The Application of Modern NMR Techniques to Problems of Structure, Stereochemistry and Conformation in Steroids: C-20 Stereochemistry and C-17 Side-chain Conformation in C-20 Substituted Pregnanes; Structure and Conformation in Ring A and Ring B Cyclosteroids and Cyclopropanosteroids.

By

Ronald Kirk Marat

A Thesis
Submitted to the Faculty of Graduate Studies
in Partial Fulfilment of the Requirements
for the Degree of

Doctor of Philosophy

Department of Chemistry
University of Manitoba
Winnipeg, Manitoba

ISBN 0-612-13339-7

Name _____

Dissertation Abstracts International and *Masters Abstracts International* are arranged by broad, general subject categories. Please select the one subject which most nearly describes the content of your dissertation or thesis. Enter the corresponding four-digit code in the spaces provided.

Chemistry - Pharmaceutical
SUBJECT TERM

0491
SUBJECT CODE

UMI

Subject Categories

THE HUMANITIES AND SOCIAL SCIENCES

COMMUNICATIONS AND THE ARTS
Architecture 0729
Art History 0377
Cinema 0900
Dance 0378
Fine Arts 0357
Information Science 0723
Journalism 0391
Library Science 0399
Mass Communications 0708
Music 0413
Speech Communication 0459
Theater 0465

EDUCATION
General 0515
Administration 0514
Adult and Continuing 0516
Agricultural 0517
Art 0273
Bilingual and Multicultural 0282
Business 0688
Community College 0275
Curriculum and Instruction 0727
Early Childhood 0518
Elementary 0524
Finance 0277
Guidance and Counseling 0519
Health 0680
Higher 0745
History of 0520
Home Economics 0278
Industrial 0521
Language and Literature 0279
Mathematics 0280
Music 0522
Philosophy of 0998
Physical 0523
Psychology 0525
Reading 0535
Religious 0527
Sciences 0714
Secondary 0533
Social Sciences 0534
Sociology of 0340
Special 0529
Teacher Training 0530
Technology 0710
Tests and Measurements 0288
Vocational 0747

LANGUAGE, LITERATURE AND LINGUISTICS
Language
- General 0679
- Ancient 0289
- Linguistics 0290
- Modern 0291

Literature
- General 0401
- Classical 0294
- Comparative 0295
- Medieval 0297
- Modern 0298
- African 0316
- American 0591
- Asian 0305
- Canadian (English) 0352
- Canadian (French) 0355
- English 0593
- Germanic 0311
- Latin American 0312
- Middle Eastern 0315
- Romance 0313
- Slavic and East European 0314

PHILOSOPHY, RELIGION AND THEOLOGY
Philosophy 0422
Religion
- General 0318
- Biblical Studies 0321
- Clergy 0319
- History of 0320
- Philosophy of 0322

Theology 0469

SOCIAL SCIENCES
American Studies 0323
Anthropology
- Archaeology 0324
- Cultural 0326
- Physical 0327

Business Administration
- General 0310
- Accounting 0272
- Banking 0770
- Management 0454
- Marketing 0338

Canadian Studies 0385
Economics
- General 0501
- Agricultural 0503
- Commerce-Business 0505
- Finance 0508
- History 0509
- Labor 0510
- Theory 0511

Folklore 0358
Geography 0366
Gerontology 0351
History
- General 0578
- Ancient 0579
- Medieval 0581
- Modern 0582
- Black 0328
- African 0331
- Asia, Australia and Oceania 0332
- Canadian 0334
- European 0335
- Latin American 0336
- Middle Eastern 0333
- United States 0337

History of Science 0585
Law 0398
Political Science
- General 0615
- International Law and Relations 0616
- Public Administration 0617

Recreation 0814
Social Work 0452
Sociology
- General 0626
- Criminology and Penology ... 0627
- Demography 0938
- Ethnic and Racial Studies 0631
- Individual and Family Studies 0628
- Industrial and Labor Relations 0629
- Public and Social Welfare 0630
- Social Structure and Development 0700
- Theory and Methods 0344

Transportation 0709
Urban and Regional Planning 0999
Women's Studies 0453

THE SCIENCES AND ENGINEERING

BIOLOGICAL SCIENCES
Agriculture
- General 0473
- Agronomy 0285
- Animal Culture and Nutrition 0475
- Animal Pathology 0476
- Food Science and Technology 0359
- Forestry and Wildlife 0478
- Plant Culture 0479
- Plant Pathology 0480
- Plant Physiology 0817
- Range Management 0777
- Wood Technology 0746

Biology
- General 0306
- Anatomy 0287
- Biostatistics 0308
- Botany 0309
- Cell 0379
- Ecology 0329
- Entomology 0353
- Genetics 0369
- Limnology 0793
- Microbiology 0410
- Molecular 0307
- Neuroscience 0317
- Oceanography 0416
- Physiology 0433
- Radiation 0821
- Veterinary Science 0778
- Zoology 0472

Biophysics
- General 0786
- Medical 0760

EARTH SCIENCES
Biogeochemistry 0425
Geochemistry 0996
Geodesy 0370
Geology 0372
Geophysics 0373
Hydrology 0388
Mineralogy 0411
Paleobotany 0345
Paleoecology 0426
Paleontology 0418
Paleozoology 0985
Palynology 0427
Physical Geography 0368
Physical Oceanography 0415

HEALTH AND ENVIRONMENTAL SCIENCES
Environmental Sciences 0768
Health Sciences
- General 0566
- Audiology 0300
- Chemotherapy 0992
- Dentistry 0567
- Education 0350
- Hospital Management 0769
- Human Development 0758
- Immunology 0982
- Medicine and Surgery 0564
- Mental Health 0347
- Nursing 0569
- Nutrition 0570
- Obstetrics and Gynecology .. 0380
- Occupational Health and Therapy 0354
- Ophthalmology 0381
- Pathology 0571
- Pharmacology 0419
- Pharmacy 0572
- Physical Therapy 0382
- Public Health 0573
- Radiology 0574
- Recreation 0575
- Speech Pathology 0460
- Toxicology 0383

Home Economics 0386

PHYSICAL SCIENCES
Pure Sciences
Chemistry
- General 0485
- Agricultural 0749
- Analytical 0486
- Biochemistry 0487
- Inorganic 0488
- Nuclear 0738
- Organic 0490
- Pharmaceutical 0491
- Physical 0494
- Polymer 0495
- Radiation 0754

Mathematics 0405
Physics
- General 0605
- Acoustics 0986
- Astronomy and Astrophysics 0606
- Atmospheric Science 0608
- Atomic 0748
- Electronics and Electricity 0607
- Elementary Particles and High Energy 0798
- Fluid and Plasma 0759
- Molecular 0609
- Nuclear 0610
- Optics 0752
- Radiation 0756
- Solid State 0611

Statistics 0463

Applied Sciences
Applied Mechanics 0346
Computer Science 0984
Engineering
- General 0537
- Aerospace 0538
- Agricultural 0539
- Automotive 0540
- Biomedical 0541
- Chemical 0542
- Civil 0543
- Electronics and Electrical 0544
- Heat and Thermodynamics ... 0348
- Hydraulic 0545
- Industrial 0546
- Marine 0547
- Materials Science 0794
- Mechanical 0548
- Metallurgy 0743
- Mining 0551
- Nuclear 0552
- Packaging 0549
- Petroleum 0765
- Sanitary and Municipal 0554
- System Science 0790

Geotechnology 0428
Operations Research 0796
Plastics Technology 0795
Textile Technology 0994

PSYCHOLOGY
General 0621
Behavioral 0384
Clinical 0622
Developmental 0620
Experimental 0623
Industrial 0624
Personality 0625
Physiological 0989
Psychobiology 0349
Psychometrics 0632
Social 0451

Nom _____

Dissertation Abstracts International est organisé en catégories de sujets. Veuillez s.v.p. choisir le sujet qui décrit le mieux votre thèse et inscrivez le code numérique approprié dans l'espace réservé ci-dessous.

_____ ☐☐☐ U·M·I

SUJET — CODE DE SUJET

Catégories par sujets

HUMANITÉS ET SCIENCES SOCIALES

COMMUNICATIONS ET LES ARTS
Architecture 0729
Beaux-arts 0357
Bibliothéconomie 0399
Cinéma 0900
Communication verbale 0459
Communications 0708
Danse 0378
Histoire de l'art 0377
Journalisme 0391
Musique 0413
Sciences de l'information 0723
Théâtre 0465

ÉDUCATION
Généralités 515
Administration 0514
Art 0273
Collèges communautaires 0275
Commerce 0688
Économie domestique 0278
Éducation permanente 0516
Éducation préscolaire 0518
Éducation sanitaire 0680
Enseignement agricole 0517
Enseignement bilingue et multiculturel 0282
Enseignement industriel 0521
Enseignement primaire. 0524
Enseignement professionnel 0747
Enseignement religieux 0527
Enseignement secondaire 0533
Enseignement spécial 0529
Enseignement supérieur 0745
Évaluation 0288
Finances 0277
Formation des enseignants 0530
Histoire de l'éducation 0520
Langues et littérature 0279
Lecture 0535
Mathématiques 0280
Musique 0522
Orientation et consultation 0519
Philosophie de l'éducation 0998
Physique 0523
Programmes d'études et enseignement 0727
Psychologie 0525
Sciences 0714
Sciences sociales 0534
Sociologie de l'éducation 0340
Technologie 0710

LANGUE, LITTÉRATURE ET LINGUISTIQUE
Langues
- Généralités 0679
- Anciennes 0289
- Linguistique 0290
- Modernes 0291

Littérature
- Généralités 0401
- Anciennes 0294
- Comparée 0295
- Médiévale 0297
- Moderne 0298
- Africaine 0316
- Américaine 0591
- Anglaise 0593
- Asiatique 0305
- Canadienne (Anglaise) 0352
- Canadienne (Française) 0355
- Germanique 0311
- Latino-américaine 0312
- Moyen-orientale 0315
- Romane 0313
- Slave et est-européenne 0314

PHILOSOPHIE, RELIGION ET THÉOLOGIE
Philosophie 0422
Religion
- Généralités 0318
- Clergé 0319
- Études bibliques 0321
- Histoire des religions 0320
- Philosophie de la religion 0322

Théologie 0469

SCIENCES SOCIALES
Anthropologie
- Archéologie 0324
- Culturelle 0326
- Physique 0327

Droit 0398
Économie
- Généralités 0501
- Commerce-Affaires 0505
- Économie agricole 0503
- Économie du travail 0510
- Finances 0508
- Histoire 0509
- Théorie 0511

Études américaines 0323
Études canadiennes 0385
Études féministes 0453
Folklore 0358
Géographie 0366
Gérontologie 0351
Gestion des affaires
- Généralités 0310
- Administration 0454
- Banques 0770
- Comptabilité 0272
- Marketing 0338

Histoire
- Histoire générale 0578
- Ancienne 0579
- Médiévale 0581
- Moderne 0582
- Histoire des noirs 0328
- Africaine 0331
- Canadienne 0334
- États-Unis 0337
- Européenne 0335
- Moyen-orientale 0333
- Latino-américaine 0336
- Asie, Australie et Océanie 0332

Histoire des sciences 0585
Loisirs 0814
Planification urbaine et régionale 0999
Science politique
- Généralités 0615
- Administration publique 0617
- Droit et relations internationales 0616

Sociologie
- Généralités 0626
- Aide et bien-être social 0630
- Criminologie et établissements pénitentiaires 0627
- Démographie 0938
- Études de l' individu et de la famille 0628
- Études des relations interethniques et des relations raciales 0631
- Structure et développement social 0700
- Théorie et méthodes. 0344
- Travail et relations industrielles 0629

Transports 0709
Travail social 0452

SCIENCES ET INGÉNIERIE

SCIENCES BIOLOGIQUES
Agriculture
- Généralités 0473
- Agronomie. 0285
- Alimentation et technologie alimentaire 0359
- Culture 0479
- Élevage et alimentation 0475
- Exploitation des pâturages 0777
- Pathologie animale 0476
- Pathologie végétale 0480
- Physiologie végétale 0817
- Sylviculture et faune 0478
- Technologie du bois 0746

Biologie
- Généralités 0306
- Anatomie 0287
- Biologie (Statistiques) 0308
- Biologie moléculaire 0307
- Botanique 0309
- Cellule 0379
- Écologie 0329
- Entomologie 0353
- Génétique 0369
- Limnologie 0793
- Microbiologie 0410
- Neurologie 0317
- Océanographie 0416
- Physiologie 0433
- Radiation 0821
- Science vétérinaire 0778
- Zoologie 0472

Biophysique
- Généralités 0786
- Medicale 0760

SCIENCES DE LA TERRE
Biogéochimie 0425
Géochimie 0996
Géodésie 0370
Géographie physique 0368
Géologie 0372
Géophysique 0373
Hydrologie 0388
Minéralogie 0411
Océanographie physique 0415
Paléobotanique 0345
Paléoécologie 0426
Paléontologie 0418
Paléozoologie 0985
Palynologie 0427

SCIENCES DE LA SANTÉ ET DE L'ENVIRONNEMENT
Économie domestique 0386
Sciences de l'environnement 0768
Sciences de la santé
- Généralités 0566
- Administration des hôpitaux 0769
- Alimentation et nutrition 0570
- Audiologie 0300
- Chimiothérapie 0992
- Dentisterie 0567
- Développement humain 0758
- Enseignement 0350
- Immunologie 0982
- Loisirs 0575
- Médecine du travail et thérapie 0354
- Médecine et chirurgie 0564
- Obstétrique et gynécologie 0380
- Ophtalmologie 0381
- Orthophonie 0460
- Pathologie 0571
- Pharmacie 0572
- Pharmacologie 0419
- Physiothérapie 0382
- Radiologie 0574
- Santé mentale 0347
- Santé publique 0573
- Soins infirmiers 0569
- Toxicologie 0383

SCIENCES PHYSIQUES
Sciences Pures
Chimie
- Généralités 0485
- Biochimie 487
- Chimie agricole 0749
- Chimie analytique 0486
- Chimie minérale 0488
- Chimie nucléaire 0738
- Chimie organique 0490
- Chimie pharmaceutique 0491
- Physique 0494
- PolymÈres 0495
- Radiation 0754

Mathématiques 0405
Physique
- Généralités 0605
- Acoustique 0986
- Astronomie et astrophysique 0606
- Électronique et électricité 0607
- Fluides et plasma 0759
- Météorologie 0608
- Optique 0752
- Particules (Physique nucléaire) 0798
- Physique atomique 0748
- Physique de l'état solide 0611
- Physique moléculaire 0609
- Physique nucléaire 0610
- Radiation 0756

Statistiques 0463

Sciences Appliqués Et Technologie
Informatique 0984
Ingénierie
- Généralités 0537
- Agricole 0539
- Automobile 0540
- Biomédicale 0541
- Chaleur et thermodynamique 0348
- Conditionnement (Emballage) 0549
- Génie aérospatial 0538
- Génie chimique 0542
- Génie civil 0543
- Génie électronique et électrique 0544
- Génie industriel 0546
- Génie mécanique 0548
- Génie nucléaire 0552
- Ingénierie des systèmes 0790
- Mécanique navale 0547
- Métallurgie 0743
- Science des matériaux 0794
- Technique du pétrole 0765
- Technique minière 0551
- Techniques sanitaires et municipales 0554
- Technologie hydraulique 0545

Mécanique appliquée 0346
Géotechnologie 0428
Matières plastiques (Technologie) 0795
Recherche opérationnelle 0796
Textiles et tissus (Technologie) 0794

PSYCHOLOGIE
Généralités 0621
Personnalité 0625
Psychobiologie 0349
Psychologie clinique 0622
Psychologie du comportement 0384
Psychologie du développement 0620
Psychologie expérimentale 0623
Psychologie industrielle 0624
Psychologie physiologique 0989
Psychologie sociale 0451
Psychométrie 0632

THE APPLICATION OF MODERN NMR TECHNIQUES TO PROBLEMS OF STRUCTURE, STEREOCHEMISTRY AND CONFORMATION IN STEROIDS: C-20 STEREOCHEMISTRY AND C-17 SIDE-CHAIN CONFORMATION IN C-20 SUBSTITUTED PREGNANES; STRUCTURE AND CONFORMATION IN RING A AND RING B CYCLOSTEROIDS AND CYCLOPROPANOSTEROIDS

BY

RONALD KIRK MARAT

A Thesis submitted to the Faculty of Graduate Studies of the University of Manitoba in partial fulfillment of the requirements of the degree of

DOCTOR OF PHILOSOPHY

Contents

List of Figures vii
List of Tables x
Abstract xi
Acknowledgements xiii

1 Introduction 1

1.1 NMR and Steroids 1

1.1.1 NMR Parameters 3

Chemical Shifts 3

Vicinal H-H Coupling Constants 5

Vicinal C-H Coupling Constants 5

Geminal H-H Coupling Constants 7

Long-Range Couplings 9

Nuclear Overhauser Enhancements 10

1.1.2 NMR Techniques 20

NOE Difference Spectroscopy 21

Difference Double Resonance (DDR) Spectroscopy 22

^{1}H Detected 1D DEPT and INEPT 23

J Resolved Spectroscopy 23

Homonuclear Correlation Spectroscopy 24

2D-TOCSY 26

2D-NOE Spectroscopy (NOESY) 27
2D Rotating Frame NOE Spectroscopy (ROESY) 27
Heteronuclear Correlation Spectroscopy 29
2D Carbon-Carbon Correlation 30
1D Experiments Using Selective Pulses 31
1D COSY 31
1D TOCSY 31
1D ROESY and NOESY 32
1.2 Conformation and Activity 32
1.3 Structure-Activity Relationships in Cardiac Glycosides 34
1.3.1 The Digitalis Glycosides 34
1.3.2 Na^+,K^+-ATPase 37
Structural Features 37
Mechanism of Inhibition 37
1.3.3 The Separation of Therapeutic and Toxic effects 39
1.3.4 Structure-Activity Relationships of the C-17 Sidechain 42
Cyclic C-17 Substituents 43
Open-chain C-17 Substituents 43
1.3.5 Cardiotonic 5β,14β-pregnanes 43
1.3.6 Re-evaluation of C-17 Side-Chain Conformation in Naturally Occurring Cardiac Glycosides 53
1.4 Cyclosteroids and Cyclopropanosteroids 55
1.4.1 Cyclosteroids as Potential Mechanism-Based Enzyme Inhibitors 55
Aromatase (P-450$_{AROM}$) Inhibitors 58

2 Experimental **66**
2.1 Samples 66
2.1.1 Cardiotonic Pregnanes 66
2.1.2 Cyclosteroids and Cyclopropanosteroids 66

2.1.3 Naturally Occurring Cardiac Glycosides 67
2.2 Spectroscopic Methods 67

3 Results **70**
3.1 Cardiotonic Pregnanes 70
3.1.1 Conformational and Configurational Analysis 70
20(R)- and 20(S)-Nitro-5β-pregne-3β,14β-diol 3-acetate (**1** and **2**) . . 74
5β-Pregnane-3β,14β,20(R)- and 20(S)-triol 3,20-diacetate (**3** and **4**) . 76
5β-Pregnane-3β,14β,20(R)- and 20(S)-triol 3-acetate (**5** and **6**) 76
20(R)- and 20(S)-Acetamido-3β-(α-L-pyranorhamnosyl)oxy-5β-pregnan-14β-ol (**7** and **8**) 78
20(R)- and 20(S)-Amino-3β-(α-L-pyranorhamnosyl)oxy-5β-pregnan-14β-ol (**9** and **10**) 78
20(R)- and 20(S)-Acetamido-5β-pregn-14-en-3β-ol (**11** and **12**) 78
5β-Pregn-14-ene-3β,20(R)- and 20(S)-diol 3-acetate (**13** and **14**) . . . 78
20(R)- and 20(S)-Trifluoroacetamido-5β-pregn-14-en-3β-ol 3-trifluoroacetate (**15** and **16**) 78
17β-Nitromethyl-3β-(α-L-pyranorhamnosyl)oxy-5β-androstan-14β-ol (**17**) 79
17β-Hydroxymethyl-3β-(α-L-pyranorhamnosyl)oxy-5β-androstan-14β-ol (**18**) 79
14α-Hydroxy-(tri-O-benzyoyl-α-L-rhamnopyranosyl)oxy-5β,17α-pregnane 21-carboxylic acid 14,21-lactone (**19**) 80
14β-Hydroxy-(tri-O-benzoyl-α-L-rhamnopyranosyl)oxy-5β-pregnane 21-carboxylic acid 14,21-lactone (**20**) 80
21-Nitro-3β-(α-L-rhamnopyranosyl)oxy-5β-pregnane-14β,20(R)-diol (**21**) 80
20(R)-(*tert*-Butyldimethylsiloxy)-21-nitro-3β-(tri-O-benzoyl-α-L-rhamnopyranosyl)oxy-5β-pregn-14β-ol (**22**) 80

20(R)-Methoxy-21-nitro-3β-(α-L-rhamnopyranosyl)oxy-5β-pregnane-14β-ol (**23**) 81
21-Nitro-3β-(tri-O-benzoyl-a-L-rhamnopyranosyl)oxy-5β-pregn-20,21-en-14β-ol (**24**) 81
14β-Hydroxy-3β-(a-L-pyranorhamnosyl)oxy-5β-androstan-17β-acrylic acid (**25**) 82
3.1.2 C-17 Side-chain Conformation in Naturally Occurring Cardiac Glycosides and their Genins 82
Digoxigenin 83
Digitoxigenin and Digitoxigenin-3-acetate 84
Digoxin and Digitoxin 84
3.1.3 C-17 Side-chain Conformations Predicted by Molecular Mechanics and Semi-Empirical Molecular Orbital Methods 95
C-20 Substituted Pregnanes and 21-Norpregnanes 95
C-21 Substituted Pregn-20,21-enes (**24** and **25**) 98
Digoxigenin and Digitoxigenin 98
3.2 Cyclosteroids and Cyclopropanosteroids 99
3.2.1 Determination of Structures 99
19(S)-Bromo-17β-(*tert*-butyldimethylsiloxy)-5β,6β-dibromomethylene-9α,19-cyclo-10α-androstan-3-one (**42**) 99
19(S)-Bromo-5β,6β-[(R)-bromomethylene]-17β(*tert*-butyldimethylsiloxy)-9α,19-cyclo-10α-androstan-3-one (**43**) 101
19(S)-Bromo-5β,6β-[(S)-bromomethylene]-17β(*tert*-butyldimethylsiloxy)-9α,19-cyclo-10α-androstan-3-one (**44**) 101
19(S)-Bromo-5β,6β-17β(*tert*-butyldimethylsiloxy)-9α,19-cyclo-10α-androst-4-en-3-one (**45**) 110
17β-*tert*-Butyldimethylsiloxy-19,19-dichloro-5α,19α-cycloandrostan-3-one (**35**) 110

17β-*tert*-Butyldimethylsiloxy-19,19-dichloro-5β,19-cycloandrostan-3-one (**32**) 110
17β-*tert*-Butyldimethylsiloxy-19(S)-chloro-5α,19α-cycloandrostan-3-one (**36**) 110
17β-*tert*-Butyldimethylsiloxy-19(R)-chloro-5α,19α-cycloandrostan-3-one (**37**) 110
17β-*tert*-Butyldimethylsiloxy-19(S)-chloro-5β,19-cycloandrostan-3-one (**33**) 111
17β-*tert*-Butyldimethylsiloxy-19(R)-chloro-5β,19-cycloandrostan-3-one (**34**) 111
19(R)-Hydroxy-5β-19-cycloandrostane-3,17-dione (**40**) 111
3.2.2 Spectral Analysis 111
3.2.3 Conformational Analysis 122
Ring A Cyclopropanosteroids (**26 - 31**) 130
5β,19β-Cycloandrostanes (**32-34, 38-41**) 133
5α,19α-Cycloandrostanes (**35-37**) 135
9α,19α-Cycloandrostanes (**42-45**) 136
19(R)-Acetoxy-1β,19-cyclo-5α-androstane-3,17-dione (**46**) 136

4 Discussion **140**

4.1 Cardiotonic Pregnanes 140
4.1.1 ^{13}C Shifts 140
4.1.2 Comparison of Experimentally Determined C-17 Side-chain Conformations with Those Predicted by Molecular Mechanics and Semi-Empirical Molecular Orbital Methods 142
Cardiotonic Pregnanes 142
Digoxigenin 143
Digoxin 144
Digitoxigenin and Digitoxigenin-3-acetate 144

4.1.3 The Relationship between C-17 Side-Chain Structure and Conformation to Biological Activity 145
C-20 Substituted Pregnanes 145
C-20 Substituted 21-Norpregnanes 149
C-21 Substituted Pregn-20,21-enes (**24** and **25**) 151
4.1.4 Suggestions for Further Research 151
4.2 Cyclosteroids and Cyclopropanosteroids 153
4.2.1 Cyclopropane Induced Chemical Shifts 153
4.2.2 NOEs and Internuclear Distances 154
4.2.3 The Relationship of Ring A Structure and Conformation to Biological Activity 155
4.2.4 Suggestions for Further Research 157

Bibliography **160**

List of Figures

1.1 General steroid structure and numbering 2

1.2 $^3J(1\alpha, 2\beta)$ in a 3-one steroid 6

1.3 J_{gem} in a cyclohexanone fragment as predicted by the Barfield-Grant equation 8

1.4 Energy level diagram for a two spin system 11

1.5 Population level diagram for a two spin system 14

1.6 Structures of some naturally occurring cardiac glycosides. 36

1.7 Pregnanes **1 - 10**. 46

1.8 Pregnenes **11 - 16**. 47

1.9 21-Norpregnanes **17** and **18**. 48

1.10 Typical reaction scheme used to produce cardiotonic pregnanes 49

1.11 Cardiotonic C-21 Substituted pregnanes **19-25** 50

1.12 The two probable lactone side-chain conformations in digitoxin-like cardiac glycosides 53

1.13 Proposed scheme for the use of cyclopropanes as enzyme inhibitors . 57

1.14 Biosynthesis of estrone and estradiol 59

1.15 Accepted mechanism for the first two steps in estrogen synthesis . . . 60

1.16 Proposed mechanism for the third step in estrogen synthesis 61

1.17 Cyclosteroids and cyclopropanosteroids **26 - 37**. 63

1.18 Cyclosteroids and cyclopropanosteroids **38 - 46**. 64

3.1 Conformations in Pregnanes **1** - **16** viewed as a Newman projection along the C-17–C-20 bond 75
3.2 Fully coupled ^{13}C spectrum of the C-22 carbon in digoxigenin and digitoxin 86
3.3 Fully coupled ^{13}C spectrum of the C-21 carbon in digoxigenin and digitoxin 87
3.4 ROESY spectrum of digoxin in a 1:1 mixture of $CDCl_3$ and DMSO-d_6 at 313 K 92
3.5 Expanded ROESY spectrum of the C-21 and C-22 protons of digoxin in a 1:1 $CDCl_3$ DMSO-d_6 mixture 93
3.6 ROESY spectrum of the C-21 and C-22 protons of digitoxin in a 1:1 $CDCl_3$ DMSO-d_6 mixture 94
3.7 Lowest energy conformations of digoxigenin as predicted by AM1 calculations 97
3.8 Proposed reaction scheme for synthesis of 19,5-cyclosteroids 100
3.9 Resolution enhanced 500 MHz proton spectrum of **42** 102
3.10 Proton detected carbon-proton correlation spectrum of **42** 103
3.11 Proton detected carbon-proton correlation spectrum of **42** with extracted rows 104
3.12 COSY spectrum of **42** 105
3.13 Proton detected carbon-proton correlation spectrum of **43**, one of the reduction products of **42** 106
3.14 Proton detected carbon-proton correlation spectrum of **44**, one of the reduction products of **42** 107
3.15 Steady-state NOE difference spectrum of **44** while irradiating the C-19 cyclopropyl proton 108
3.16 Steady-state NOE difference spectrum of **44** while irradiating the 5,6-cyclopropyl proton 109

3.17 Proton detected carbon-proton correlation spectrum of **29** 120
3.18 1D TOCSY spectra of **31** at various mixing times 121
3.19 Experimental and simulated 500 MHz ring A spectrum of **37** 123
3.20 Steady state NOE difference spectrum of **27** irradiating H-1β 132
3.21 Ring A conformations in **26** - **40** viewed along the C-5–C10 bond . . 138
3.22 Ring A conformations in **35** - **46** viewed along the C-5–C10 bond . . 139

4.1 Proposed preferred C-17 side-chain locations for Na^+,K^+-ATPase inhibition. 146
4.2 Relative MM3 strain energies as a function of rotation angle about the C-17–C-20 bond for nitropregnanes **1** and **2**, and 21-nor-nitropregnane **17** 147
4.3 Relative MM3 strain energies as a function of rotation angle about the C-17–C-20 bond for hydroxypregnanes **5** and **6**, and 21-nor-hydroxypregnane **18** 148
4.4 A plot of % NOE as a function of $1/r^6$ (in Å) for two series of structural isomers 156
4.5 Possible difficulties in the binding of a 19(S)-hydroxy-5β,19β-cyclosteroid to aromatase in the model of Oh and Robinson 158

List of Tables

3.1 Coupling constants and NOE values for **1** to **16** (part 1 of 3) 71

3.2 Coupling constants, NOE values and rotating frame NOE values for some naturally occurring cardiac glycosides and their aglycones. . . . 85

3.3 ^{13}C Shifts in **1-25** (part 1 of 4) 88

3.4 Conformation of C-17 sidechain as predicted by molecular mechanics and semi-emperical molecular orbital methods. 96

3.5 ^{1}H Shifts in **26-46** (part 1 of 5) 112

3.6 ^{13}C Shifts in **26-46** (part 1 of 3) 117

3.7 Ring A coupling constants in Hz for **26 - 46** (part 1 of 4) 124

3.8 Cyclopropane fragment coupling constants in **26-31** and **41** 128

4.1 Comparison of C-17 sidechain conformation and configuration compared to receptor binding as measured in a [^{3}H]ouabain radioligand binding assay. 152

Abstract

Coupling constants and nuclear Overhauser effect (NOE) measurements have been used to establish the C-20 configuration and the conformation about the C-17–C-20 bond in a series of twenty-five C-20 substituted 5β,14β-pregnanes, 5β-pregn-14-enes, 5β,14β,21-norpregnanes and related compounds. In the 14β-pregnane series the conformation of the C-17 side-chain is variable while in the pregnenes the side-chain adopts a conformation in which H-17 is *anti* to H-20. In the 21-nor compounds a C-20 hydroxyl adopts a conformation *anti* to H-17, while a C-20 nitro group is *anti* to C-13. The methods described are the first reliable nuclear magnetic resonance (NMR) method for determining the C-20 stereochemistry in these compounds. The C-17 lactone conformation in digoxin, digitoxin, digoxigenin, digitoxigenin and digitoxigenin-3-acetate was re-investigated. The lactone ring exists in an equilibrium of two conformers where the C-21 protons or the C-22 proton are alternately *syn* to H-17. A comparison of experimentally determined conformations with those predicted by molecular mechanics and semi-empirical molecular orbital methods, the effects of conformation on ^{13}C chemical shifts and a discussion of the relationship between conformation and cardiotonic activity are included. Observed conformations are compared with receptor binding as measured in a [^{3}H] ouabain radioligand binding assay.

Proton and carbon NMR data are provided for twenty-one ring A and ring B cyclosteroids and cyclopropano (or methylene) steroids. Structural and stereochemical problems were solved by a combination of 2D NMR and NOE difference spectroscopy. Shift assignments were made using standard 2D NMR techniques, while ring A proton sub-spectra were extracted from a 1D total correlation spectroscopy (TOCSY) experiment. Coupling constants were obtained from iterative spin system simulation of these sub-spectra. Ring A conformations were determined from the two and three bond proton-proton couplings and NOE measurements. The utility and limitations

of extended Karplus-type equations, the effect of cyclopropyl groups on vicinal and geminal couplings, cyclopropane induced chemical shifts and the relationship between ring A conformation and potential aromatase inhibitor activity are discussed.

Acknowledgements

I am very grateful to Dr. John Templeton for taking me on as a student under somewhat unusual circumstances. I would also like to thank Dr. Ted Schaefer for his continual advice and encouragement. None of the spectroscopic studies described in this thesis would have been possible without the synthetic talents of Yangzhi Ling, Weiyang Lin, Rakesh Gupta and Talal Zeglam.

I also appreciate the licence given to me by the Chemistry Department that allowed me to pursue these studies while in their employ.

My biggest debt of gratitude is owed to my family: Diana, Andrea and Kevin, who I am sure have suffered more than I through this long process.

Finally, I would like to thank the sport of squash racquets, which has prevented me from turning into an amorphous blob during the last few years and has enabled me to overcome several severe cases of "writer's block" by allowing me to vent my frustrations on a small rubber ball.

Chapter 1

Introduction

1.1 NMR and Steroids

Throughout the development of NMR spectroscopy there has been a close association between NMR and steroids. From the earlier pioneering work by Zurcher[1,2] on the proton shifts of the axial C-18 and C-19 methyl groups, and an early NMR text based entirely on steroid examples,[3] to the development of modern two dimensional techniques, steroids have provided many useful test cases. There are good reasons for this. The rigid polycyclic steroid skeleton (Figure 1.1) with faces clearly differentiated by the angular methyl groups is an almost ideal system for the study of substituent effects on proton chemical shifts and coupling constants. There is an almost infinite variety of naturally occurring and synthetic steroids available. Furthermore, since steroids are a biologically and economically important class of compounds, the development of new NMR techniques for their structural elucidation is of more than academic importance.

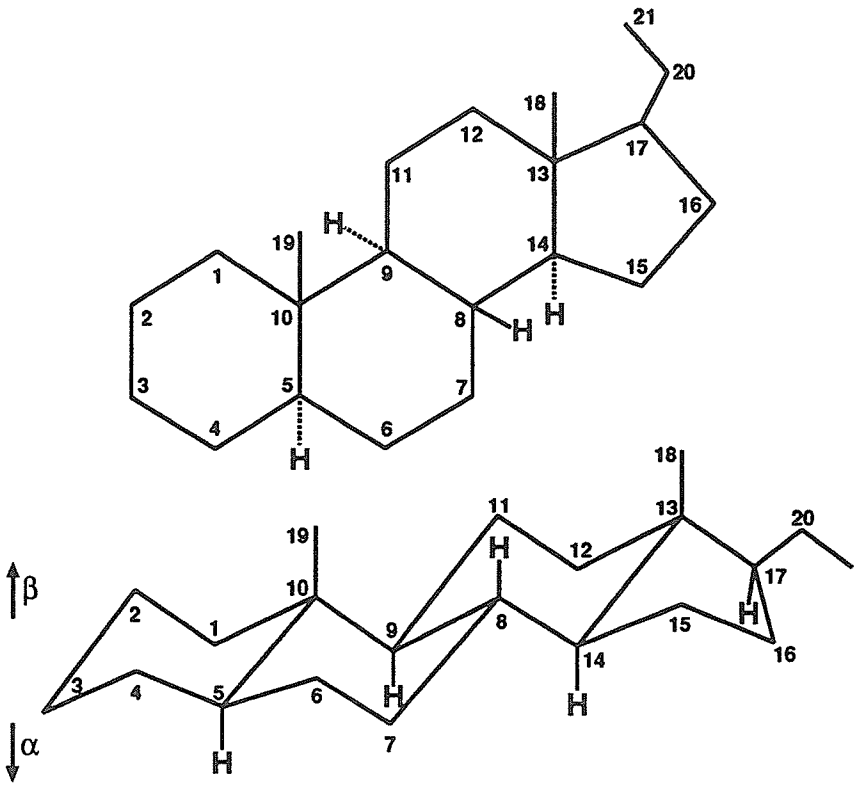

Figure 1.1: General steroid structure and numbering. The upper face, as drawn, is conventionally labelled β, while the lower face is labelled α. Variations in stereochemistry occur at C-5, C-14 or both.

1.1.1 NMR Parameters

Chemical Shifts

The proton chemical shifts of the C-10 and C-13 methyl groups are very sensitive to substitution in the steroid skeleton, often over many bonds. These substituent effects are generally transmitted *via* magnetic anisotropy and dipole effects, and are not usually the result of inductive (through bond) effects. Indeed, the rigidity of the steroid skeleton makes it an ideal system for the study of such effects. Tables of additive substituent shifts to be added to the base value for the parent androstanes have been collected and published in an NMR text by Bhacca and Williams.[3] With these tables it is possible to predict the shifts of the C-10 and C-13 methyl groups for many patterns of substitution. Deviations from additivity can occur, usually when steric factors, hydrogen bonding or conjugation force a conformational change. For example, the substituent shift for the 4-en-3-one group cannot be derived from the sum of the individual 4-ene and 3-one moieties. Similarly, a bulky 2β-substituent can force a conformational change in a 3-one or 4-en-3-one steroid resulting in an anomalous shift for the C-10 methyl.[4,5] Useful as these substituent shift values may have been in the past, they have for most purposes been replaced by more modern methods.

Only since the development of high field spectrometers and two dimensional techniques has it been possible to assign routinely the steroid ring proton resonances. Typically, twenty or more proton signals occur in just under 2 ppm and on low field spectrometers appear as an almost featureless broad absorption band.

In cyclohexane rings the axial protons are generally shielded by *ca.* 0.3 to 0.6 ppm with respect to equatorial protons. These shift differences are the result of long-range shielding effects associated with the anisotropies of the magnetic susceptibilities of the C-C single bonds. Axial protons are in the shielding region of the C-C bonds at the 2 and 3 positions with respect to the position in question, while equatorial protons

are in the de-shielding region. The same general relationship holds true in steroids, but the shift difference between the axial and equatorial protons can be much larger, especially for protons near ring junctions. For example, the shift difference between the axial and equatorial C-7 protons is often greater than 1 ppm. Presumably, this is the result of additional shielding/deshielding of the protons by the C-14–C-15 bond. This may be contrasted with the shift differences between the C-2 and C-3 protons which are often less than 0.3 ppm. The shift differences in the cyclopentyl D ring are usually much smaller than those in the A, B and C rings. Although these patterns are useful for the assignment of steroid proton spectra, they can easily be upset by substitution. For example, the shift difference between the axial and equatorial C-12 protons in testosterone is reduced from 0.77 ppm to 0.25 ppm upon addition of a 17α methyl group.[6]

Several groups[7,8] have produced a table of substituent effects on ring proton shifts in steroids based on the complete analysis of a series of steroids at 500 MHz. The substituents included were oxo and F, Cl, Br, I and OH in both axial and equatorial environments. The substituent effects were reported for both axial and equatorial protons on α, β and γ carbons. These tables have only been made possible by the development of high field spectrometers and modern methodology.

Carbon chemical shifts are perhaps of even greater utility to steroid chemists than the proton shifts. Carbon signals can usually be observed individually even on fairly basic instrumentation. However, except at the highest magnetic fields, many of the proton shifts overlap and can be difficult to assign. The first extensive compilation of steroid ^{13}C shift data was by Blunt and Stothers.[9] From the basic chemical shift table they derived tables of additive substituent shifts which can be used to predict the carbon shifts of an unknown steroid based on the assignments of a similar compound. In subsequent years many other tabulations of steroid carbon shifts have been added to the data base,[10–25] making ^{13}C spectroscopy one of the principal methods for establishing steroid structures. ^{13}C studies of steroids have also led to the development

of empirical rules and formulae for the calculation of ^{13}C shifts in six-membered rings in general.[11,12,16,26]

Vicinal H-H Coupling Constants

Many empirical extensions to the original Karplus[27] equation have been proposed for the extraction of dihedral angles from vicinal coupling constants.[28–33] All of these methods suffer from a number of limitations. In a critique of their earlier work, Ōsawa *et al*[33] reported data which show a number of serious discrepancies between experimental coupling constants and those predicted by their equation. In several conformationally flexible molecules, couplings of 2-5 Hz were predicted for protons where the experimentally observed couplings were 10-12 Hz, and *vice versa*. The principal problem seems to be the use of dihedral angles predicted by molecular mechanics calculations, and not the form of the equation relating ^3J(HH) and dihedral angle. In these cases, the reported calculated couplings were population weighted averages, and it appears that molecular mechanics is unable to provide sufficiently accurate conformational energies. A review of these methods has recently appeared,[34] and the method of Haasnoot *et al*[29] has been extended to include solvent effects.[35]

Figure 1.2 shows a comparison of $^3J(1\alpha, 2\beta)$ in a 3-one steroid predicted by four different models. As is clearly evident, the determination of accurate torsion angles is unlikely with these methods, although it is certainly possible to assign a general conformation to the ring. These equations are also very useful for determining the effects of substitution on conformation in cases where that substitution is not likely to have an intrinsic effect on the couplings.

Vicinal C-H Coupling Constants

Three bond *H*-C-C-*C* couplings are positive and vary as a function of dihedral angle with maxima at 180° and 0° in a manner similar to vicinal H-H couplings. Coupling through three σ bond varies in a Karplus-like manner and as rough approximation

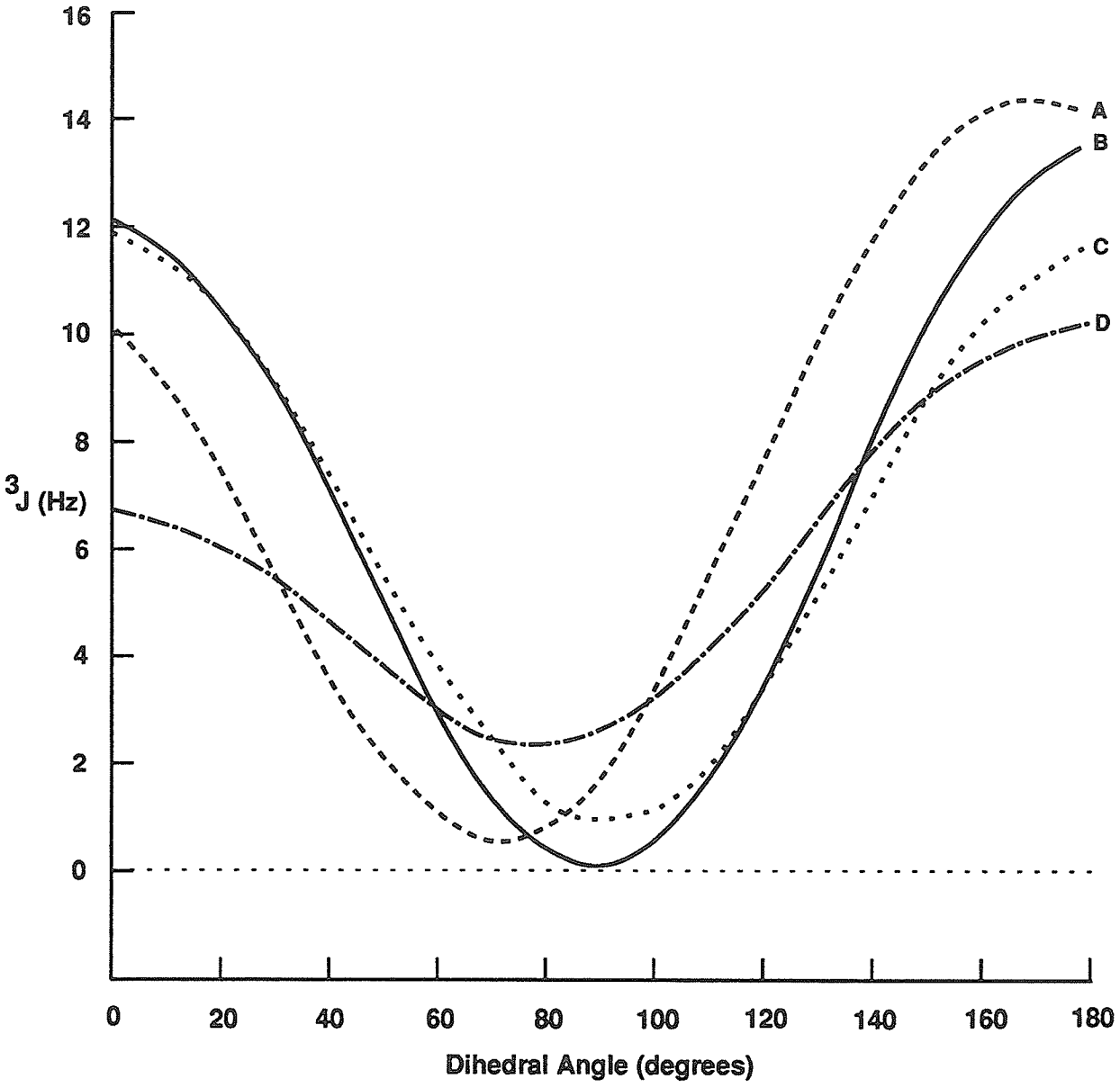

Figure 1.2: $^3J(1\alpha, 2\beta)$ in a 3-one steroid as predicted by the methods of Colucci *et al*[30] (A), Haasnoot *et al*[29] (B), Smith and Barfield[28,31] (C), and Imai and Ōsawa[32,33](D). The curves were generated with the Mathematica[36] program on an HP 9000/730 computer.

^3J(H-C-C-C) = 0.6 ^3J(H-C-C-H) in an analogous situation.[37] In general, an electronegative substituent on the coupling carbon will cause an increase in $^3J(CH)$ while substitution at the central or H-terminal carbon will cause a decrease in $^3J(CH)$.[38] An added complication, not relevant in H-H vicinal couplings, is the hybridization of the terminal coupling carbon. *Anti* couplings range from *ca.* 6 Hz to 9 Hz while *gauche* couplings range from *ca.* 0.5 Hz to *ca.* 3.5 Hz.[39] A minimum of *ca.* 0 Hz occurs at a dihedral angle of 90°. However, obtaining values for $^3J(H-C)$ in steroids can be very difficult as fully coupled carbon spectra are heavily overlapped and the low sensitivity requires large (> 40 mg) sample sizes. Summers *et al*[40] have employed the sensitivity of peak intensity to coupling constant in the HMBC experiment (Section 1.1.2) as a method for estimating the magnitude of this coupling, turning what is ordinarily a nuisance into an asset. With this technique they were able to confirm that ring A in 4-androstene-3,17-dione exists in a half chair conformation and to determine that ring D exists in an envelope conformation with H-15β and H-16α pseudo-axial.

Geminal H-H Coupling Constants

Although far less frequently used than vicinal couplings, geminal couplings are stereospecific when adjacent to a π system. A formal description of the effect based on valence bond theory was presented by Barfield and Grant.[42] The π electron contribution to the geminal coupling is negative and varies as a function of the dihedral angle between the methylene group and the adjacent π bond. The π contribution to the geminal coupling is a maximum when the π bond bisects the H-C-H angle (C-C–C-C torsion angle of 0°).* The relationship between $^2J_{gem}$ and C–C torsion angle is illustrated in Figure 1.3. The agreement between the Barfield-Grant equation and experiment is quite good in the range of θ=0° to 60°.[43–45] For torsion angles in the range of 90° the agreement is less certain, with valence bond theory[42] pre-

*The definition of torsion angle used here is 30° less than that used by Barfield and Grant[42]

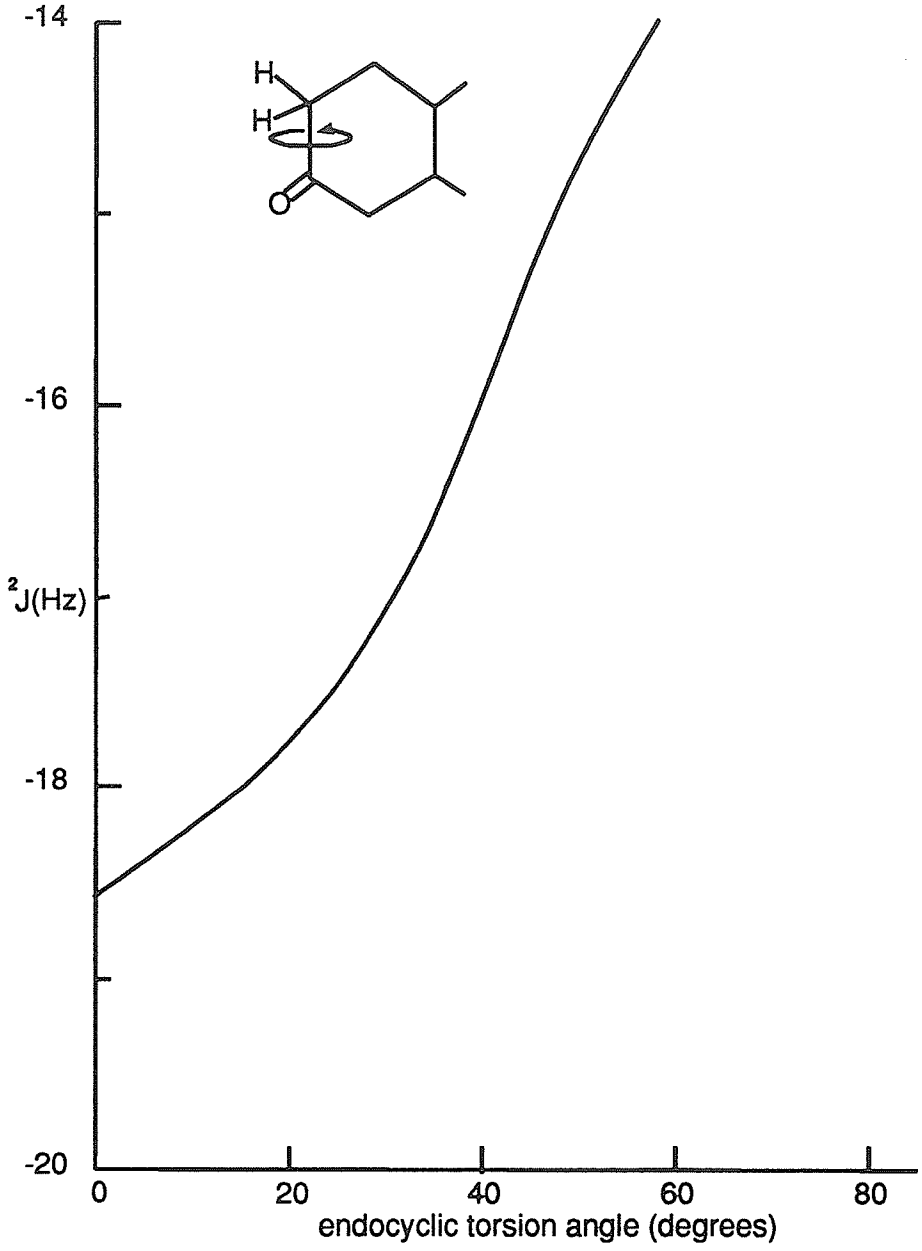

Figure 1.3: J_{gem} in a cyclohexanone fragment as predicted by the Barfield-Grant equation.[41,42]

dicting a negative π contribution to J_{gem} and molecular orbital theories predicting a positive contribution.[46,47] The resolution of this dilemma has been hampered by the lack of compounds with this particular geometry. In a low temperature NMR study of a deuterated cyclooctanone Montecalvo and St.-Jacques[48] have shown that the Barfield-Grant equation is incorrect in the vicinity of θ=90°, and confirmed a positive contribution to ^2J in the range θ=60° to 120°. It must also be noted that geminal couplings are sensitive to the C-CH_2-C bond angle and to electronegativity and orientation of substituents.[43–45,49,50]

Several studies have employed $^2J(2\alpha, 2\beta)$ and $^2J(4\alpha, 4\beta)$ to determine the ring A conformation in 3-one and 4-ene-3-one steroids.[4,5,41]

Long-Range Couplings

Long-range coupling is generally considered to be coupling over four or more chemical bonds. Such couplings, although small, are highly stereospecific. Long-range couplings in saturated systems are generally maximum when there is a planar "zig-zag" arrangement of atoms. For four bond couplings this is known as the "W" (or "M") configuration. Four bond couplings between equatorial protons in cyclohexane rings are a typical example of this arrangement. In acyclic compounds conformational averaging usually results in long-range couplings that are vanishingly small. Long-range couplings are also enhanced when one of the intervening atoms is sp^2 hybridized.

In steroids, four-bond couplings are frequently observed and can provide useful structural and conformational information. Unfortunately, they also limit the ultimate resolution obtainable in steroid spectra. The most frequently observed four bond couplings are those from the C-10 and C-13 methyl groups where they often can be seen in COSY spectra or can be revealed by difference double resonance techniques. In a 5α-steroid the C-10 methyl group has a *ca.* 0.5 Hz couplings to H-1α. Couplings to H-5 and H-9 are smaller but can be detected as cross-peaks in a suit-

able COSY spectrum. In a 5β-steroid the *cis* A/B ring junction affords the wrong geometry for the C-10 methyl to H-1α and C-10 methyl to H-5 couplings. The lack of these couplings, which can often be detected by a C-10 methyl peak that is sharper than usual, is a useful method for determining C-5 stereochemistry. The C-13 methyl group couples to H-12α and H-17α. Coupling to H-14α is much smaller and is rarely observed. In most steroids C-17 is substituted and the assignment of H-17 rarely presents a problem. The C-12 protons, however, are often obscured and the C-10 methyl to H-12α coupling, which is usually clearly visible in the COSY spectrum, is a good starting point for the assignment of the ring C protons. In 4-ene-3-one steroids four-bond couplings are also observed from H-4 to H-2α and H-6β.

Nuclear Overhauser Effects (NOEs)

The nuclear Overhauser effect has become a standard technique for demonstrating the spatial proximity of nuclei in organic molecules. The Overhauser effect in general terms is the change in the integrated intensity of the magnetic resonance signal of one spin when another is irradiated. The original Overhauser effect[51] referred to change in a nuclear signal in a paramagnetic sample when the electrons were irradiated. By far more common today, however, is the internuclear experiment. The application of the nuclear Overhauser effect to problems of configuration and conformation in solution was first demonstrated by Anet and Bourn.[52] The size of the NOE was found to correlate directly with internuclear distance,[53] and in favourable instances can be used to determine internuclear distances quantitatively.[54]

Consider the case of two chemically shifted but uncoupled nuclei, I and S (Figure 1.4). There are four energy levels, conventionally labelled $\beta\beta$ through $\alpha\alpha$. There are four single quantum transitions: two I spin transitions with transition probability W_I, two S spin transitions with transition probability W_S, a zero quantum transition with transition probability W_0, and a double quantum transition with transition probability W_2. In the absence of coupling the two I spin transitions are degenerate

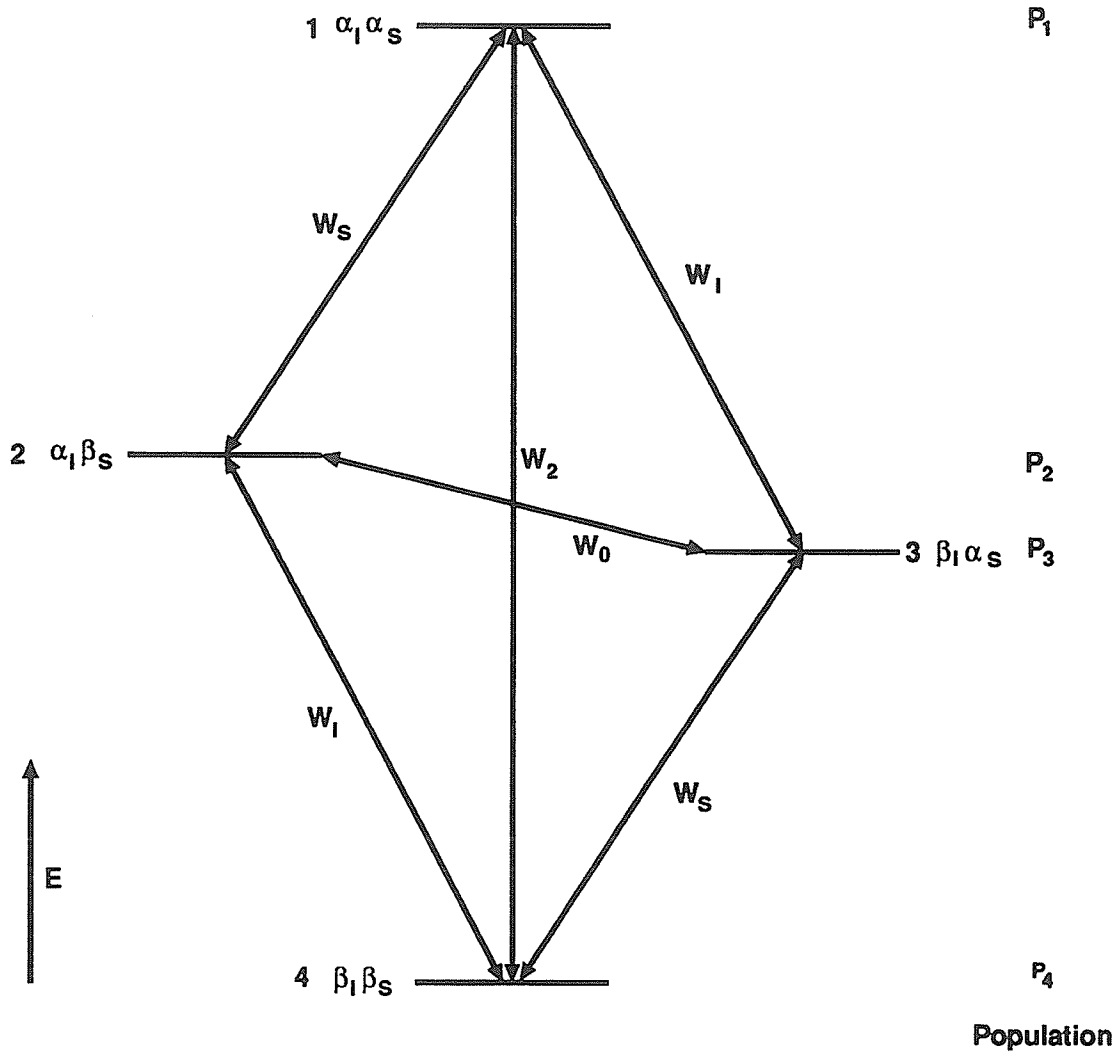

Figure 1.4: Energy level diagram for a two spin system. The frequency of a transition is goverened by the energy difference between the levels. At equilibrium, the population of each level is dictated by Boltzman's law.

as are the two S spin transitions. Irradiation at the S spin frequency will equilibrate levels 1 with level 2 and level 3 with level 4 (Figure 1.5). This is a non-equilibrium situation but, in the absence of any re-distribution mechanism the *relative* populations of level 1 compared to level 3 and level 3 compared to level 4 do not change. Thus, there is no change in the I spin resonance intensity.

Any non-equilibrium system will try to return to equilibrium if it can. In the case of the two spin system described above, this re-distribution can be accomplished by the double and zero quantum transitions and by the single quantum transition W_I These transitions can be stimulated by the fluctuating magnetic field at the I spin created by the combination of the S spin magnetic dipole and molecular rotation. These transitions are therefore stimulated by the same mechanism responsible for dipole-dipole relaxation and this is the only relaxation mechanism capable of stimulating the double and zero quantum transitions. Since level 1 is de-populated with respect to equilibrium, and level 4 has a surplus of population with respect to equilibrium, the double quantum transition will tend to re-populate level 1 from level 4. Since S spin irradiation leads to rapid equilibration of level 1 with level 2 and level 3 with level 4, the effect of W_2 is to increase the population of level 1 with respect to level 3 and level 2 with respect to level 4. The I spin resonance intensity is governed by these population differences, so the net effect of W_2 is to increase the NMR signal intensity of the I spin. W_0, on the other hand, will move population from level 2 to level 3 (level 2 having a surplus of population and level 3 having a deficit), resulting in a net *decrease* in the I spin intensity. The dipole-dipole transition probabilities are given by[55]

$$W_I = \frac{3}{20}\frac{\gamma_I^2\gamma_S^2\hbar 2}{r^6}\frac{\tau_c}{1+\omega_I^2\tau_c^2} \tag{1.1}$$

$$W_0 = \frac{1}{10}\frac{\gamma_I^2\gamma_S^2\hbar^2}{r^6}\frac{\tau_c}{1+(\omega_I-\omega_S)^2\tau_c^2} \tag{1.2}$$

$$W_2 = \frac{3}{5}\frac{\gamma_I^2\gamma_S^2\hbar^2}{r^6}\frac{\tau_c}{1+(\omega_I+\omega_S)^2\tau_c^2} \tag{1.3}$$

It is very important to distinguish between the transition probabilities W which are transfer rates and have units of s^{-1}, and the transition frequencies ω which are angular velocities in rad s^{-1} and are 2π times the conventional NMR frequencies in Hz. For a homonuclear proton NOE experiment on a modern instrument, the single quantum transition frequencies, $\omega_I/2\pi$ and $\omega_S/2\pi$ correspond to a frequency of approximately 500 MHz. The frequency of the double quantum transition will be given by $(\omega_I+\omega_S)/2\pi$ or approximately 1 GHz, while the frequency of the zero quantum transition will be given by $(|\omega_I-\omega_S|)/2\pi$ and will be at most a few KHz. The zero quantum frequency is, in fact, the chemical shift difference between I and S.

For a small molecule in a mobile solvent, the molecular correlation time τ_c is much shorter than the Larmor frequency and the terms $\omega_I^2\tau_c^2$, $(\omega_I-\omega_S)^2\tau_c^2$ and $(\omega_I+\omega_S)^2\tau_c^2$ become vanishingly small compared to 1. Thus, W_2 is six times more effective at redistributing population than W_0 and 4 times more effective than W_S. The nuclear Overhauser effect will therefore result in an enhancement of the I spin signal and will quantitatively be given by

$$\eta = \frac{W_2 - W_0}{2W_S + W_2 + W_0}\frac{\gamma_S}{\gamma_I} \tag{1.4}$$

The dipole-dipole transition probabilities are also strongly dependent on internuclear distance $(1/r^6)$, but in the absence of any other relaxation mechanism this would only effect the *rate* of population redistribution and NOE build-up. However, as internuclear distance increases and dipole-dipole relaxation becomes less effective other relaxation mechanisms will contribute to W_S (but not to W_2 or W_0). These

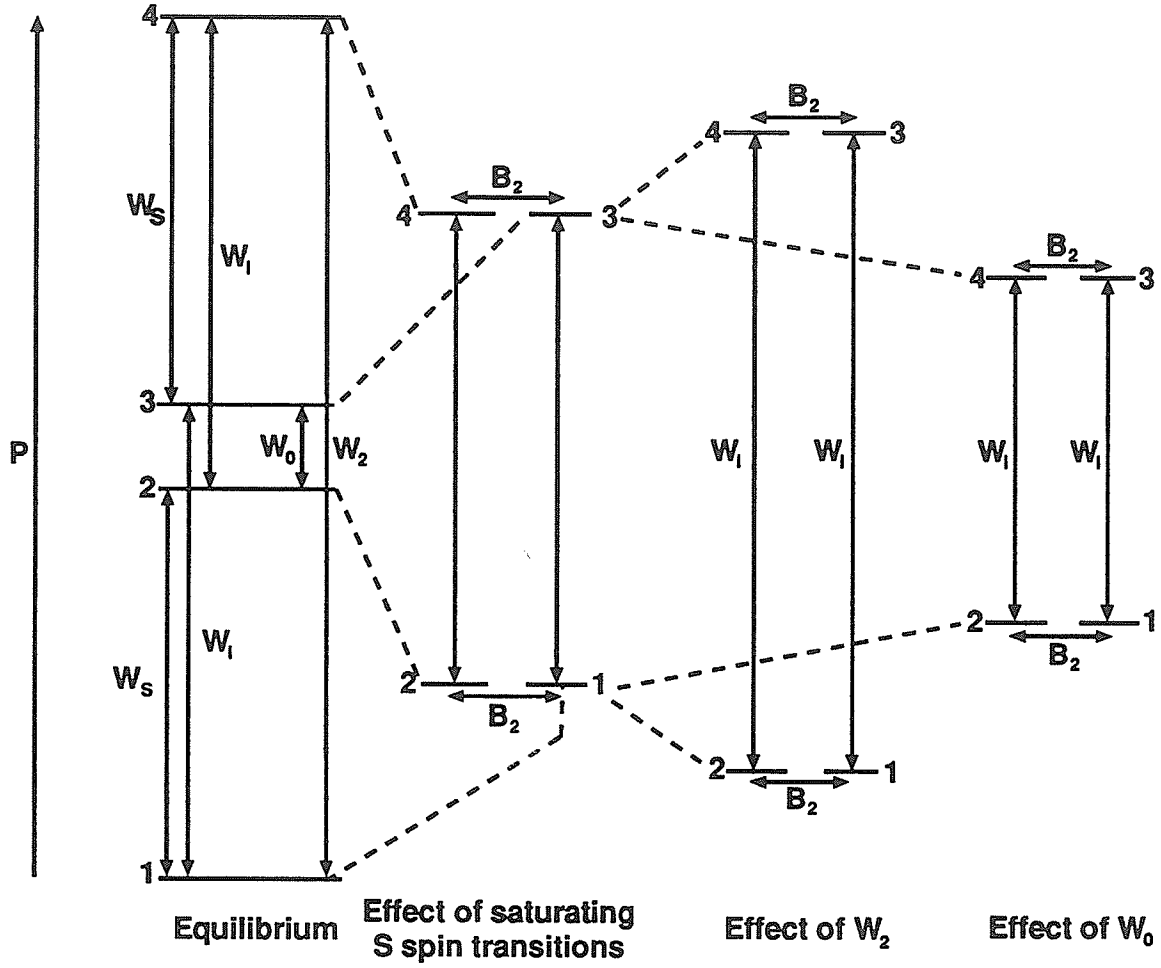

Figure 1.5: Population level diagram for a two spin system. The *intensity* of each transition is governed by the population difference between the upper and lower levels. The saturating field (B_2) forces levels 1 and 2 to be equally populated and levels 3 and 4 to be equally populated, creating a non-equilibrium situation. W_2 will pump population between levels 1 and 4 and thus increase the intensity of the I transitions, while W_0 will pump population between levels 2 and 3 and thus decrease the intensity of the I spin transitions.

other mechanisms constitute a "leakage pathway" and will serve to reduce the NOE. As the internuclear distance increases W_S starts to dominate the denominator of Equation 1.4 and in the limit where $2W_S >> W_2 - W_0$ the NOE vanishes. It is the relative decrease of dipole-dipole relaxation compared to other relaxation pathways at increasing internuclear distance that leads to the dependence of NOE on internuclear distance. The degree of NOE observed at I when S is irradiated depends on the contribution to the spin-lattice relaxation of I by dipole-dipole interaction from S.

Note that in the absence of any other information or assumptions (about, say, other relaxation mechanisms) it is not possible in principle to measure directly internuclear distances from two-spin NOEs. Bell and Saunders[53] have shown, however, that for a set of similar compounds, in the same solvent, under identical conditions, plots of log(% NOE) *vs* log r are good straight lines with slopes of -6 for both H–H and CH_3–H interactions. This implies that it is possible in favourable circumstances to compare two-spin NOEs within a molecule or between similar molecules (for example, a pair of isomers) under identical conditions and to obtain information about relative internuclear distances. This information is often sufficient for assigning stereochemistry or conformation. The steep dependence of dipole-dipole relaxation on distance means that one stereoisomer or conformer will often be expected to have a substantial NOE while another will be expected to have none. It must be pointed out that stereochemistries assigned by NOE measurements are always much more reliable when *both* stereoisomers are available for measurement.

The above description is valid for a two spin system. Steroids, of course, have considerably more than two spins. In discussing NOE in multi-spin systems, it is useful to establish the following definitions:

1. I_{zi} is the observable z magnetization of spin i. This is equivalent to signal intensity.

2. I_{0i} is the equilibrium z magnetization of i in the absence of any NOE.

3. T_{1i} is the longitudinal relaxation time of i, $R_i = T_{1i}^{-1}$.

4. $\sigma_{ij} = \sigma_{ji}$ are the cross relaxation rates between i and j.

5. $\rho_{ij} = \rho_{ji}$ are the dipole-dipole relaxation rates between i and j. $\rho_{ij} = \rho_{ij} = 2\sigma_{ij}$.

6. ρ_i^* is the relaxation rate of i due to processes other than dipole-dipole relaxation by j.

These relaxation rates are related to the two-spin transition probabilities above by:

$$\rho_I = 2W_I + W_0 + W_2$$

$$\rho_S = 2W_S + W_0 + W_2$$

$$\sigma_{IS} = \sigma_{SI} = W_2 - W_0$$

The overall relaxation rate of i will therefore be

$$R_i = \sum_{j \neq i} \rho_{ij} + \rho_i^* \tag{1.5}$$

The expression for the rate of change of intensity as a function of time can then be given by

$$\frac{dI_{zi}}{dt} = -R_i(I_{zi} - I_{0i}) - \sum_{j \neq i} \sigma_{ij}(I_{zj} - I_{0j}) \tag{1.6}$$

Equation 1.6 is known as the generalized Solomon[56] equation.† Because of the steep dependence of dipole-dipole relaxation on distance, it is rarely necessary to consider more than three spins when dealing with steroids.

Following the notation of Noggle and Schirmer,[55] the saturated spins are designated as s, the observed or detected spins as d, and all other spins as n. $f_d(s)$ is the fractional NOE observed at d when s is saturated and $f_n(s)$ is the fractional NOE at n caused by saturation of s. Solving Equation 1.6 for steady state ($dI_z/dt = 0$) a general expression for steady state homonuclear multi-spin NOE can then be written as

$$f_d(s) = \sum_s \frac{\rho_{ds}}{2R_d} - \sum_n \frac{\rho_{dn} f_n(s)}{2R_d} \tag{1.7}$$

This essentially means that any enhancement of n by s will result in a decrease in the NOE observed at d if there is significant dipole-dipole relaxation of d by n. It may therefore be naive to presume that absence of an NOE necessarily precludes spatial proximity. The maximum NOE observed at d when the relaxation of d is totally dominated by dipole-dipole relaxation by s ($\rho_{ds} = R_d$, $\rho_{dn} = 0$) is thus 0.5.

For a three-spin amx spin system there are six possible NOEs and if it is possible to measure all six NOEs then it is possible to get a measure of internuclear distances. If $f_a(x)$ refers to the fractional NOE observed at a upon irradiation of x, and r_{ax} refers to the internuclear separation of a and x, etc., then ratios of internuclear distances can be obtained from equations such as

$$\left(\frac{r_{ax}}{r_{am}}\right)^6 = \frac{\gamma_x^3 f_a(m) + f_a(x) f_x(m)}{\gamma_m^3 f_a(x) + f_a(m) f_m(x)} \tag{1.8}$$

†For a rigorous derivation of Equation 1.6 see Noggle and Schirmer[55] or Neuhaus and Williamson.[57]

$$\left(\frac{r_{xa}}{r_{xm}}\right)^6 = \frac{\gamma_a^3}{\gamma_m^3}\frac{f_x(m) + f_x(a)f_a(m)}{f_x(a) + f_x(m)f_m(a)} \tag{1.9}$$

$$\left(\frac{r_{mx}}{r_{ma}}\right)^6 = \frac{\gamma_x^3}{\gamma_a^3}\frac{f_m(a) + f_m(x)f_x(a)}{f_m(x) + f_m(a)f_a(x)} \tag{1.10}$$

Since virtually all steroid NOE studies involve homonuclear NOEs the ratios involving γ will normally reduce to unity.

Unfortunately, in steroids, spectral overlap usually prevents the measurement of enough NOEs to measure internuclear distances directly. There are some some specific three-spin cases, however, which commonly occur and should be considered.

Consider the case where irradiation of a results in a substantial enhancement of m (typically a geminal pair). The NOE observed at x then depends on the proximity of x to both a and m. If $f_m(a)\rho_{mx}/2R_x$ is greater than $\rho_{ax}/2R_x$ then the enhancement of m by a will result in a negative NOE to x. This usually implies that x is much closer to m than it is to a, and can be a useful method for demonstrating proximity of m and x when direct NOE measurements between m and x are not possible (usually because of spectral crowding). However, if $f_m(a)\rho_{mx}/2R_x$ is comparable to $\rho_{ax}/2R_x$ then the direct effect of the irradiation of a on x and the indirect effect of m on x will cancel and no NOE will be observed at x. This may lead to an erroneous conclusion about the location of x.

If necessary, multi-spin effects can be circumvented by observing the rate of NOE build-up rather than the actual enhancement itself.[‡] When extrapolated to zero time the rate of intensity change, dI_{xi}/dt is proportional only to the cross relaxation rate between the irradiated and the observed spins. All the other $\sigma_{ij}(I_{zj} - I_{0j})$ terms in Equation 1.6 except that for the saturated spin become zero. Conceptually, this is quite easy to understand. At zero time no indirect effects can occur as no intensities

[‡]This technique is commonly used by biochemists for macromolecules where multi-spin effects (known in this case as spin diffusion) are quite severe.

except for that of the saturated spin have changed. If we return to our two spin (IS) nomenclature used earlier, at $t = 0$

$$dI_z/dt = \sigma_{IS} I_{0z} \tag{1.11}$$

This is an important result in that it can give us a direct measure of two-spin cross relaxation (σ_{IS}) independent of multi-spin effects and R_I. If one assumes that all r_{ij} have the same correlation time, τ_c, (an approximation at best) then we can measure internuclear distances by comparing cross relaxation rates with those of a pair of known r_{ij}.

$$\left(\frac{r_{ij}}{r_{kl}}\right)^6 = \left(\frac{\sigma_{ij}}{\sigma_{kl}}\right) \tag{1.12}$$

For steroid and other natural product studies, geminal pairs are a natural choice for distance calibration. The major drawback to this technique is the necessity of measuring NOEs at short irradiation or mixing times where the NOEs may be small and hard to detect. If frequency stepping is employed to irradiate the lines of a multiplet short irradiation times can result in unequal saturation of the multiplet lines. This unequal saturation will create an INEPT-like transfer of magnetization to any coupled nuclei. The resultant change in intensity of the coupled nucleus caused by the polarization transfer will be indistinguishable from the NOE, making frequency switching inappropriate for the measurement of the short irradiation time NOEs.

Maes *et al*[58] have employed the initial rate approximation to a study of the molecular structure of [1,2,5]oxadiazolo[3′,4′,3,4]-5α-pregn-16-en-20-one. NOEs were measured from NOESY cross-peak volumes, and the measured internuclear distances were found to be in good agreement with those determined by x-ray crystallography.

NOE measurements have also been used to study the interaction between an

enzyme and its steroid substrate. When bound to an enzyme, a steroid takes on the characteristic τ_c of the enzyme. These correlation times are well into the region of spin diffusion, and rapid cross relaxation gives rise to large negative NOEs between the steroid protons and between the steroid protons and the enzyme protons. If the bound steroid is in equilibrium with a large pool of unbound steroid, these NOEs will be retained in the unbound steroid because of its much longer spin-lattice relaxation times. It is this unbound steroid that is actually observed and, depending on the molecular weight of the enzyme, the bound steroid may not even be observable. This is known as a transferred NOE experiment and it can give information on the conformation of the steroid while bound to the enzyme. NOEs between the steroid and the enzyme give important information on the steroid binding site. This technique has been used by Kuliopulos *et al*[59] to study the mechanism and stereochemistry of reactions catalyzed by Δ^5-3-ketosteroid isomerase. The steroid concentration was 6 mM while the enzyme concentration was 200 μM. Details of the binding of the steroid ring A to the enzyme's active site and of the stereochemistry of the enolization were presented.

1.1.2 NMR Techniques

The principal problems with the NMR spectroscopy of steroids are the lack of information in the carbon spectrum and the excessive complexity of the proton spectrum. The carbon spectrum gives only a single parameter, the chemical shift, for each carbon. The proton-proton couplings observed in the proton spectrum give important structural information, but the information is often unavailable because of severe overlap of the bands.

Various techniques can be used to assign the multiplicity of carbon spectra, with polarization transfer (Distortionless Enhancement *via* Polarization Transfer - DEPT[60] and Insensitive Nuclei Enhanced via Polarization Transfer - INEPT[61]) and J modulation[62] techniques replacing older techniques such as single frequency off-

resonance decoupling. The proton spectrum consists of singlets from the angular methyl groups and/or acetyl groups; perhaps a few low field multiplets from protons on substituted carbons; and hundreds of lines in the region between 0.5 and 2.0 ppm from the remainder of the protons in the molecule. The resolving power of modern instruments, especially with the application of computer resolution enhancement, is such that virtually every two and three bond coupling to every proton in this region can be resolved.

The challenge is to sort out the overlap and assign the signals to the appropriate protons. There are two principal ways in which this may be done. One can be selective in the information which is recorded, or one can spread the information into two (or more) dimensions.

NOE Difference Spectroscopy

The nuclear Overhauser enhancement or NOE is a fundamental NMR parameter giving important structural information and can also be a method for selectively observing certain nuclei in a crowded spectrum. The application of NOE difference spectroscopy to steroids was first reported by Farrant *et al*[63,64] who used it to assign the α face of 6α-methyl-17α-acetoxyprogesterone. In this technique, a reference spectrum is subtracted from a spectrum in which the peaks of a particular proton have been pre-irradiated for a period of time comparable to T_1 (typically 3 to 5 seconds for steroids.) In the resultant difference spectrum only protons that are close to the irradiated proton remain – all others cancel. Many earlier spectrometers could only irradiate at a single frequency and could therefore only pre-irradiate singlets or narrow multiplets. Modern spectrometers, (since *ca.* 1982) can irradiate multiplets by stepping the frequency over each line, and NOE's can be observed from wide multiplets with minimum danger of affecting neighbouring peaks. Frequency stepping can however generate off resonance excitation from modulation sidbands. The use of shaped pulses on each line rather than discontinuous steps avoid this effect, but

has not been reported in the literature. Improvements in spectrometer stability have given spectroscopists the ability to measure NOEs well below the 1% level.

In steroids the most commonly irradiated protons are those of the C-10 and C-13 methyl groups. For a 5α,14α steroid irradiation of the C-10 methyl protons will result in observable NOEs to protons on the β face of rings A and B, while irradiation of the C-13 methyl protons will result in observable NOEs to protons on the β face of rings C and D. The NOEs will also generally be stronger to the β face protons that are also axial. In a 5β steroid, on the other hand, ring A bends under the plane of the molecule and many of the ring-A NOEs will be missing. This can be a useful method of differentiating a 5α from a 5β steroid.

Difference Double Resonance (DDR) Spectroscopy

In this technique a control spectrum is subtracted from a spectrum where one or more of the protons is decoupled. In the resulting difference spectrum, only those protons that are J-coupled to the irradiated proton will be observed while all others will cancel. his technique works best when the couplings between the irradiated group and the observed nuclei are vanishingly small, and the decoupling only results in a slight narrowing of the peaks. This situation results in clean multiplet patterns (less the coupling to the irradiated nucleus, of course.) When the couplings are larger, the decoupling results in a gross change in the multiplet structure and the resulting difference spectrum is very complex. Again, the C-10 and C-13 methyl groups serve as convenient nuclei for irradiation as they have small (*ca.* 0.5 Hz) couplings to several nuclei on the α face of the steroid. In 5α,14α steroids, the C-10 methyl couples to H-1α and H-5 while the C-13 methyl couples to H-17α and H-12α. In 5β steroids, however, H-1α and H-5 do not have the correct "W" configuration for coupling to the C-10 methyl. This results in a sharper more intense methyl singlet and can be a convenient method for the determination of C-5 stereochemistry. In 4-en-3-one steroids H-4 is usually clear of other resonances and difference double resonance can

therefore be used to obtain isolated spectra of the C-2 and C-6 protons. Bloch-Siegert shifts often limit the utility of this technique by creating large frequency dependent subtraction artifacts, although computer methods for removing Bloch-Siegert shifts have been presented.[65]

A number of groups have used DDR techniques for the assignment and analysis of steroid spectra,[4,65] often combined with NOE difference spectroscopy, and a review article has been published by Sanders and Mersh.[66]

Inverse or Proton Detected 1D DEPT and INEPT

It is possible to perform the DEPT and INEPT experiments (section 1.1.2), commonly used to assign the multiplicity of ^{13}C spectra, with proton detection.[67,68] In this way it is possible to obtain isolated spectra of methine, methylene or methyl protons. There does not yet appear to be any examples of this technique being applied to steroids, however. This may be due to the difficulty in suppressing signals from the ^{12}C isotopomers on older spectrometers, or it may be due to the availability of the much more selective two-dimensional techniques.

J Resolved Spectroscopy

In principal, 2D J resolved spectroscopy provides a spectrum in which shifts and couplings are separated on two orthogonal frequency axes.[69] A projection along the F_2 axis should give a "broad-band decoupled" proton spectrum in which each proton gives a single line rather than a multiplet. F_1 slices at each proton shift should then give the multiplet structure of that proton. Unfortunately, the technique is very sensitive to strong coupling. That is, when the size of the coupling constant between two protons approaches the chemical shift difference between those protons a number of spurious peaks and multiplet distortions occur which render the spectra very difficult to interpret. It is generally not possible to predict in advance from the molecular structure when strong coupling is likely to occur. In this sense, the

technique is said to be "non-robust". Nevertheless, since it is an easy technique to implement on most spectrometers, it was the first two-dimensional NMR technique to be applied to steroids. The use of J spectroscopy for the analysis of proton spectra of steroids was first used by Hall and Sanders who reported the complete assignment of 1-dehydrotestosterone[70] and 11α-hydroxytestosterone.[71] Other steroids for which the technique has been successful include 17α-acetoxy-6α-methylprogesterone[63] and 3α-aminopregn-5-en-20-one.[72]

Wong and Clark[41,73] have used the related selective indirect J spectroscopy to determine $^2J(2\alpha, 2\beta)$ in a series of 4-en-3-one steroids. This coupling is sensitive to the torsion angle of the C-2–C-3 bond and is thus a measure of ring A conformation. Spectra were recorded with a digital resolution of 2 Hz per data point but the coupling constants were reported to have an accuracy of $\pm$0.2 Hz. Furthermore, no attention was paid to the possibility of strong coupling and its effects on the J spectrum. When one of these couplings was re-investigated at high-resolution with full spin-system iterative simulation, the earlier reported value was found to be considerably in error.[4]

A recent report employs selective pulses to reduce the experiment to a series of two spin systems.[74] The technique, known as SERF (for *se*lective *ref*ocusing), results in exclusively doublet multiplicity in the F_1 dimension. 3α-Hydroxy-5α-androstan-17-one was used as a test case where a number of reasonable couplings were reported. Whether the technique will prove practical in a general case is yet to be proven, and the effects of strong coupling are uncertain. It is a requirement that the frequencies of all nuclei pairs of interest be known in advance, but this should not be a problem if the standard sequence of experiments used to assign the resonances has already been performed.

Homonuclear Correlation Spectroscopy

Homonuclear correlation is usually accomplished *via* the COSY (*co*relation *s*pectro*sc*o*py*) pulse sequence[75] and is one of the most common two-dimensional NMR tech-

niques. The usual format can be thought of as having the normal one-dimensional spectrum running along the diagonal with off diagonal peaks indicating J coupling. Other formats, such as SECSY[76,77] (*s*pin-*e*cho *c*orrelation *s*pectroscop*y*) and FOCSY[77] (*f*old-over corrected *c*orrelation *s*pectroscop*y*), are less commonly used and for steroids appear to offer no real advantage over COSY. Two dimensional TOCSY (*t*otal *c*orrelation *s*pectroscop*y*) or homonuclear Hartman-Hahn spectra[78] can extend the correlations out into the coupling network beyond directly coupled spins, but often result in a matrix that is too crowded for interpretation. COSY is a simple experiment to perform; data processing is straightforward; it is not terribly demanding on spectrometer resources; and it is relatively insensitive to strong coupling and experimental abuse. A 45° mixing pulse can reduce crowding on the diagonal and give information on the relative signs of couplings. The relative signs of couplings can be used to distinguish vicinal from geminal couplings. Cross sections of COSY spectra show fine structure resulting from proton-proton coupling and can be used for the estimation of coupling constants. However, the magnitude mode presentation of most COSY spectra and digital resolution will often set a lower limit to the size of the coupling constants that can be observed. Addition of a fixed delay into the evolution time[79] will allow relatively small (*ca.* 0.2 Hz) couplings to be observed as cross peaks even in cases where the splitting is not observable in the one-dimensional spectrum. Such a delay can result in the loss of cross-peaks from larger couplings, however.

The skeleton protons of a steroid can be considered to be one large contiguous spin system. Provided that at least a few multiplets can be assigned with certainty, it is possible, in principle, to work through the COSY spectrum assigning all of the other multiplets. In practice, severe overlap will usually make this difficult except with heavily functionalized steroids.

Relayed Coherence Transfer (RCT)[80] is essentially a multi-step COSY experiment. If nucleus A is coupled to nucleus B and nucleus B is coupled to nucleus C but C is not coupled to A, COSY will show cross-peaks between A and B and between B and C. A

RCT experiment, however, will also show an A-C cross-peak resulting from the two-step magnetization transfer: A to B, B to C. The main application of RCT to steroids is in the identification or observation of multiplets that are obscured in a conventional COSY spectrum. Hughes[81] has employed RCT in a study of 17α- and 17β-estradiol. Relayed magnetization transfer was demonstrated from the C-13 methyl to H-12α to H-11β. The degree of magnetization transfer is a function of the J values and delays in the pulse sequence so that successful application of RCT requires at least a good estimate of the sizes of the couplings involved. The TOCSY experiment can provide the same information as the RCT experiment without foreknowledge of the J values.

2D TOCSY

Heteronuclear cross polarization using Hartmann-Hahn matched fields has become commonplace in solid state NMR spectroscopy. In liquids, dipolar interactions average to zero and spins are coupled only *via* scaler (J) coupling. However, Hartmann-Hahn cross polarization can be performed in liquids and the magnetization is exchanged between spins at a rate determined by J. For the technique to work, the mismatch in the fields seen by the two species must be less than the interaction between the spins. Since J couplings in liquids are much smaller than dipolar coupling in solids achieving a Hartmann-Hahn match in liquids is far more difficult than in solids.

In homonuclear systems both spins see the *same* field and in principle it would seem that the Hartmann-Hahn match would be automatic. Unfortunately, resonance offset effects reduce the effective field so that only nuclei equidistant from the B_1 frequency are effectively matched. This problem can be overcome by replacing the continuous B_1 field with a composite pulse sequence similar to that used for composite pulse broad-band decoupling. Of course, a homonuclear cross-polarization experiment does nothing to improve sensitivity, but it does provide a method for correlating nuclei *via* J coupling. The two-dimensional experiment is performed with a non-selective 90° pulse along the X' axis followed by a Waltz-17[82] spin lock along the Y' axis which

serves as the mixing time. Purge pulses (on the order of ms) may be placed before and after the spin lock if desired. The mixing period is followed by an evolution time and the detection period. For short mixing times (10 to 20 ms) the information obtained is essentially the same as for COSY; off-diagonal peaks indicate J coupling between peaks on the diagonal. At longer mixing times (>40ms) the magnetization propagates out into the spin system and cross-peaks can be observed between nuclei several couplings away. If A is coupled to B, and B is coupled to C, then magnetization can be transfered from A to B and from B to C and a cross-peak will be observed between A and C even though A and C are not directly coupled. For steroids the practical limit for the mixing times is *ca.* 150 ms. At this point cross peaks are observed for protons 3 to 4 couplings (4 to 5 carbons) remote and the spectrum becomes too complex.

2D-NOE Spectroscopy (NOESY)

NOESY has the same matrix form as COSY, but the cross-peaks demonstrate NOE between protons rather than coupling. There have been relatively few reports on the application of NOESY to steroids[5,6] principally because it is difficult to avoid confusing COSY impurity peaks and because NOE difference spectroscopy is far more sensitive and provides better resolution. Many of the cross-peaks observed in NOESY spectra of steroids are from geminal pairs and therefore provide little structural information.

2D Rotating Frame NOE Spectroscopy (ROESY)

As molecular weight and spectrometer frequency increase, NOEs become smaller and eventually vanish at $\omega\tau_c = 1.118$.[§] At this point, the zero quantum transition probability W_0 and the double quantum transition probability W_2 become equal. For values of $\omega\tau_c$ larger than 1.118 (larger molecules, viscous solvents, very high frequencies) the

[§]See the description of NOE in Section 1.1.1

NOE becomes negative. These negative NOEs are the norm for macromolecules like proteins but are not commonly observed in small molecules like steroids. There is one important class of steroids for which this appears to be an exception, however. The cardiac glycosides, particularly in viscous solvents such as DMSO or water, show very little NOE on high field spectrometers. Near the cross-over point the NOEs are also very sensitive to local variations in the effective τ_c and are less reliable as a structural parameter. In the determination of the structure of forbeside C (A steroid with a five sugar carbohydrate chain at C-7, just slightly heavier than a typical cardiac glycoside), a series of NOE difference spectra were presented where all NOEs are clearly negative.[83] No mention of this fact was made in the paper and the nuclear Overhauser effects were repeatedly referred to as "enhancements" even though the irradiation resulted in a net *decrease* in the intensity of the observed signal.

Rotating-frame NOEs under spin-locked conditions, however, are always positive and increase monotonically with increasing τ_c. This experiment was introduced by Bothner-By *et al*[84] and was extended to the two dimensional ROESY experiment by Bax and Davis.[85] It is a very useful substitute for NOESY in situations where traditional NOEs are very small. The use of rotating frame NOEs has become indispensable in the study of smaller oligosaccharides, nucleic acids, peptides and proteins.

The pulse sequence for the two-dimensional ROESY experiment is similar to that used for the TOCSY experiment, but with the spin-lock field reduced by approximately an order of magnitude. The mixing times used in ROESY are governed by $T_1\rho$ rather than J and are therefore considerably longer than those used for TOCSY. Whereas TOCSY usually uses a composite pulse (eg. WALTZ) mixing sequence in order to reduce the offset dependence of B_1 the use of this sort of sequence is specifically avoided in ROESY. The similarity of the TOCSY and ROESY pulse sequences means that contamination of ROESY spectra with TOCSY cross peaks is a serious problem. The opposite phase of the ROESY and TOCSY cross peaks can result in cancellation of signals in cases where both TOCSY and ROESY cross peaks are expected between

two nuclei. This problem is partially but not completely eliminated by the lower spin-lock field and the avoidance of resonance-offset compensating pulse sequences. Recently Huang and Shaka[86] have proposed a ROESY mixing sequence, based on phase alternating 180° and 360° pulses, which eliminates TOCSY type peaks.

ROESY has been used to help establish the structures of saponins[87] and tenacigenins.[88]

Heteronuclear Correlation Spectroscopy

Experiments which correlate the ^{13}C shifts with the proton shifts have probably become the most frequently used two-dimensional NMR technique for steroids. A number of experiments can be used for carbon proton correlation. Carbon detected experiments include HETCOR[89] (*het*eronuclear *cor*relation) which correlates the shifts *via* the one bond carbon-proton coupling, and COLOC[90] (*co*rrelation by *lo*ng range coupling) which correlates the shifts *via* two, three and four bond couplings. Proton detected (sometimes called "inverse") experiments include HMQC[91] (*h*eteronuclear *m*ultiple *q*uantum *c*oherence) and HSQC[92] (*h*eteronuclear *s*ingle *q*uantum *c*oherence) for one bond correlations and HMBC[93] (*h*eteronuclear *m*ultiple *b*ond *c*orrelation) for multiple bond correlations.

In two-dimensional NMR it is usually easier to obtain high resolution in the detection dimension than the evolution dimension. The selection of proton or carbon detection, therefore, depends on where the resolution is required. Since steroid carbon spectra are generally much better resolved than proton spectra, the proton detected experiments are usually the obvious choice. Furthermore, spreading the crowded proton spectrum into the *ca.* twenty times greater carbon chemical shift range enables one to extract proton multiplets which would be totally obscured in the proton spectrum. These multiplet patterns and their associated coupling constants are the key to obtaining structural and conformational information.

Proton detected experiments do, however, require good stability for suppression

of the 100 times stronger signals from the ^{12}C isotopomers and provisions for carbon decoupling while observing protons. Most if not all modern spectrometers have the required equipment and stability. Maximum-entropy/linear prediction methods can be employed in cases where time constraints have resulted in a short evolution dimension. For steroids, HSQC (in our experience, at least) seems to provide better sensitivity and F_1 resolution than HMQC.

2D Carbon-Carbon Correlation

Correlation of carbons *via* the carbon-carbon homonuclear coupling with suppression of the 100 fold more intense singly labelled isotopomer is possible with the INADEQUATE (*i*ncredible *n*atural *a*bundance *d*oubl*e* *qua*ntum *t*ransfer *e*xperiment) experiment.[94]

Several reports on the application of INADEQUATE to steroids appear in the literature. Kruk *et al*[95] have used INADEQUATE for the unambiguous assignment of all 27 carbons in vitamin D_3. The technique has also been applied in the elucidation of the structures of some anti-viral steroids from the sponge *petrosia weinbergi*.[96] As elegant as the experiment is, the information provided by INADEQUATE can be obtained on a much smaller sample by a combination of proton-proton correlation spectroscopy (COSY or TOCSY), carbon-proton correlation spectroscopy (HMQC or HSQC or HETCOR) and long-range carbon-proton correlation spectroscopy (HMBC or COLOC). Many if not all of these techniques will likely have been run on the sample in any event, rendering the INADEQUATE experiment redundant. One situation in which INADEQUATE may have an advantage is where there are chains of quaternary carbons and correlations *via* protons cannot be used. These situations are not frequently found in steroids.

1D Experiments Using Selective Pulses

As useful as two dimensional experiments are, they are not necessarily appropriate in all cases. Data storage or experiment time constraints may limit digital resolution and the size or accuracy of couplings that can be observed. An alternative is to record selective rows of a two dimensional experiment by the use of selective pulses. Many such experiments have been proposed.[97]

For example, 1D COSY can be used to obtain spectra of all protons coupled to the proton receiving the selective pulse. This experiment yields spectra which are anti-phase in the active coupling. This can be useful for the discrimination of active and passive couplings, but can also cause cancellation of overlapping peaks and a confusing multiplet structure. The addition of a refocusing period and a Z-filter can be used to give in-phase multiplets but requires a knowledge of the active coupling. Extensions to COSY such as the DISCO and RELAY experiments can be readily applied to the 1D COSY experiment as well.

1D TOCSY has potential advantages over 1D COSY. In-phase multiplets are obtained without the use of refocusing periods, and by varying the mixing period multiplets at varying "depths" in the spin system may be observed. For mixing times on the order of 20 ms, only directly coupled protons are observed. At 100 ms, protons can be observed three to four couplings (four to five carbons) removed. This tends to be the practical limit for steroids: longer mixing times give spectra with resonances which are often too overlapped.

The 1D TOCSY experiment, as well as 1D ROESY and 1D NOESY, require inphase magnetization at the start of the mixing period. Unfortunately, in all selective excitation experiments precession of off-resonance multiplet components during the pulse creates considerable out of phase magnetization. Pulses which have a flatter excitation profile for amplitude (such as a sinc pulse) are invariably longer and even worse at generating out-of-phase magnetization than simpler pulses such as Gaussian. Several methods have been proposed to overcome this problem. The

Gaussian selective pulse can be replaced with a half-Gaussian pulse followed by a non-selective 90° pulse,[98] or by a 270° self-refocusing Gaussian pulse.[99] Cascades of Gaussian pulses have also been proposed.[100] The addition of a Z filter to the end of the pulse sequence[97,101] also serves to remove phase anomalies in the resultant spectrum. Other modifications which improve the selectivity and sensitivity of the technique have been proposed by Bircher *et al.*[102]

1D equivalents of the NOESY and ROESY experiment have also been proposed.[97] For steroids, 1D NOESY does not seem to offer any advantages over NOE difference spectroscopy. For larger steroids, such as cardiac glycosides, NOEs are often very small because of the reasons detailed in Section 1.1.1. Rotating frame NOEs, however, do not go through this minimum and selective ROESY may have application in these cases.

The utility of 1D TOCSY for extraction of sub-spectra from steroid spectra will be demonstrated in Section 3.2.2. At the current time there appear to be no reports in the literature of any selective pulse experiments being applied to steroids.

1.2 Conformation and Activity

Conformational analysis is an important part of the drug design process. The relationship between ring A conformation and the activity of several classes of steroid hormones has been discussed by many workers. Duax's group has correlated progestational activity with ring A conformation in 4-ene-3-one steroids,[103–105] and has published a review on the correlation of conformation with biological activity.[106] They concluded that $1\alpha,2\beta$ sofa or inverted $1\beta,2\alpha$ half-chair conformations were favoured for binding to the progesterone receptor. However, existence of the sofa conformation in solution has been questioned,[4] and the ring-A conformation is likely an equilibrium of two interconverting half-chair conformations. Bohl *et al*[107] have studied the relative stabilities of the ring A conformations in progesterone and its 19-nor and 9-ene

derivatives by molecular mechanics methods. They concluded that the differences in progesterone binding affinities is not due to the ability to form an inverted ring A conformation, but is determined by steric interactions with the C-10 methyl group. Wolff *et al*[108] have discussed changes in the anabolic to androgenic ratio in androgen derivatives based on changes induced in the ring A conformation resulting from unsaturation or cyclopropanation. The relationship of ring A conformation and activity has been reviewed by Vida.[109] Roldan *et al*[110] have postulated a correlation between the curvature of ring A towards the α face of the steroid and the inhibition of thymocyte RNA synthesis by natural adrenal steroids and a series of 1,4-diene analogs. Ring A conformational data for a series of 6-substituted 4-ene-3-one androstanes have been used to probe the nature of the 5α-reductase, androgen receptor and progesterone receptor active sites. Synthesis of a selective 5α-reductase inhibitor with little androgenic activity (i.e. androgen receptor binding) would be an important advance in the treatment of androgen dependent prostate cancer.

Considerable interest has also been shown in the relationship between C-17 sidechain conformation and activity. For example, in the 22-hydroxy and 22-methoxy derivatives of 1α,25-dihydroxyvitamin D3, the 22(S)-isomers were at least 30 times more effective than the corresponding 22(S)-isomers in receptor binding studies.[111] These differences were attributed to a "zig-zag" sidechain conformation which is energetically favourable for the 22(S)-isomers but is unfavourable for the 22(R)-isomers. Likewise, the conformation of the C-17 sidechain is thought to be important for activity in cardiac glycosides, and a good correlation is found between the location of the C-23 carbonyl and enzyme affinity.[112] The preferred conformation is thought to have the C-23 carbonyl between C-13 and H-17.[112–114] ¶

NMR has become a preferred method for these studies because of its unique ability to provide reliable conformational data on steroids in solution. Crystal packing forces

¶A more detailed discussion of C-17 sidechain conformation and activity in cardiac glycosides is given in Section 1.3.4.

make x-ray crystallographic studies of steroid conformation less reliable than NMR methods. While molecular mechanics and molecular orbital methods can provide insight on possible conformations, and on the forces leading to specific conformations, they are not a substitute for experimental data.

It must be noted, however, that the conformation observed in solution is not necessarily the same as that of the steroid bound to a receptor. Any energy required to force the steroid into the conformation required for binding must therefore be factored into energetics of the steroid-receptor equilibrium. Since most steroids are relatively hydrophobic and are generally transported by serum proteins, it is reasonable to study their conformations in organic solvents.

1.3 Structure-Activity Relationships in Cardiac Glycosides

1.3.1 The Digitalis Glycosides

The application of purple foxglove (*Digitalis purpurea*) extracts to the treatment of "dropsy" (myocardial insufficiency) was first described by the English physician William Withering in 1785.[115] It is now known that this plant contains several compounds of a class of steroids known as cardiac glycosides. These compounds increase the force of contraction of the heart muscle while at the same time decreasing beat frequency. The net effect is an overall increase in cardiac efficiency.[116,117] Modern therapeutic uses of cardiac glycosides include treatment of congestive heart failure, cardiac arrhythmias and cardiogenic shock. These compounds are, however, extremely toxic and the margin between therapeutic and toxic doses is small. One report estimates that cardiac glycosides are responsible for one-half of all drug-induced deaths in hospitals.[118]

Most of the pharmacological activity of Withering's extracts was due to the cardiac

glycosides gitaloxin and digitoxin (Figure 1.6).[119] Digitoxin was isolated from *Digitalis purpurpea* in 1930, and became the first of the isolated glycosides to be used in practice. The more polar digoxin (Figure 1.6), isolated from *Digitalis lanata*, has become the principal cardiac glycoside in use today primarily because of its more rapid onset and shorter duration of action.[120] In general, the less polar glycosides show good absorption from the gastrointestinal tract but bind strongly to serum proteins (which delays their action), while the more polar glycosides show less protein binding but are not readily absorbed orally.

Related steroids are also found in the sea onion or squill (*Scilla maritima*), *Strophanthus* seeds and the wood of the ouabaia tree (*Acocanthera schimperi*). From the latter two sources the extremely potent and water soluble glycoside ouabain (Figure 1.6) can be extracted. Radioactive (tritium labelled) ouabain is often used in competitive receptor binding studies of cardiac glycosides. Extracts containing ouabain are used as arrow poisons in Africa, testament to their extreme potency.

The steroid glycosides are believed to improve cardiac efficiency through direct action on the enzyme Na^+,K^+-ATPase located in the cardiac muscle membrane. This enzyme is responsible for the transport of sodium ions from the cell interior to the extracellular fluid and potassium ions in the reverse direction. Inhibition probably results from a conformational change in the enzyme caused by the binding of the steroid. Energy for ion transport is derived from the hydrolysis of adenosine triphosphate (ATP) to adenosine diphosphate (ADP). The steroid binds to a receptor site in the extracellular domain of the enzyme and thereby inhibits its action. The resulting increase in intracellular sodium ion concentration leads to increased force of contraction[116] for which the mechanism is explained in detail in the following section. Renal Na^+,K^+-ATPase is also inhibited by the steroid, resulting in decreased reabsorption of sodium ions by the kidney. This explains the natriuretic and diuretic side-effects of cardiac glycoside therapy.

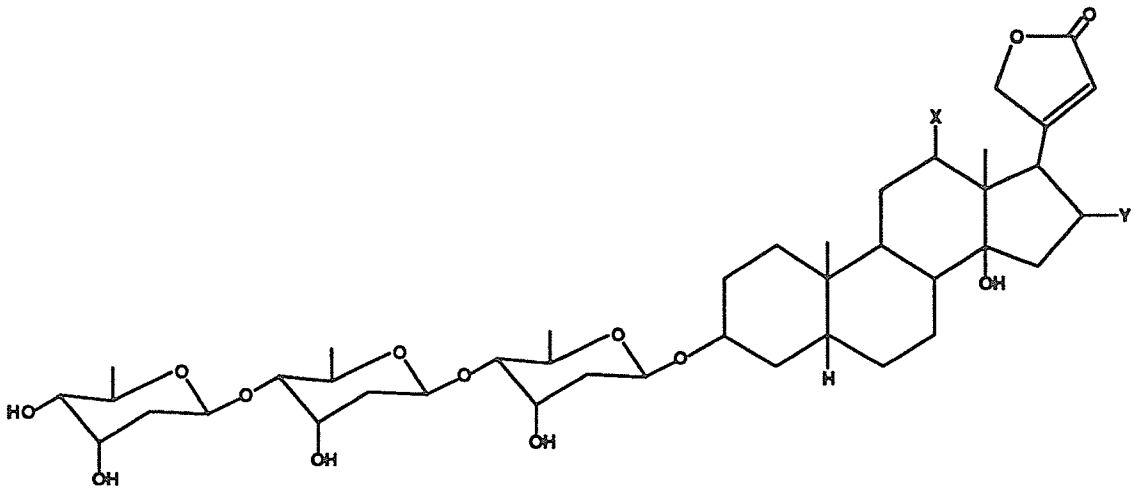

X=H Y=H **digitoxin**

X=H Y=C(O)OH **gitaloxin**

X=OH Y=H **digoxin**

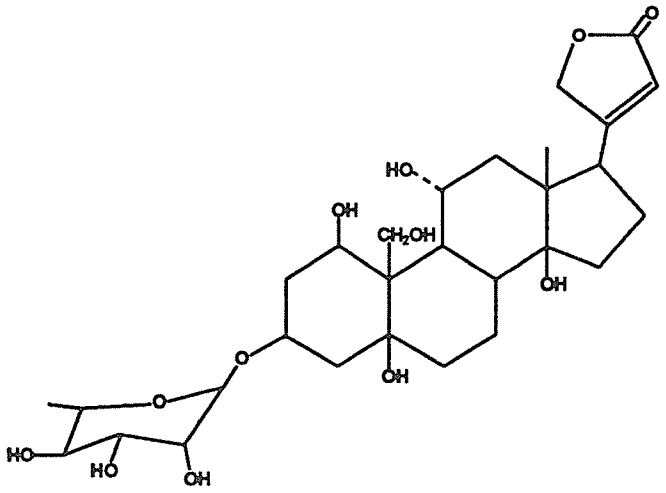

ouabain

Figure 1.6: Structures of some naturally occurring cardiac glycosides.

1.3.2 Na^+,K^+-ATPase

Structural Features

The Na^+,K^+-ATPase enzyme protein complex consists of two and possibly three polypeptide chains, designated α,β and γ.[121] The α subunit consists of approximately 1,000 amino acid residues and has a molecular weight of approximately 112,000. The β subunit is a sialoglycoprotein with approximately 300 amino acid residues and a total molecular weight (including carbohydrate) of 55,000. The α and β subunits are both membrane bound. The γ subunit is a lipoprotein with an approximate molecular weight of 10,000. Whether the γ subunit is an integral part of the enzyme or not is the subject of some controversy. It has been proposed that Na^+,K^+-ATPase exists in two conformational forms, one of which is catalytic while the other serves a regulatory function, and that the two conformers form a dimer which is the single enzyme functional unit.[122] There is, however, no experimental evidence for the way in which the polypeptides that make up the enzyme monomer are located relative to each other.

The α subunit contains both the catalytic site and cardiac glycoside binding site. Isoforms of the α subunit have been known for some time,[123] and it seems clear that the various isoforms are expressed by separate genes.[124] Studies of the human genome have found genes for at least three isoforms of the α subunit,[125] and there may be distinct biochemical roles for each of the isozymes. The ratio of the various isoforms is expressed in a species and tissue specific manner,[126] resulting in the vast differences observed in sensitivity to cardiac glycosides.

Mechanism of Inhibition

It is generally thought that moderate inhibition of Na^+,K^+-ATPase indirectly results in an increase in intracellular Ca^{2+}. Less enzyme is available for restoration of the Na^+,K^+ balance, but the remaining non-inhibited enzyme will act faster because of

the increased intracellular Na^+. The ion balance will thus be restored before the next cardiac cycle, but it will take longer than usual. This is the so-called "Na^+ pump lag" and will result in a *transient* increase in intracellular Na^+. The transient increase in Na^+ results in a transient increase in Ca^{2+} via activation of the Ca^{2+}/Na^+ antiport mechanism. Since Ca^{2+} inhibits the effects of the inhibitory proteins troponin and tropomyocin, the spontaneous reaction between actin and myosin (which results in muscle contraction) will be promoted.

Excessive inhibition reduces Na^+/K^+ transport to such an extent that normal diastolic Na^+ levels cannot be obtained before the next contraction. It is this *sustained* increase in intracellular Na^+ and Ca^{+2} that is believed to be responsible for digitalis toxicity. Since therapeutic and toxic effects arise via the same mechanism, it would seem, according to this mechanism, that the margin between therapeutic and toxic doses should be more or less fixed.

Erdmann *et al* have reported that in the rat (which has a very low sensitivity to cardiac glycosides) ouabain produces a cardiotonic effect at concentrations far below those required for inhibition of Na^+,K^+-ATPase.[127,128‖] These workers went on to state: "one example of proven positive inotropic glycoside effect without concomitant inhibition of Na^+,K^+-ATPase would suffice to question the whole present concept of cardiac glycoside mechanism of action."[128] It is not known whether this low dose response is actually due to some other mechanism or possibly due to a particularly sensitive isoform of the enzyme. Other workers[129,130] have concluded that these results were an artefact of the *in vivo* procedure and that inhibition of Na^+,K^+-ATPase had actually occurred.

‖The statement "below those required for for inhibition..." requires examination, as there should be no threshold effect in enzyme inhibition. Are the authors meaning, perhaps, that the concentrations were below those required for *significant* inhibition?

1.3.3 The Separation of Therapeutic and Toxic effects

The major toxic effect of cardiac glycosides is arrhythmia, with less serious clinical manifestations of digitalis toxicity including nausea, fatigue, vomiting, diarrhoea and a variety of CNS effects including visual disturbances and vertigo. It is generally believed that the toxic and therapeutic effects are inseparable in that they both result from inhibition of several isozymes in various parts of the body.[121] However, this belief is now being challenged in that the correlation between toxic and cardiotonic effects in some cardiac glycosides is poor and that some Na^+,K^+-ATPase inhibiting (and toxic) compounds are not cardiotonic.[131–134] This leads to speculation that different mechanisms might be involved. That some steroids bind to the cardiac glycoside receptor site of Na^+,K^+-ATPase and yet show no cardiotonic effects suggests that the mechanism of action of these compounds is not identical with interaction with the enzyme.[135] Although there appears to be no doubt that a receptor for cardiac glycosides is located on the extracellular domain of the enzyme, it is not yet certain whether this receptor is responsible for the cardiotonic effects of cardiac glycosides and whether it is also responsible for toxicity.

A number of possible mechanisms exist which could provide a basis for separating inotropic and toxic effects.

1. The two effects may be associated with different subfractions or isoforms of Na^+,K^+-ATPase. Ouabain is known to vary in its affinity for different isoforms of the α subunit of the enzyme, and it is reasonable to postulate that different receptors would then vary in their sensitivity to different digitalis analogues. It may also be possisble that non cardiac toxic effects may be associated with differences in sensitivity to cardiac glycosides by other tissue forms of Na^+,K^+-ATPase.

2. Na^+,K^+-ATPase is known to exist in at least two conformational forms – the catalytic or E_1 form and the regulatory or E2 form. Therapeutic effect may be

associated with a particular conformation of the enzyme and the toxic effects with another.[136] Different digitalis analogues may differ in their affinity to the two conformers.

3. Therapeutic effects may be caused by inhibition of Ca^{2+}-ATPase rather than Na^+,K^+-ATPase,[137] in which case the two enzymes could easily differ in their sensitivity to cardiac glycosides.

4. Inotropic or toxic effects may be the result of effects of the autonomic nervous system rather than by effects on the cardiac muscle. Na^+,K^+-ATPase is found in all eukaryotic cells and it would not not be surprising if cardiac glycosides had profound effects on tissues other than heart muscle. The exceptional sensitivity of myocardial Na^+,K^+-ATPase to cardiac glycosides seems to be due not to increased affinity of this isozyme to the drug but rather due to the serious consequences of the inhibition. Gilles and Quest[138,139] have suggested that a large component of the therapeutic effects of digitalis arise from effects on the autonomic nervous system while many of the toxic effects result from central nervous system effects. According to these workers, the beneficial effects of cardiac glycoside therapy on patients with congestive heart failure are due in large part to reflexogenic effects.

It seems clear, therefore, that there is sufficient evidence to demonstrate a separation of therapeutic and toxic effects and that there are a number of probable mechanisms by which this separation might occur. A systematic evaluation of structure and activity of compounds structurally similar to the cardiac glycosides may prove very useful in the search for safer digoxin replacements.

Steroid-Enzyme Interaction

In the generally accepted model of cardiac glycoside interaction with the receptor site of Na^+,K^+-ATPase there are four distinct areas of steroid-enzyme interaction.[121]

1. Hydrogen bonding to the carbonyl of the C-17 sidechain α,β-unsaturated lactone.[140–142] This interaction is believed to be responsible for *ca.* 20 kJ/mol of the steroid-receptor binding energy.

2. Hydrophobic interactions between the α face of the steroid framework and the receptor.

3. Hydrogen bonding to the 3′ or 4′ hydroxyl of the first C-3 sugar moiety. It is of interest that glycosides with a single 3β-O-digitoxosyl substituent show stronger receptor binding than those with the 3β-O-tridigitoxosyl chain of digitoxin and digoxin. This interaction appears to be highly specific in that gomphoside, with a rigid 3,4 ring-fused sugar, shows potent cardiotonic activity when the 3′-hydroxyl group is axial but much weaker activity when this hydroxyl is oxidized to the ketone or converted to the 3′-equatorial hydroxyl. In one example, a monosaccharide was found to have 500 times the activity of the corresponding aglycone.[143]

4. Binding to the β face of the steroid framework through hydrophobic interactions or possibly hydrogen bonds in glycosides such as ouabain which have extensive β-face hydroxylation.

The stereochemistry at C-5 does not seem to be critical for activity. Canarigenin (Δ^5) and uzarigenin (5α) have receptor binding energies only slightly lower than the corresponding 5β-aglycone digitoxigenin.

In contrast to the C-5 stereochemistry, having a *cis* C/D ring junction (14β stereochemistry) seems essential to cardiotonic activity. In fact, having a *trans* ring junction (14α stereochemistry) tends to promote cardiodepression.[144] Whereas 14α stereochemistry (such as found in the androgens, progestins, estrogens and the corticosteroids) yields a relatively flat steroid structure, the 14β stereochemistry of the cardiac glycosides results in a markedly bent structure. Presumably, the displacement of the C-17 sidechain caused by this bending could result in this difference in activity.

The 14β-hydroxyl is also not essential to activity, although its removal results in a significant decrease in receptor binding.[145]

1.3.4 Structure-Activity Relationships of the C-17 Sidechain

The older model states that the C-17 sidechain is the first point of attachment of the steroid to the enzyme and the single most important functional group in the molecule. Reduction of the 20,22 double bond or α stereochemistry at C-17 results in an almost total lack of activity.[146]

Although it was once thought that the C-17 β-unsaturated lactone was essential, it is now know that this is not necessarily true. Steroids with a wide variety of both cyclic and open-chain C-17 β-substituents have been found to bind to Na^+,K^+-ATPase and to possess cardiotonic activity.[121] Many of the structure-activity relationships developed for the C-17 sidechain were formulated by correlating the activity of these molecules with the structure of the sidechain, often with assumptions being made about the conformation about the C-17–C-20 bond. It was inferred from these studies that the location of the C-23 ketone was critical for activity and that displacement of the carbonyl of 2.2 Å from its "ideal" location, as determined from molecular mechanics calculations, resulted in a ten-fold loss of potency.[147,148,112,113] In fact, a plot of Na^+,K^+-ATPase binding ability (log I_{50}) as a function of displacement from the carbonyl position in digitoxigenin results in a reasonable straight line ($r^2 = 0.98$).[112] The natural conclusion was that binding occurs through a hydrogen bond to the lactone carbonyl. Repke's group has estimated that the binding energy of the C-17 sidechain is about equivalent to one hydrogen bond (*ca.* 20 kJ/mol).[121] Ring D conformation is also thought to be important in that it relates directly to the side-chain location.[149]

The preferred conformation for the lactone sidechain was thought to be one in which C-23 carbonyl lay between H-17 and C-13.[112–114] This conformation was reportedly confirmed by an NMR study.[150] Thomas *et al*[151] have proposed that there

are two binding sites for the lactone ring.

Cyclic C-17 Substituents

A six-member pentadienolide ring, as is found in the bufadieneolide (toad toxins) are more potent than the digitalis type glycosides at inhibition of Na^+,K^+-ATPase,[152,153] suggesting that this might be a preferred structure.

Open-chain C-17 Substituents

Studies in which the lactone ring was replaced with a sterically and electronically similar open-chain equivalent were first performed by Thomas's group,[154–156] who investigated a series of $\alpha\beta$-unsaturated analogues of digitoxin. Activity was assessed by measuring both enzyme inhibition and cardiotonic activity. They concluded that a co-planar arrangement of C=C double bond and a heteroatom were required for activity. They also concluded that attachment occurred *via* hydrogen bonding to the heteroatom and electrostatic attraction to the π bond. A partial positive charge on C-20 was considered an important feature.[151,152]

1.3.5 Cardiotonic 5β,14β-pregnanes

LaBella's group has reported that the progesterone derivative chlormadinone acetate can inhibit Na^+,K^+-ATPase.[157,158] This suggests the possibility of an endogenous progesterone-like steroidal hormone acting on the digitalis receptor of heart muscle. However, this compound has cardiodepressive rather than cardiotonic activity. Restoration of the *cis* C/D ring junction and the 14β-hydoxyl group results in pregesterone derivatives with both Na^+,K^+-ATPase inhibitory activity and cardiotonic activity,[159] although it is only 1/500th as potent as ouabain. Further work has yielded pregnanes[160–163] and 21-norpregnanes[164] with receptor affinities comparable to the naturally occurring cardiac glycosides. It was proposed that the differences in response observed with these compounds represented a balance between cardiotonic

effects due to Na^+,K^+-ATPase inhibition and cardiodepressive effects linked to membrane stabilization.[159,165]

The relationships between the C-20 substituent, receptor binding and cardiotonic activity are, however, still quite unclear. For example, 20-nitro-14-hydroxy-3β-(α-L-rhamnopyranosyloxy)-21-nor-5β,14β-pregnane binds to the digitalis receptor of heart muscle with an affinity (IC_{50}=12nM/l) close to that of digitoxigenin (IC_{50}=8nM/l).[164] However, preliminary studies indicate that this compound does not produce a strong positive inotropic effect in dogs. It appears that strong Na^+,K^+-ATPase binding may be a necessary but not sufficient requirement for cardiotonic activity.

It has also been found that, in contrast to the digitalis glycosides, these pregnanes promote sodium and water excretion by the kidneys but have little effect on potassium excretion.[166,167] This potassium sparing diuresis may have practical clinical applications. The overall therapeutic indices of some of these compounds are close or superior to digitoxin.[168]

During the synthesis and pharmacological studies of a series of these cardiotonic 5β,14β-pregnanes, **1** - **10** (Figure 1.7), pregnenes **11** - **16** (Figure 1.8) and norpregnanes **17** and **18** (Figure 1.9) it proved necessary to determine the C-20 stereochemistry.[161] The synthetic procedures (Figure 1.10) resulted in mixtures of the C-20 epimers or compounds of unknown C-20 stereochemistry, necessitating separation and determination of the C-20 configuration. Direct correlation of the NMR data with configuration was not adequate because of differences in the conformation of the side-chain, requiring knowledge of both the C-20 configuration and the side chain conformation.

A knowledge of the side-chain conformation is also essential in understanding the structure-activity relationships of these molecules.

The series was continued with compounds **19** - **25** (Figure 1.11). In **19** and **20** it was necessary to determine the C-17 stereochemistry and compound identity. In **21** - **23** it was necessary to determine the C-20 stereochemistry and the conformation of

the side-chain, while in **24** and **25** it was necessary to determine the configuration of the double bond and the side-chain conformation.

A number of NMR methods have been proposed for determining the C-20 stereochemistry and the conformation about the C-17–C-20 bond in 20-substituted pregnanes and related compounds.[169–175] Most of these methods, however, have been applied only to the more common 14α hormonal steroids. As early as 1963 chemical shift data for a series of epimeric 20-hydroxy- and 20-acetoxy-steroids were reported.[169] The epimeric Δ^{16}-20-hydroxysteroids and their acetylated derivatives could be differentiated by the relative ^{1}H chemical shifts of the C-13 methyl groups. The corresponding saturated compounds on the other hand showed no such consistent behaviour. In 5β,14β-20(R,S)-hydroxypregnanes, C-16, C-18 and C-20 are considerably deshielded in the 20(R)-alcohol compared with the 20(S)-alcohol.[170] These shifts were postulated to be the result of greater shielding of the ring D carbons by the C-20 methyl in the S-epimer compared with the R, although no conformational data were given. In a series of 5α,14α-20(R,S)-aminopregnanes no such consistent trend in the carbon shifts could be observed.[171] Pyridine induced shifts of the C-18 protons are generally greater in 20(R)-hydroxypregnanes than in the corresponding 20(S)-compounds owing to hydrogen bonding of the pyridine to the C-20 hydroxyl, and the different relationship of the magnetically anisotropic pyridine ring to these protons in the two epimers.[172] Similar pyridine induced shifts have been observed in 20(R)- and 20(S)-hydroxy-23-norcholanoic acids.[173] The presence of other groups, such as 14β-hydroxy, capable of hydrogen bonding with pyridine and which are in the vicinity of ring D, may lead to a misinterpretation of the induced shifts.

Because of the rotational freedom about the C-17–C-20 bond, it is not possible to solve the conformational and configurational problems independently, nor can any single piece of data adequately answer both questions. All of the previously reported techniques for determining the C-20 stereochemistry can generally only be applied to a narrow range of compounds and make assumptions about the side chain conformation.

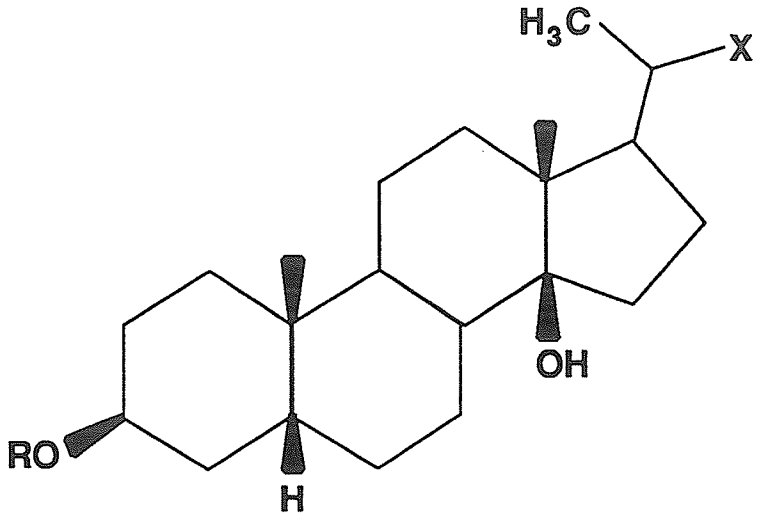

	R	X
1	Ac	(R)-NO_2
2	Ac	(S)-NO_2
3	Ac	(R)-OAc
4	Ac	(S)-OAc
5	Ac	(R)-OH
6	Ac	(S)-OH
7	Ac	(R)-NHAc
8	Ac	(S)-NHAc
9	α-L-rhamnose	(R)-NH_2
10	α-L-rhamnose	(S)-NH_2

Figure 1.7: Pregnanes **1** - **10**.

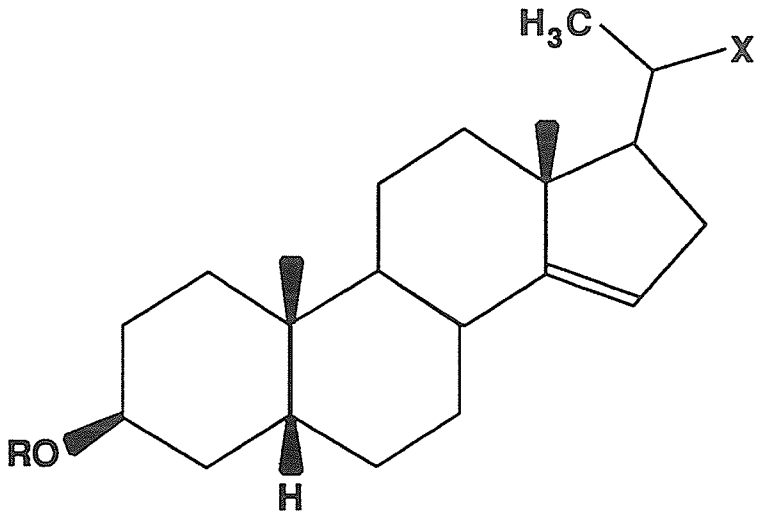

	R	X
11	H	(R)-NHAc
12	H	(S)-NHAc
13	Ac	(R)-OH
14	Ac	(S)-OH
15	$COCF_3$	(R)-$NHCOCF_3$
16	$COCF_3$	(S)-$NHCOCF_3$

Figure 1.8: Pregnenes **11** - **16**.

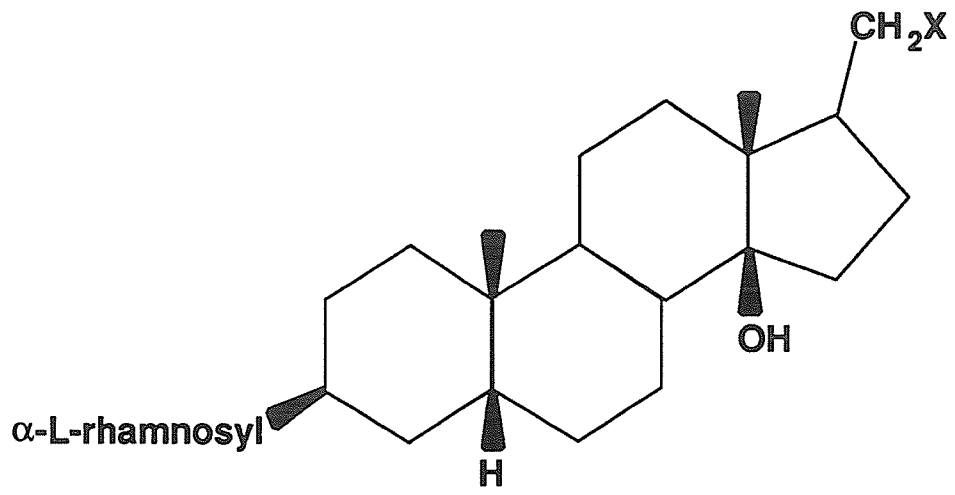

X

17 NO_2

18 OH

Figure 1.9: 21-Norpregnanes **17** and **18**.

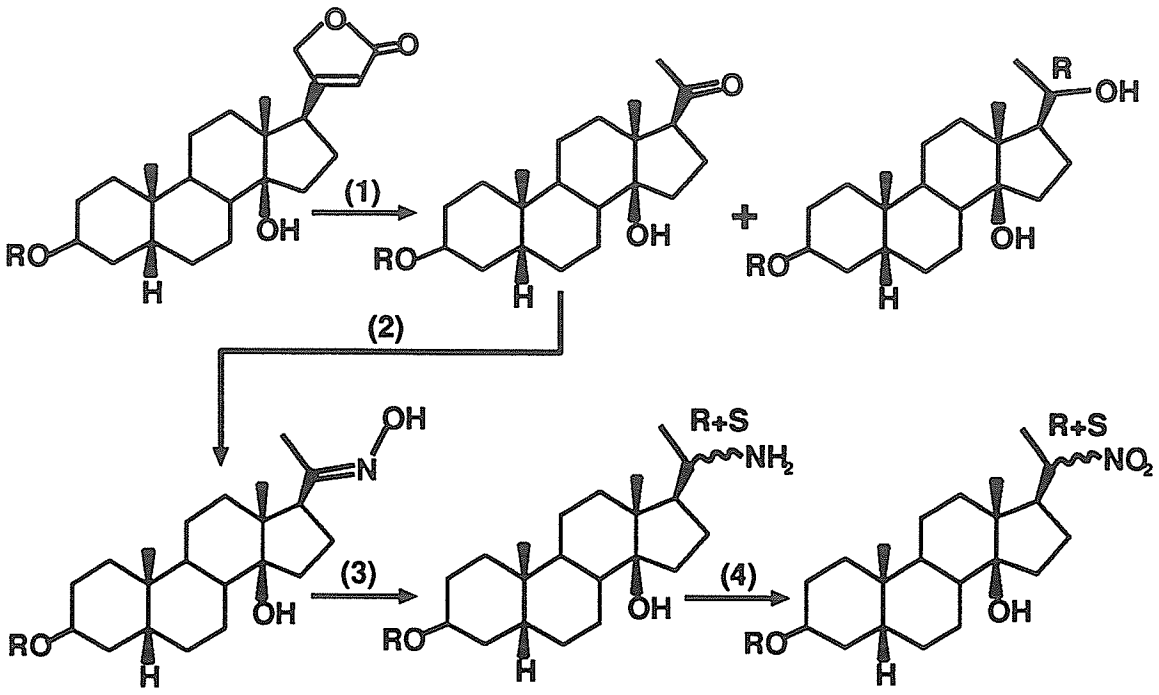

Figure 1.10: Typical reaction scheme used to produce cardiotonic pregnanes.[161]

(1) Treatment of the lactone with ozone and zinc-acetic acid produced the C-20 ketone.

(2) Reaction of the C-20 ketone with $NH_2OH.HCl$-pyridine produced the *trans* oxime.

(3) Reduction of the oxime with sodium in 1-propanol produced an epimeric mixture of the 20-amines.

(4) Oxidation of the amines with dimethyldioxirane produced the 20-nitro epimers.

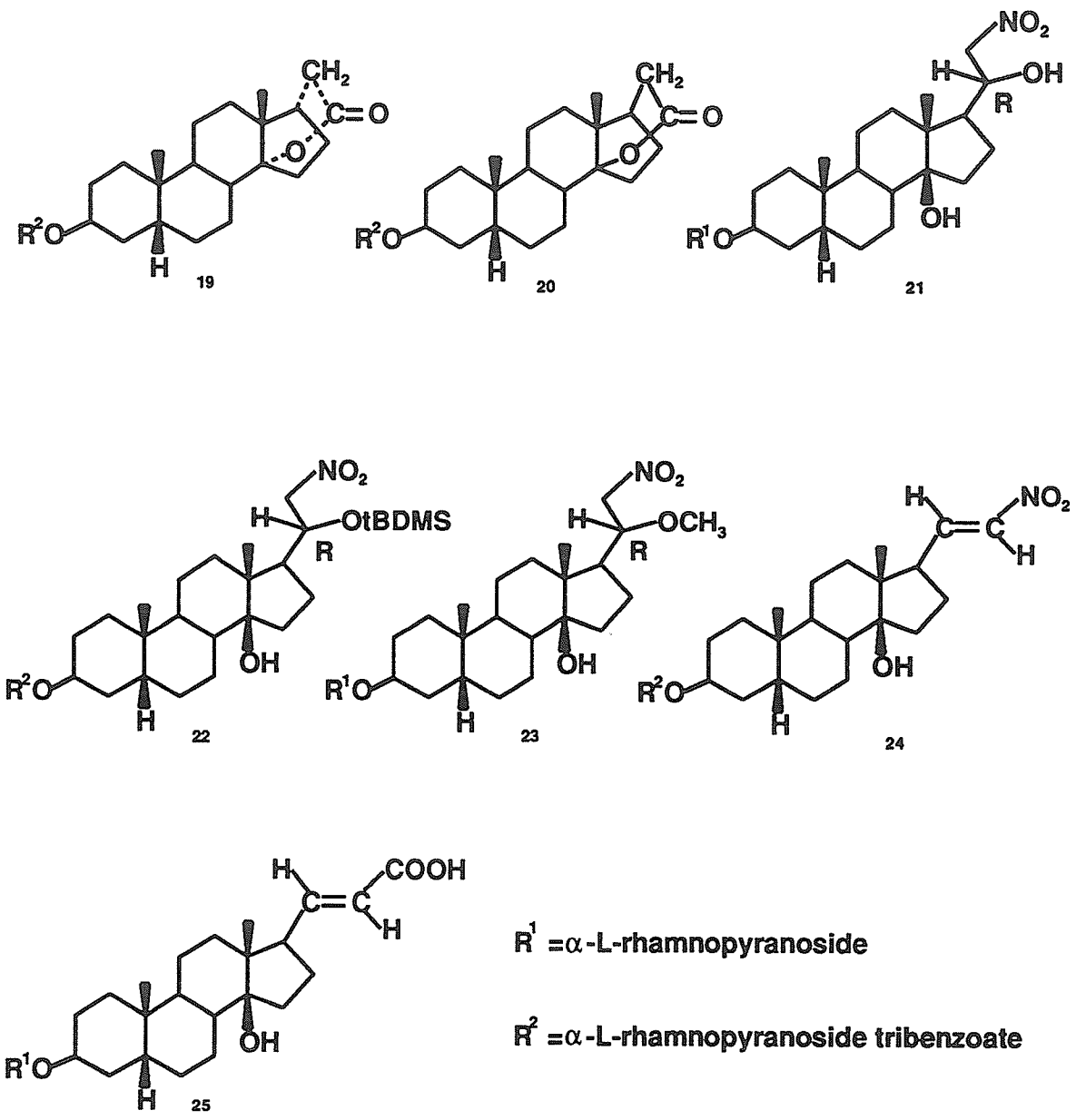

Figure 1.11: Cardiotonic pregnanes **19-25**

Methods that use coupling constants to determine the conformation often neglect the fact that several conformations can have similar couplings, and require that the stereochemistry be independently known.

It was the purpose of this work to develop a method, based on coupling constants and NOE measurements, for the simultaneous determination of the C-20 stereochemistry and C-17 side chain conformation in 20-substituted pregnanes and pregnenes. The method should ideally be independent of the C-20 substitution, C-14 stereochemistry and substitution elsewhere in the molecule.

The three-bond coupling between H-17 and H-20, $^3J(17,20)$, is dependent on the dihedral angle between them according to the Karplus relationship.[27] This relationship has been empirically extended to include the effects of electronegativity and orientation of substituents.[29] Couplings estimated in this manner were considered by the original workers reliable to *ca* 0.5 Hz, but experience has shown that 1 Hz would be a more reasonable estimate. Using such an extended Karplus equation, it is possible to estimate that *gauche* couplings between H-17 and H-20 in C-20 substituted pregnanes should range from 1.6 to 3.3 Hz, while *anti* couplings should range from 10.4 to 11.6 Hz. Deviations from these values can occur when the geometry is forced away from the normal staggered conformation or when there is a significant population of other rotational conformers. In general, the observed coupling will be the weighted average of those in all populated conformers. However, it is likely, because of steric interactions between the C-13 methyl group and the bulky C-20 substituents, that one conformer will predominate. It should also be noted that the two possible conformations where H-17 and H-20 are *gauche* (dihedral angles of +60° and -60°) do not necessarily display equivalent couplings, and that this difference in coupling is predicted to increase with increasing electronegativity of the C-20 substituent. For example, in the 20(R)-hydroxy compound **5**, $^3J(17,20)$ is calculated to be 3.3 Hz when H-20 is *anti* to C-13 and 1.8 Hz when *anti* to C-16. In the corresponding S epimer the situation is reversed and $^3J(17,20)$ is calculated to be 1.7 Hz when *anti*

to C-13 and 3.3 Hz when *anti* to C-16. In situations where there is ambiguity, NOE measurements can be used to locate H-20 uniquely.

The nuclear Overhauser enhancement observed at spin B when spin A is irradiated depends on the degree of dipole-dipole relaxation of B by A compared with all of the other possible relaxation mechanisms of B. If there are other spins which have an NOE from A and in turn are partly responsible for the relaxation of B, a decrease in the observed NOE of B can occur.** Because of these effects, it is rarely possible to measure accurately absolute internuclear distances in small molecules using NOE.[55] Nevertheless, because of the strong (r^{-6}) dependence of NOE on internuclear distance, qualitative or even semi-quantitative comparison of relative distances in similar compounds is a reliable procedure.

NOE measurements between the C-13 and C-20 methyls can then be used to determine the orientation of the C-20 methyl. Other NOE's, such as from the C-20 methyl to H-16β or from H-20 to H-17 can also be used. These are especially useful if only one member of a pair of epimers is available, or if the chemical shift difference between the methyls is too small for reliable NOE measurements.

The prediction of conformation in organic compounds, including steroids, by molecular mechanics and semi-empirical molecular orbital methods has become very fashionable. If the conformation about the C-17–C-20 bond could be reliably predicted by these methods then the task of assigning the C-20 stereochemistry would become easier. Even if the C-20 configuration is known, knowledge of the conformation is of interest in structure activity studies, and many of these studies rely on conformations based on molecular mechanics methods. In this work comparison will be made between the experimentally determined conformations and conformations predicted by molecular mechanics (MM2 and MM3 level) and semi-empirical molecular orbital (AM1 level) calculations in an effort to estimate the reliability of these calculations for predicting the C-17 side-chain conformation.

**See Section 1.1.1.

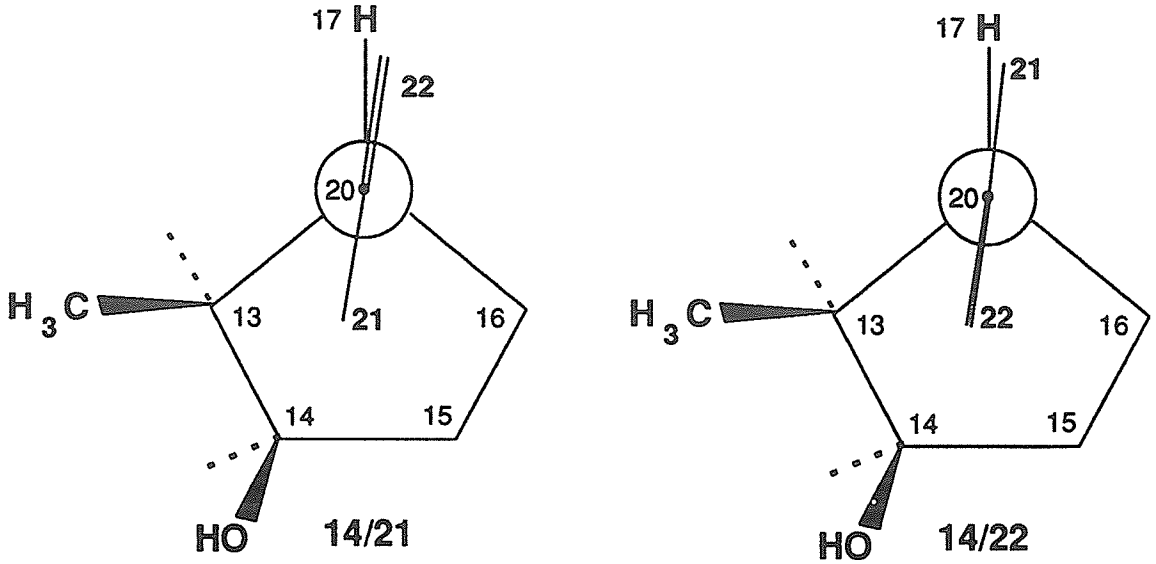

Figure 1.12: The two probable lactone side-chain conformations in digitoxin-like cardiac glycosides.

1.3.6 Re-evaluation of C-17 Side-Chain Conformation in Naturally Occurring Cardiac Glycosides

The conformation of the butenolide lactone ring and its relationship to activity in the cardiac glycosides has been the subject of considerable interest.[150] X-ray crystallographic[176–181] and molecular mechanics[147,149,182,176] investigations suggest two probable conformations, in which the orientation of the lactone ring relative to the steroid differs by approximately 180°. These have been designated as the 14/21 conformation and 14/22 conformations, depending on whether the C-21 or C-22 are situated adjacent to the C-14 hydroxyl (Figure 1.12). Based on these studies, it has been concluded that the 14/21 conformation is a requirement for binding to the digitalis receptor of Na^+,K^+-ATPase but that the energy difference between the two conformers is low in glycosides with unmodified lactone rings.[150]

X-ray studies of digoxigenin[176] and its 12β-acetate[179] have shown a mixture of the 14/21 and 14/22 conformers. Molecular mechanics also predicts that the two conform-

ers have similar energies.[182] An NMR method, based on chemical shifts induced in the C-21 and C-22 protons upon formation of the 14-trichloroacetylcarbamate derivative of digoxigenin-3,12-acetate, however, shows exclusively the 14/21 conformer.[150]

As in digoxigenin (above), the NMR shift method for digoxin showed exclusively the 14/21 conformer.[150] This is to be expected, as differences in substitution in ring-A cannot reasonably be expected to have a significant effect on the C-17 side-chain conformation.

Molecular mechanics methods predict a mixture of the 14/21 and 14/22 conformers for digitoxigenin[147,149,182,176] and its 3β-acetate.[182] The same conformation would presumably also be valid for the glycoside digitoxin, although no calculations were reported. An x-ray structure for digitoxigenin shows a 14/22 conformation for the lactone ring,[177] while a 14/21 conformation was reported for the 3β-acetate.[178] A rapidly equilibrating mixture of the 14/21 and 14/22 conformers was reportedly observed by the NMR shift method for digitoxigenin, while a 14/21 conformation was observed for the 3β-acetate and sugar peracetylated digitoxin.[150] Addition of a 16β-acetoxy group showed a mixture of conformers by the NMR method but x-ray structures showed a 14/22 conformer for the 3β-acetate[181] and a 14/21 conformer for the 3β-tridigitoxyltetraacetate.[150] Interestingly, molecular mechanics also predicts a difference in conformation depending on the 3β-substituent.[182]

Since the above conformational data seem somewhat inconsistent, it was decided to re-evaluate the lactone ring conformation in some naturally occuring cardiac glycosides and their derivatives. Unlike the cardiotonic pregnanes discussed earlier, these compounds lack any stereospecific proton-proton couplings that can be used to determine the C-17–C-20 torsion angle. However, there are two three-bond carbon-proton couplings which are suitable for this task: $^3J(H-17, C-21)$ and $^3J(H-17, C-22)$. Observation of these couplings is simply a matter of recording a fully ^{1}H coupled ^{13}C spectrum of the molecule in question. NOE measurements from the lactone ring protons are an alternative method of obtaining this information for the aglycones.

The high molecular weight of the glycosides results in very small NOEs and rotating frame NOE experiments (Section 1.1.2) are a better choice for these molecules.

1.4 Cyclosteroids and Cyclopropanosteroids

Cyclosteroids and cyclopropano (or methylene) steroids have a number of actual and potential therapeutic applications. Cyproterone acetate (6α-chloro-17α-acetoxy-1α,2α-methylene-4,6-pregnadiene-3,20-dione) is an antiandrogen used in the treatment of androgen dependent diseases such as prostate cancer, hirsuitism and acne.[183] The corresponding 9β,10α-retro steroid has been found to have significant progestational activity but is devoid of any antiandrogenic activity.[184] Introduction of a cyclopropyl group at the 1,2 position also results in a substantial increase in the progestational activity of 17α-acetoxyprogesterone and related compounds.[184,185] 17β-Hydroxy-2α,3α-cyclopropano-5α-androstane has been shown to have a relative enhancement of anabolic activity compared to androgenic activity.[108,109] It has been postulated that the activity of cyproterone and related compounds is associated with the unique electronic properties of the cyclopropyl group combined with a resistance to metabolic degradation.[186,184,187–189]

1.4.1 Cyclosteroids as Potential Mechanism-Based Enzyme Inhibitors

A mechanism-based inhibitor is one in which the normal catalytic action of the enzyme upon the inhibitor produces a reactive intermediate which in turn reacts with the enzyme to disable it. The advantage of such a mechanism-based inhibitor over competitive inhibitors is that it produces a highly selective and irreversible inhibition of the enzyme. A mechanism-based inhibitor is an inherently stable molecule which can mimic the normal substrate for an enzyme. However, when the enzyme reacts with the inhibitor in its normal fashion, the product is a highly reactive electrophilic

species. This electrophile can then react with an active-site nucleophile producing a covalent bond which permanently blocks access to the enzyme's active site. To be effective and specific the inhibitor should resemble the natural substrate as closely as possible, and the inhibiton should occur near the end of the biosynthetic pathway. It should also not serve as a substitute for the normal hormone product of the enzyme.

Inhibition of the enzymes responsible for the synthesis or metabolism of steroid hormones has application in a number of diseases. For example, prostate cancers, at least in the early stages of the disease, are dependent on androgens for growth. Inhibition of androgen synthesis is therefore an important part of the treatment of this disease. Likewise, certain breast cancers are estrogen dependent; and reduction of estrogen levels *via* inhibition of aromatase can lead to partial or even complete regression of tumors in favourable cases.[190] This method of treatment is especially useful in postmenopausal women where the majority of estrogen synthesis takes place in the peripheral adipose tissue rather than in the ovaries.[191] In such women surgical removal of the ovaries is ineffective in lowering estrogen levels. Unfortunately, the commonly used aromatase inhibitor aminogluthetimide suffers from poor selectivity and serious side effects.

Templeton[192] has proposed the use of cyclosteroids and cyclopropanosteroids as mechanism-based inhibitors of enzymes involved in the synthesis and metabolism of steroids *via* the reaction scheme shown in Figure 1.13.

There is experimental evidence to support this hypothesis. Cyclopropanol itself can serve as a mechanism-based inhibitor of methanol oxidase;[193,194] 2β,4β-cyclo-5α-androstane-3β,17β-diol 17-acetate and its 3α-epimer have been synthesized and are irreversible inhibitors of 3β-hydroxysteroid dehydrogenase.[195,196]

Inhibition studies using a variety of substrates are a useful method for studying an enzyme's active site. Petrow *et al*[197] have used a number of 6-substituted steroids including 6-spiro cyclopropyl in an x-ray study of the topography of the steroid 5α reductase active site and the androgen and progesterone receptors. A series of 20-

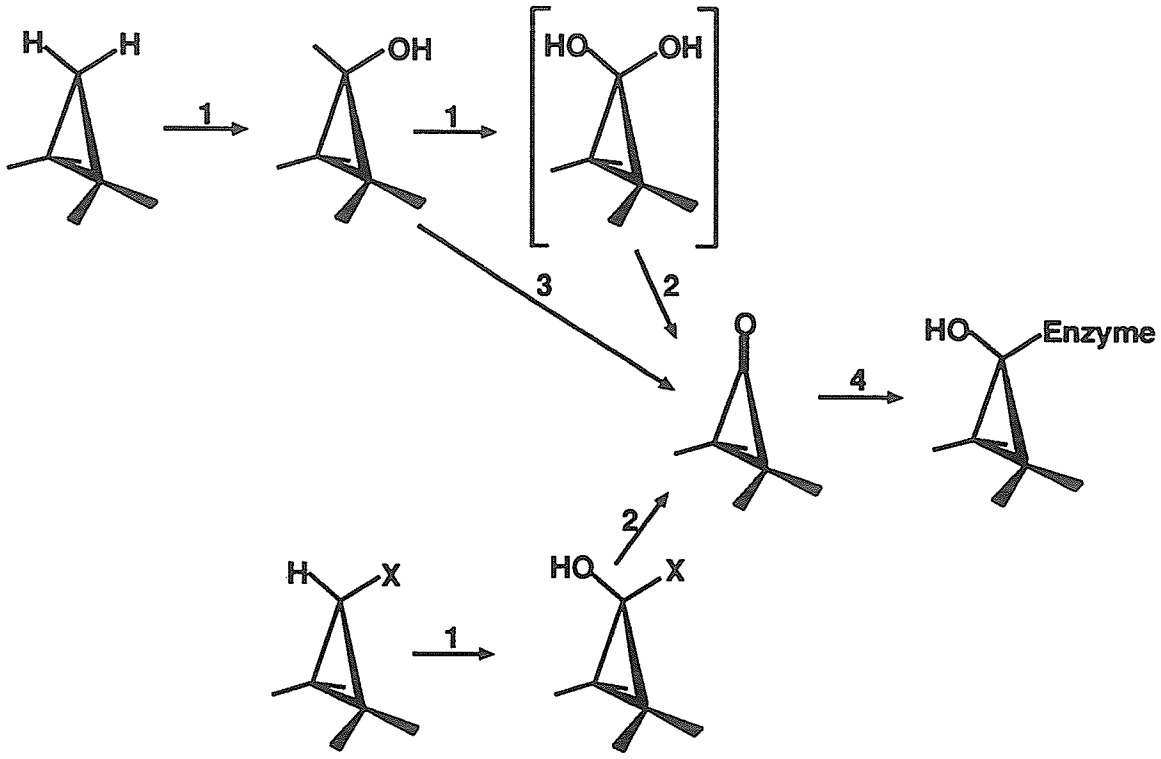

Figure 1.13: Proposed scheme for the use of cyclopropanes as enzyme inhibitors: 1. P-450 type hydroxylation; 2. Spontaneous elimination of H_2O or HX; 3. Hydrogen abstraction; 4. Attack of an enzyme active site nucleophile on the resultant electrophilic cyclopropanone, resulting in a covalent bond between the enzyme and the inhibitor.

hydroxy-17,21-cyclopregnanes have been synthesized as probes into the structure and function of the 17β,20α- and 3α,20β-hydroxysteroid dehydrogenases.[198] These are key enzymes in cortisone and progesterone synthesis and 17β,20α-dehydrogenase has been associated with a number of other biochemical processes.[199,200]

Aromatase (P-450$_{AROM}$) Inhibitors

Aromatase is the enzyme responsible for the synthesis of estrogens from androgens via aromatization of ring A (Figure 1.14.) Androst-4-ene-3,17-dione is converted to estrone and testosterone is converted to estradiol. Aromatase is one of a large family of haemoproteins designated as the cytochrome P-450 isoenzymes. The name is derived from the fact that the reduced form of the enzyme has an absorption maximum at 450 nm when complexed with carbon monoxide. These enzymes are responsible for a number of biochemical conversions of steroids through hydroxylations.

Complexation of the steroid to the enzyme results in the displacement of a water molecule from the active site and a change in the iron spin state from low to high. The resultant change in redox potential enables the enzyme to accept an electron from nicotinamide adenine dinucleotide phosphate (NADPH) *via* an electron transport chain. The reduced iron can bind molecular oxygen and then accept a second electron. The electron activates the oxygen, resulting in a breaking of the oxygen-oxygen bond. One of the oxygen atoms ends up as water while the other combines with a hydrogen abstracted from the substrate to form a hydroxyl radical. This hydroxy radical then combines with the radical formed by abstraction of the hydrogen from the substrate to form the hydroxylated substrate.

The conversion of androgens to estrogens takes place *via* three oxidative steps, each requiring one equivalent of molecular oxygen and NADPH.[201–204] The mechanism of the first two steps is thought to be well understood and involves sequential hydroxylation (with retention of configuration) of the C-10 methyl group to form the *gem*-diol, followed by elimination of water to form the aldehyde (Figure 1.15). An

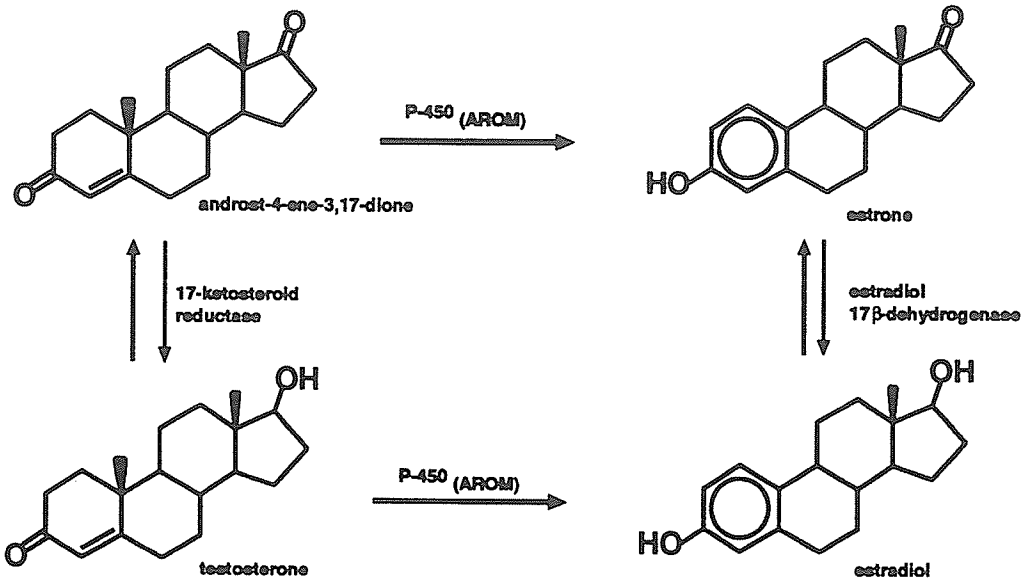

Figure 1.14: Biosynthesis of estrone and estradiol.

alternative mechanism for the second step involves hydrogen abstraction from the C-19 alcohol to form the aldehyde directly.[205] The third step involves loss of the C-10 methyl group as formic acid, and stereospecific loss of the 1β and 2β hydrogens to form the estrogen (Figure 1.16).[206,207] The original C-3 oxygen atom is retained throughout the conversion.[208] The proposed mechanism for the third step involves the nucleophilic attack of a ferric peroxy compound on the C-19 aldehyde to give an intermediate peroxide species.[209]

The proposed mechanism of estrogen synthesis imposes a number of conformational requirements on the substrate:[205]

1. The C-3 carbonyl must be situated such that it can hydrogen bond to a protonated ring nitrogen of the ^{128}His residue of the enzyme. This proton is donated to the substrate as the C-3 phenolic proton in the resulting estrogen. The hydrogen bond to the C-3 carbonyl serves to anchor the substrate in the correct position for oxidation of the C-10 methyl during the first step in the reaction.[205]

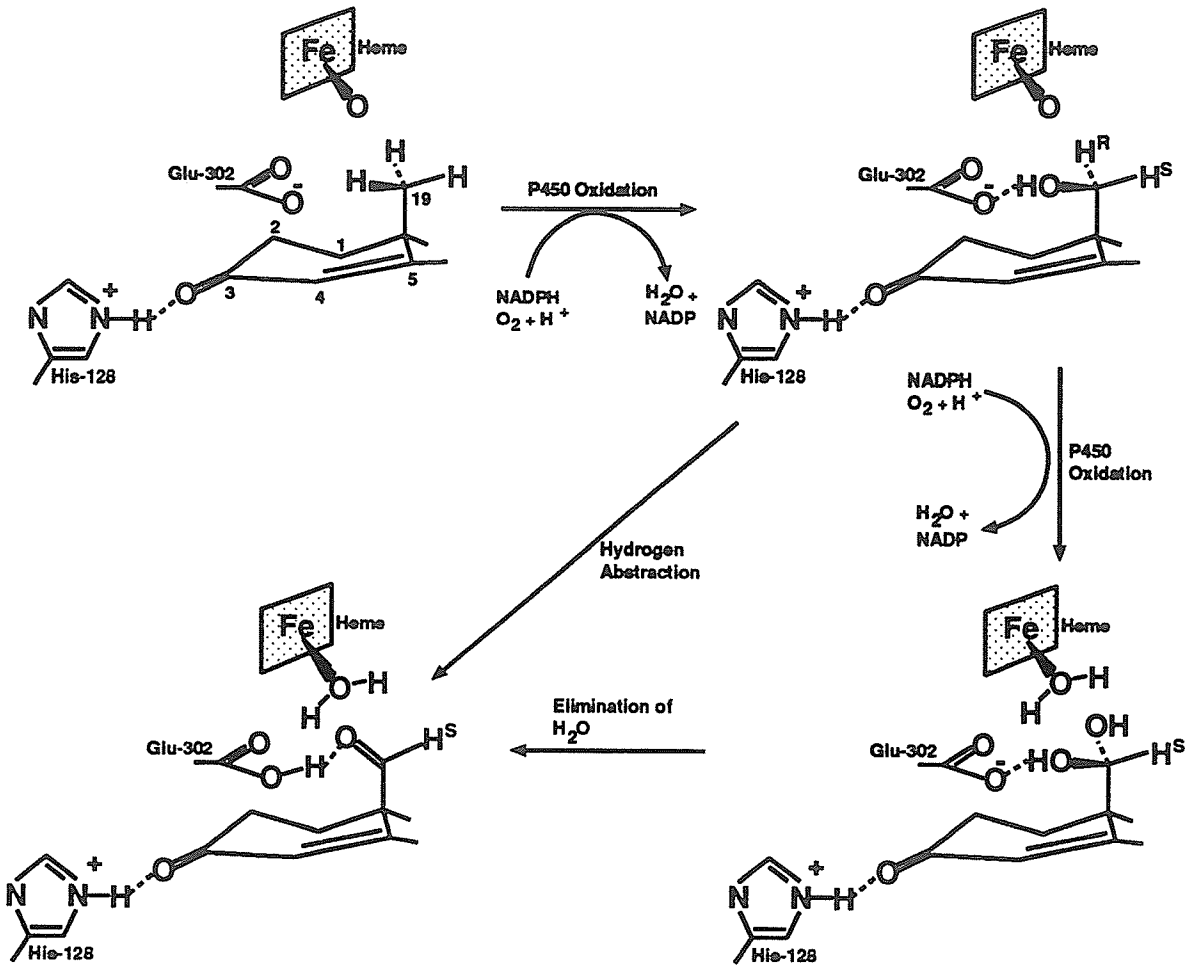

Figure 1.15: Accepted mechanism for the first two steps in estrogen synthesis as detailed by Oh and Robinson.[205]

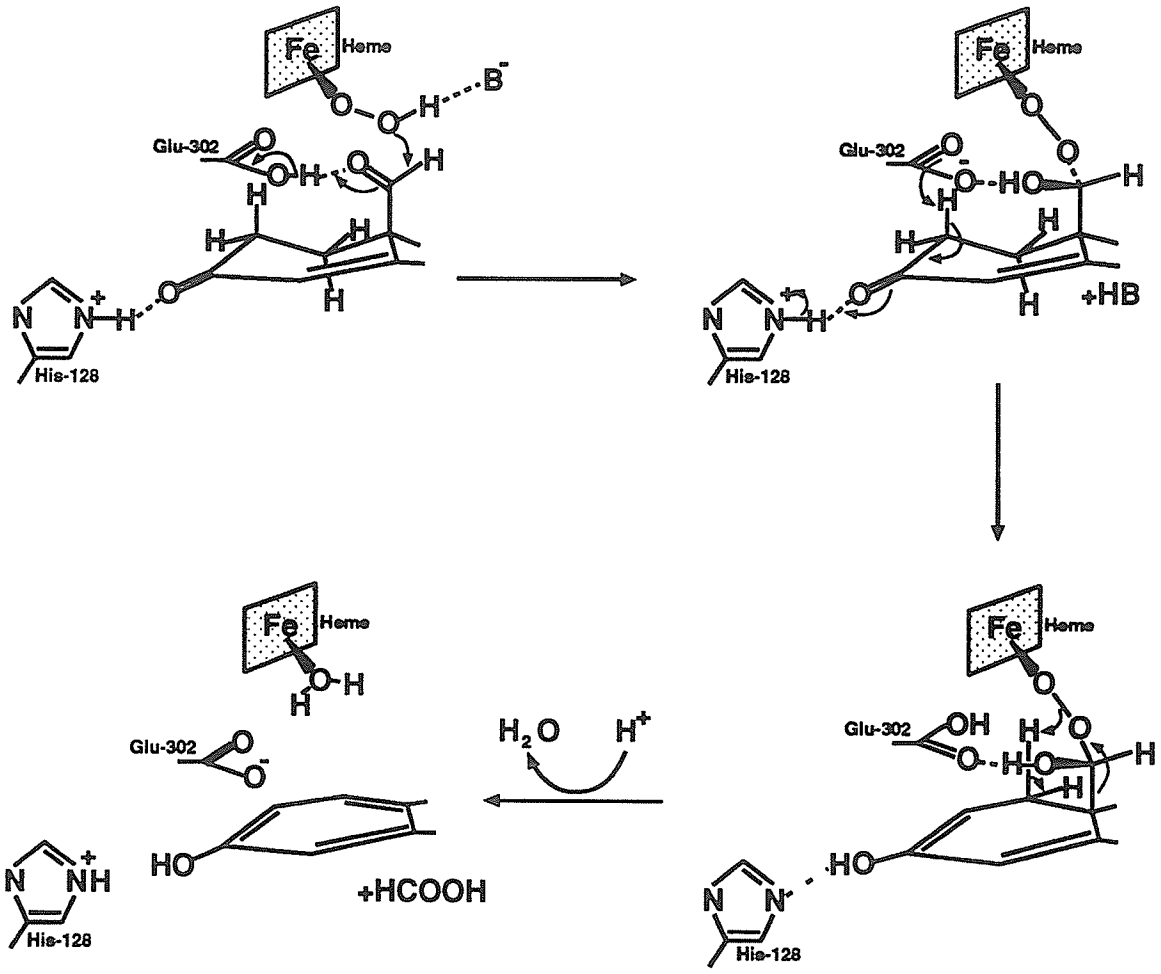

Figure 1.16: Proposed mechanism[205] for the third step in estrogen synthesis.

2. The abstraction of H-2β by the carboxylate of ^{302}Glu requires that the proton be axial.

3. The abstraction of H-1β during the cleavage of the peroxide intermediate requires that H-1β be axial. The normal ring A conformation in the substrate, however, has this proton equatorial, quite out of range for abstraction by the peroxide. The required conformational change can presumably occur during the enolization of the C-3 carbonyl.

The location of the C-3 carbonyl is probably critical to the design of effective aromatase inhibitors, while the situation of the C-1 and C-2 β hydrogens is probably of less importance as our proposed inhibitors block the enzyme before involvement of these protons.

Compounds **26** - **31** (Figure 1.17) were synthesized as part of a study on the effects of a cyclopropyl group on the androgenic to anabolic ratio of androgenic steroids and on the metabolism of a cyclopropyl group.[210,187] These molecules also serve as useful reference compounds for studying the effects of a cyclopropyl group on ring conformation in steroids. The consequences of cyclopropane formation on the NMR spectra of steroids have not been well documented. The relative structural simplicity and the lack of extensive substitution of compounds **26** - **31** makes them ideal candidates for the study of cyclopropane induced shifts and the effects of a cyclopropane ring on both geminal and vicinal proton-proton couplings. Despite the structural simplicity of **26** - **31**, their proton NMR spectra are highly overlapped and tightly coupled. One of the purposes of this work, therefore, was to develop reliable methods for the analysis of the NMR spectra of these and related molecules. Only after obtaining the NMR parameters with a reasonable degree of confidence was it possible to proceed with a conformational analysis.

Compounds **32** - **46** (Figures 1.17 and 1.18) are intermediates in the synthesis of potential mechanism-based inhibitors of P-450$_{AROM}$ as described above. In each case it is proposed that the cyclopropyl group substitute for the C-10 methyl, and

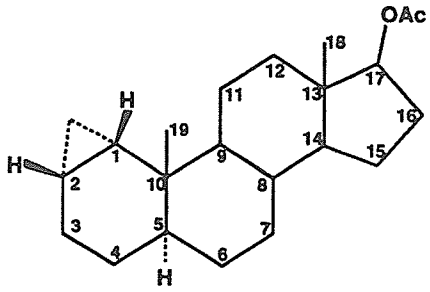

26

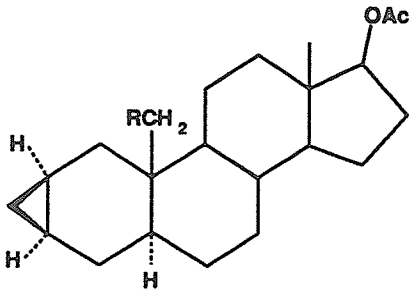

27: R=H
28: R=OH

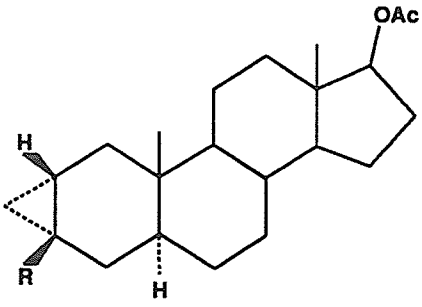

29: R=H
30: R=OCH_3

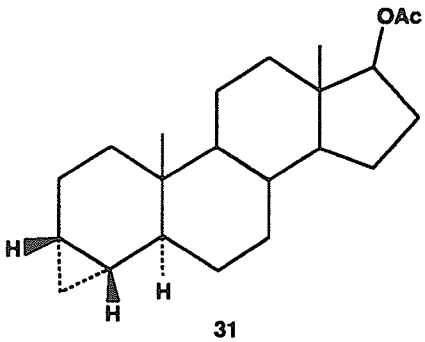

31

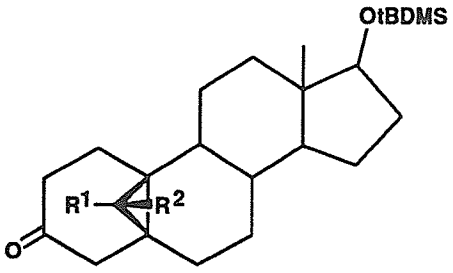

32: R^1 =Cl, R^2 =Cl

33: R^1 =Cl, R^2 =H

34: R^1 =H, R^2 =Cl

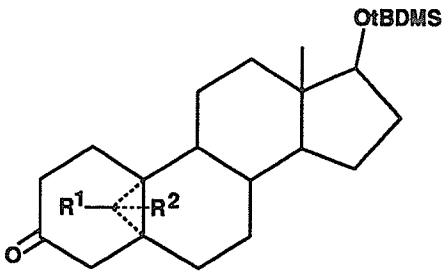

35: R^1 =Cl, R^2 =Cl

36: R^1 =Cl, R^2 =H

37: R^1 =H, R^2 =Cl

Figure 1.17: Cyclosteroids and cyclopropanosteroids **26 - 37**.

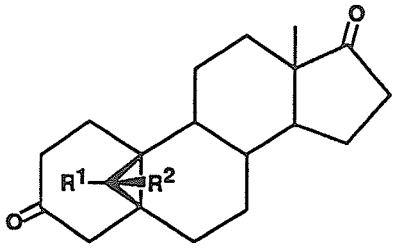

38: R^1 =OAc, R^2 =H

39: R^1 =H, R^2 =OAc

40: R^1 =H, R^2 =OH

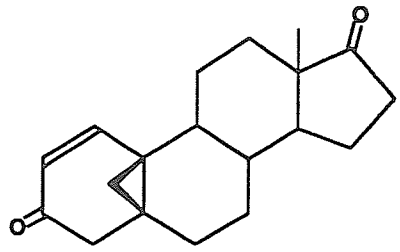

41

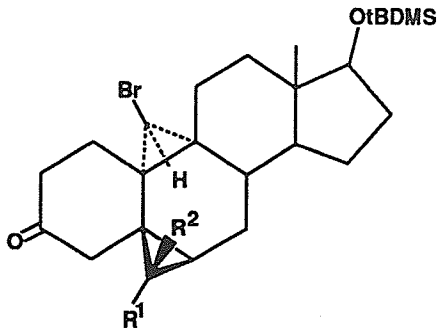

42: R^1=Br, R^2 =Br

43: R^1=H, R^2=Br

44: R^1=Br, R^2 =H

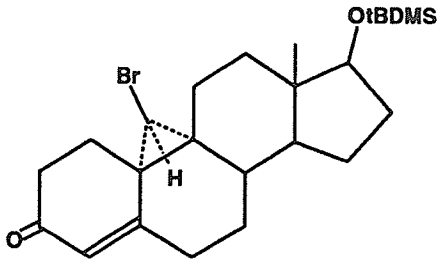

45

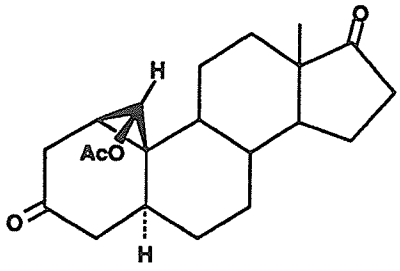

46

Figure 1.18: Cyclosteroids and cyclopropanosteroids **38 - 46.**

that oxidation of the cyclopropane or substituted cyclopropane will be followed by elimination to form the cyclopropanone (Figure 1.13). Nucleophilic attack by the enzyme on the resultant electrophilic carbonyl results in a covalent bond, thus disabling the enzyme. As an unsubstituted cyclopropane ring has proven to be relatively resistant to enzymatic hydroxylation,[187] substitution with an electronegative substituent (e.g. OH, Cl, OAc, etc.) may be necessary. In such cases, the stereochemistry at the cyclopropyl carbon substituting for the methyl becomes an important concern as rotation about the C-10–C-19 bond is no longer possible. Any observed differences in inhibitory effectiveness between the S and R substituted compounds would also give important details about the nature of the enzyme's active site. In this work, modern NMR techniques and the data obtained for **26 - 31** were applied to a number of structural and stereochemical problems associated with the synthesis of these compounds. Analyses of the coupling constants and nuclear Overhauser effects were then used to obtain reliable ring A conformational data which hopefully can be used in the development of structure-activity relationships for the molecules.

Chapter 2

Experimental

2.1 Samples

2.1.1 Cardiotonic Pregnanes

Details of the synthesis of **1-16**,[161] **17**, **18**,[164] and **19-25**[198] have been described in the literature references indicated. All syntheses were performed by Yangzhi Ling and Talal Zeglam in the Faculty of Pharmacy at the University of Manitoba.

NMR spectra of the 3β-acetates **1-8**, **13**, **14**, the trifluoro acetates **15**, **16**, the 21-norpregnanes **17**, **18** and α-L-rhamnopyranoside tribenzoates **19**, **20**, **22**, **23** were recorded as 50 to 100 mM solutions in $CDCl_3$. The 3β-glycosides **9**, **10**, **21**, **24**, **25** were recorded as 20 to 50 mM solutions in CD_3OD. The 3β-alcohols **11**, **12** were recorded as 100 mM solutions in a 1:1 mixture of $CDCl_3$ and CD_3OD. All samples were degassed by passing nitrogen through the solution.

2.1.2 Cyclosteroids and Cyclopropanosteroids

Compounds **26**, **27**, **28**, and **31** were prepared using standard methods[211] and compound **46** by an analogous procedure to that described by Templeton *et al.*[212] The syntheses of **29**,[108] **30**,[210] **32-37**,[213] **38-40**,[212] **41**[214] and **42-44**[213] have been previ-

ously described in the indicated references. Syntheses were performed by Yangzhi Ling, Weiyang Lin and R. K. Gupta in the Faculty of Pharmacy at the University of Manitoba.

Samples for NMR were *ca.* 50 mM solutions in $CDCl_3$ in 5 mm sample tubes. All samples were degassed by passing nitrogen through the solution.

2.1.3 Naturally Occurring Cardiac Glycosides

Samples of digoxigenin (97% purity), digitoxigenin (98% purity), digitoxigenin-3-acetate (99% purity) , digoxin (> 95% purity) and digitoxin (> 97% purity) were obtained from Sigma or Aldrich and prepared as 50 mM solutions in a 1:1 mixture of $CDCl_3$ and DMSO-d_6.* These samples were de-gassed by a freeze-pump-thaw sequence and stored in flame-sealed NMR tubes.

2.2 Spectroscopic Methods

^{13}C spectra were recorded on a Bruker AM300 spectrometer while two dimensional, NOE difference and 1D TOCSY spectra were recorded on a Bruker AMX500 spectrometer. For samples in $CDCl_3$ and CD_3OD, the solvent peak ($CDCl_3$: δ_C=77.0 ppm, $CHCl_3$: δ_H=7.26 ppm, CD_3OD: δ_C=49.0 ppm, CD_2HOD: δ_H=3.30 ppm) was used as the internal reference for both proton and carbon spectra. TMS was used as the reference for samples in the mixture of $CDCl_3$ and CD_3OD. With the exception of the digoxigenin, digoxin and digitoxin samples, sample temperature was controlled at 300 K for all experiments. The digoxigenin, digitoxigenin, digitoxigenin-3-acetate, digoxin and digitoxin spectra were recorded at 313 K in order to decrease the viscosity of the solvent and thereby improve resolution and shorten rotational correlation times.

*$CDCl_3$/DMSO-d_6 mixtures are commonly used[215,216] for cardiac glycosides and are a compromise between solubility and viscosity.

Carbon spectra were classified as to multiplicity with the DEPT technique.[60]

Homonuclear correlation (COSY) spectra[75] were recorded with an F_2 time domain of 1024 points and an F_1 time domain of 256 or 512 points. Zero filling yielded a 1024(real) by 1024(real) matrix after transformation. A 45° mixing pulse was employed, and spectra were displayed and plotted in the magnitude mode. Phase sensitive COSY spectra frequently result in cancellation of anti-phase multiplets, and are less suitable for the complex multiplets observed in steroid spectra.

Rotating frame NOE (ROESY) spectra[84,85] were recorded with a 300 ms mixing time and a mixing field of 2800 Hz. Homonuclear Hartmann-Hahn effects were avoided by the use of the mixing sequence of Huang and Shaka.[86] The matrix dimensions were identical to those used in the COSY experiment. Spectra were recorded processed in the phase sensitive (TPPI) mode.

Hetereonuclear correlation spectra were recorded with the proton detected single quantum coherence (HSQC) experiment,[92] with an F_2 time domain of 4096 points and an F_1 time domain of 256 points. Zero filling in F_1 and F_2 resulted in a 4096(real) by 512(real) matrix after transformation.

Proton detected multiple bond heteronuclear correlation (HMBC) spectra[93] were recorded with a low-pass J filter to suppress correlations due to the one bond couplings. The matrix dimensions were the same as for the HSQC spectra.

Difference NOE experiments were performed with a spectral width of *ca.* 2500 to 4000 Hz and a real frequency domain data size of 32,768 points, resulting in a digital resolution of 0.08 to 0.12 Hz per point. Frequency list cycling was employed to distribute long-term changes in homogeneity equally among all spectra. Multiplets were irradiated by stepping the decoupler frequency between each line of the multiplet at 200 ms intervals,[217] and each multiplet was irradiated for a total of 5 s. The irradiating field strength (calculated from the 90° pulse length and expressed as $\gamma B_2/2\pi$) was 5-7 Hz for the irradiation of multiplets and *ca.* 2 Hz for the irradiation of methyl singlets. At least 256 transients (32 transients per irradiation point with 16

loops through the frequency list) were acquired for each irradiation point in order to ensure adequate signal-to-noise ratio and cancellation of unenhanced peaks. A control spectrum was subtracted from each spectrum, and NOE values were determined by careful integration of the resulting difference spectrum. Using these techniques, NOE enhancements of less than 1% could be easily observed.

1D TOCSY experiments were performed with the Z-filtered experiment described by Kessler *et al.*[97] Ten random delays in the range of 1 - 16 ms were used in the Z-filter, and a 40 ms 270° Gaussian preparation pulse was employed.[99] Mixing times ranged from 40 ms to 100 ms, depending on the requirements of the analysis.

Spectral analyses were performed with the ASSIGN/NUMMRIT † program package on an IBM RS6000 model 350 computer.[218,219]

Molecular mechanics and semi-empirical molecular orbital calculations were performed with the Spartan program package[220] on a Hewlett-Packard 9000/730 computer. Conformational searches were performed around the C-17-C-20 bond for each of the three staggered conformations of the C-14β-hydroxyl group and likely conformations of the C-20 substituent. Full geometry optimizations were performed for each trial conformation.

†Since renamed Xsim.

Chapter 3

Results

3.1 Cardiotonic Pregnanes

3.1.1 Conformational and Configurational Analysis

The signal from H-20 is either a doublet of quartets or a quartet of doublets depending on the relative size of the couplings respectively to H-17 and the C-20 methyl protons. In compounds **7**, **8**, **11**, **12**, **15** and **16** there is an additional *ca.* 6 Hz coupling to the acetamido proton. In these compounds the multiplet from H-17 is not normally observable in a 1D spectrum owing to overlap with other signals. The ^{1}H coupling constant and NOE data are reported in Table 3.1. Although the reported couplings were determined by first order analysis of the H-20 multiplet, they are the same within experimental error at both 300 MHz and 500 MHz, and none of the multiplets observed for H-20 show any evidence of strong coupling. C-H correlation experiments also confirmed that the chemical shift of H-17 was far enough removed from H-16α and H-16β to allow a first order treatment of the spin system. The closest shift difference was 15 Hz (at 500 MHz) between H-17 and H-16β in **9**. In this case, spin system simulation confirmed that the value of ^3J(17,20) obtained from the H-20 multiplet was reliable.

Table 3.1: Coupling constants and NOE values for **1** to **16** (part 1 of 3)

Compound number	$^3J(17,20)$	nuclear Overhauser enhancements (%)[a] H-20 to C-20 CH_3	H-20 to C-13 CH_3	H-20 to H-17	C-13 CH_3 to C-20 CH_3	C-13 CH_3 to H-20
1	10.5	4.8	3.2	0	0	12.0
2	9.1	5.0	4.9	0	7.2	12.3
3	9.2	4.7	3.1	0	0	12.0
4	1.9	4.9	6.0	4.7	0	12.6
5	4.4	4.6	1.3	3.1	[b]	2.0
6	1.3	5.9	9.2	6.0	[b]	10.8
7	5.4	5.2	1.5	4.0	6.0	4.8
8	2.9	6.0	7.8	3.7	0	6.8
9	4.0	3.3	2.6	1.7	3.0	5.4
10	1.5	3.4	4.2	4.3	0	9.6
11	10.9	5.0	6.2	0	0	13.3
12	10.8	2.6	3.2	0	1.9	10.7
13	12.3	4.0	4.9	0	0	11.7
14	8.7	3.9	4.1	0	2.4	10.8
15	9.0	4.5	5.9	0	0	13.8
16	9.8	3.7	5.0	0	3.0	13.2

Table 3.1 continued... (part 2 of 3)

Compound number	nuclear Overhauser enhancements (%)[a] C-20 CH_3 to H-20	C-13 CH_3	other
1	*b*	*b*	
2	*b*	*b*	
3	7.1	0	*c*
4	5.4	0	*d*
5	5.6	*b*	
6	9.5	*b*	
7	*b*	*b*	*e,f*
8	*b*	*b*	*g,h*
9	*b*	*b*	
10	*b*	*b*	
11	9.2	0	*i*
12	10.8	2.4	*j*
13	13.8	*b*	
14	8.1	*b*	
15	*b*	*b*	*k*
16	*b*	*b*	*l*

Table 3.1 continued... (part 3 of 3)

[a] all NOEs were recorded at 500 MHz with the exception of compounds **7** and **8** which were recorded at 300 MHz.

[b] not observable because of overlap or proximity of peaks.

[c] C-13 methyl to C-20 OAc: 3.6%.

[d] C-13 methyl to C-20 OAc: 1.6%.

[e] C-13 methyl to C-20 NAc: 2.6%.

[f] C-20 NH to C-13 methyl: 2.5%.

[g] C-13 methyl to C-20 NAc: 1.2%.

[h] C-13 NH to C-13 methyl: 2.2%.

[i] C-20 methyl to H-16β: 3.9%.

[j] C-20 methyl to H-16β: 0%.

[k] C-13 methyl to C-20 NH: 0.9%.

[l] C-13 methyl to C-20 NH: 0.2%.

The coupling between the C-20 methyl protons and H-20 was independent of the configuration at C-20 and was characteristic of a rapidly rotating methyl group.

The NOE's reported in Table 3.1 are those observed at 500 MHz, except for **7** and **8** which were obtained at 300 MHz. For compounds **5**, **6**, **11**, **12** and **14**, NOE data were recorded at both 300 MHz and 500 MHz, with the 500 MHz values typically being 15% to 20% lower than the corresponding 300 MHz values and the largest difference being 24%. This decrease in NOE at higher fields is to be expected as one leaves extreme narrowing conditions. Although the NOE values were larger at 300 MHz, the superior stability and sensitivity of the 500 MHz instrument made the 500 MHz data preferable.

In compounds **5**, **6**, **13** and **14** similarity of the C-13 and C-20 methyl shifts resulted in partial saturation of one methyl when the other was saturated, precluding NOE measurements. This problem is most severe when irradiating the C-20 methyl because of the higher power required to irradiate the doublet and the frequency modulation sidebands resulting from decoupler stepping. In compounds **1**, **2**, **7-10**, **15** and **16** overlap of the C-20 methyl with other protons prevented irradiation of the C-20 methyl without causing saturation of other parts of the spectrum. These cases are noted in Table 3.1, and in each case sufficient other data were available to establish unambiguously the configuration and the conformation.

20(R)- and 20(S)-Nitro-5β-pregne-3β,14β-diol 3-acetate (1 and 2)

The coupling between H-17 and H-20 is consistent with a dihedral angle of *ca.* 180° (Figure 1.2) in both **1** and **2**. The lack of any observable NOE between these two protons is further evidence for an *anti* arrangement of H-17 and H-20. In **1**, no NOE is observed between the C-13 methyl group and the C-20 methyl group. In **2**, however, a 7.2% enhancement of the C-20 methyl group is observed. These data establish **1** as the R epimer and **2** as the S epimer, with the dominant conformations shown in Figure 3.1 A and B. In Both **1** and **2** it appears that the possibility of hydrogen

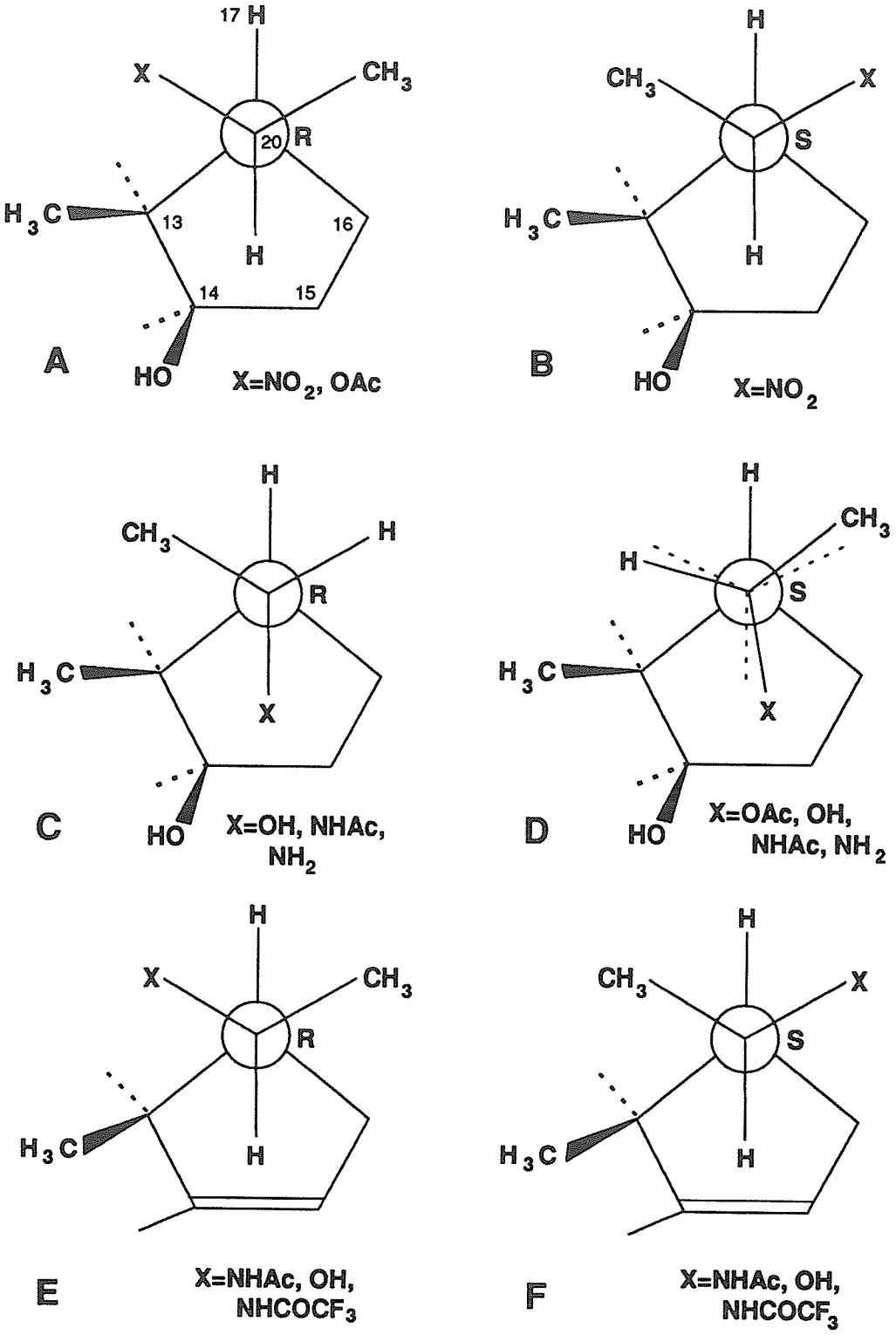

Figure 3.1: Conformations in Pregnanes **1** - **16** viewed as a Newman projection along the C-17–C-20 bond.

bonding between the C-20 substituent and the C-14 hydroxyl is not strong enough to overcome steric factors which favour H-20 over ring D.

5β-Pregnane-3β,14β,20(R)- and 20(S)-triol 3,20-diacetate (3 and 4)

The *anti* relationship of H-17 and H-20 in **3** is demonstrated by a 9.2 Hz coupling and the lack of an observable NOE between these protons. The lack of an NOE between the C-20 and C-13 methyls, and the presence of 3.6% NOE between the C-13 methyl and the C-20 acetoxy group suggest **3** as the R epimer with the conformation as shown in Figure 3.1 A. In **4**, a 1.9 Hz coupling and a 4.7% NOE are observed between H-17 and H-20. These data are consistent with a *gauche* geometry. The NOE's observed between H-20 and the C-13 methyl and between the C-13 methyl and H-20 clearly demonstrate that H-20 is proximate to the C-13 methyl as opposed to the alternate position, *anti* to C-13. A small NOE (1.6%) is observed between the C-13 methyl and the C-20 acetoxy group, consistent with **4** being the S epimer with the conformation shown in Figure 3.1 D.

5β-Pregnane-3β,14β,20(R)- and 20(S)-triol 3-acetate (5 and 6)

The value for $^3J(17,20)$ is 4.4 Hz in **5** and 1.3 Hz in **6**. Both values are consistent with a *gauche* relationship of H-17 and H-20. The predicted couplings, based on the extended Karplus equation,[29] are 1.8 Hz in **5** and 1.7 Hz in **6**. These couplings did not change significantly when the solvent was changed from $CDCl_3$ to a 1:1 mixture of $CDCl_3$ and CD_3OD. The high value in **5** may indicate a significant population of other rotational conformers (eg. Figure 3.1 A), while the low value in **6** suggests a slight twisting away from a perfectly staggered geometry towards one in which the dihedral angle between H-17 and H-20 is closer to 70° - 80°. This appears to be a general trend as the *gauche* coupling in **4**, **6**, **8** and **10** (Figure 3.1 D) is consistently lower than the *gauche* coupling in **5**, **7** and **9** (Figure 3.1 C). Evidence for this twisting is also seen in the NOE data, where a relatively large enhancement is seen between H-20 and the

C-13 methyl. In a perfectly staggered geometry, models indicate that the distance between H-20 and the C-13 methyl is approximately the same in conformers where H-20 is *anti* to H-17 and in conformers where H-20 is *gauche* to H-17 but *anti* to C-16. However, the NOE's in the latter situation are much larger than those observed in the former. Since the NOE observed between H-20 and the C-13 methyl is much larger in **6** than in **5**, it is reasonable to conclude that H-20 in **6** is approximately *anti* to C-16 while in **5** H-20 is *anti* to C-13. The probable conformation of **5** is shown in Figure 3.1 C, while that of **6** is shown in Figure 3.1 D. These results contrast with those obtained for a series of 14α-pregnanes by Lee *et al*,[174] in which H-17 was found to be *anti* to H-20 in the R epimer and to subtend a dihedral angle of 153° with H-20 in the S epimer of 20-hydroxypregn-4-en-3-one. This latter result was based on a 7.5 Hz value for $^3J(17,20)$. Because of the low NMR frequencies available at the time (100 MHz), it is possible that the observed coupling is the result of a virtual coupling effect, and that the true coupling is much larger, suggesting a dihedral angle closer to 180°. It is also possible that there is a significant population of conformers in which H-17 is *gauche* to H-20. Interestingly, $^3J(17,20)$ in 18-oximino-20(S)-hydroxypregn-4-en-3-one was reported[174] to be 3.5 Hz, from which a dihedral angle of 129° (H-17, H-20 approximately *anticlinal*) was calculated. While it is possible that hydrogen bonding between the C-20 hydroxyl group and the oximino nitrogen could force this nearly eclipsed conformation, the reported coupling is also consistent with a *gauche* arrangement of H-17 and H-20. Robinson and Hofer[175] have also predicted an *anti* arrangement of H-17 and H-20 in 20-substituted 14α pregnanes based on models and chemical shift arguments. It is likely that in **5** and **6** hydrogen bonding between the C-20 and 14β hydroxyl groups is responsible for the observed conformations, even though in **5** this results in steric interaction of the C-20 methyl and C-20 hydroxyl with the C-13 methyl.

20(R)- and 20(S)-Acetamido-3β-(α-L-pyranorhamnosyl)oxy-5β-pregnan-14β-ol (7 and 8)

The value of $^3J(17,20)$ is 5.4 Hz in **7** and 2.9 Hz in **8**. These values are both clearly within the range expected for a *gauche* coupling. In **7** a 6% NOE is observed between the C-13 methyl and the C-20 methyl while in **8** no NOE can be observed. In **8**, however, there is a much larger NOE observed between H-20 and the C-13 methyl than in **7**. These data establish **7** as the R epimer with the acetamido group *anti* to H-17 in both compounds (Figure 3.1 C and D). As with **5**, it appears that hydrogen bonding between the C-20 substituent and the C-14 hydroxyl forces the R epimer into a conformation which for steric reasons would not ordinarily be expected.

20(R)- and 20(S)-Amino-3β-(α-L-pyranorhamnosyl)oxy-5β-pregnan-14β-ol (9 and 10)

The value for $^3J(17,20)$ is suggestive of a *gauche* relationship between H-17 and H-20 in both **9** and **10**. The somewhat larger value in **9** is again suggestive of finite populations of other rotational conformers. An NOE is observed between the C-20 methyl and the C-13 methyl in **9** and is absent in **10**. In **10**, a larger NOE is observed from the C-13 methyl to H-20 and from H-20 to the C-13 methyl than in **9**. These data demonstrate the spatial proximity of the C-13 methyl to the C-20 methyl in **9** and to H-20 in **10**, thus establishing the stereochemistry and conformations shown in Figure 3.1, C and D.

20(R)- and 20(S)-Acetamido-5β-pregn-14-en-3β-ol (11 and 12), 5β-Pregn-14-ene-3β,20(R)- and 20(S)-diol 3-acetate (13 and 14), and 20(R)- and 20(S)-Trifluoroacetamido-5β-pregn-14-en-3β-ol 3-trifluoroacetate (15 and 16)

The value for $^3J(17,20)$ clearly indicates that H-17 is *anti* to H-20 in **11** - **16**. Further evidence for this arrangement is seen in the lack of NOE between H-17 and H-20 in

these compounds. These data are consistent with the results reported by Lee *et al*[174] for a series of 20-substituted 14α pregnanes, although the coupling constant values that they report are *ca.* 1 to 2 Hz lower than we observe in the pregn-14-enes. This discrepancy may simply be the result of virtual coupling effects in the earlier work. With the location of H-17 being clearly established, location of the C-20 methyl establishes both the configuration and conformation. In all of the pregn-14-enes **11** to **16** there is a clearly observable NOE between the C-20 and C-13 methyls in the S epimers that is not seen in the R epimers. In **11** there is an NOE between the C-20 methyl and H-16β which is absent in **12**. The conformations of **11-16** are shown in Figure 3.1, E and F. In **11-16** there is no possibility of hydrogen bonding between the C-20 substituent and the C-14 hydroxyl making the conformers with H-20 over ring D preferred for steric reasons.

17β-Nitromethyl-3β-(α-L-pyranorhamnosyl)oxy-5β-androstan-14β-ol (17) and 17β-Hydroxymethyl-3β-(α-L-pyranorhamnosyl)oxy-5β-androstan-14β-ol (18) (21-norpregnanes)

In **17**, one of the C-20 protons has an *anti* coupling of 10.3 Hz to H-17, while the other H-20 proton has a *gauche* coupling of 5.3 Hz. The geminal coupling between the two C-20 protons is -12.5 Hz. A 6.1% NOE of the C-20 proton *gauche* to H-17 and a 1.9% NOE of the C-20 proton *anti* to H-17 are observed when the C-13 methyl is irradiated. The nitro group must therefore be *anti* to C-13. In **16**, both of the protons are *gauche* to H-17 with couplings of 3.3 and 3.4 Hz, the geminal coupling being -10.7 Hz. One of the protons has a 5.1% NOE from the C-13 methyl (*anti* to C-16), while the other has a 1.0% NOE (*anti* to C-13). This places the hydroxyl over ring D *anti* to H-17.

14α-Hydroxy-(tri-O-benzyoyl-α-L-rhamnopyranosyl)oxy-5β,17α-pregnane 21-carboxylic acid 14,21-lactone (19)

In contrast to **20** only relatively small NOEs (*ca.* 2%) were observed from the C-13 methyl to the C-20 protons. However, a substantial NOE was observed from the C-13 methyl group to H-17 (6.0%), with a corresponding NOE observed from H-17 to the C-13 methyl (3.5%). These data clearly establish that the C-17 sidechain has α stereochemistry.

14β-Hydroxy-(tri-O-benzoyl-α-L-rhamnopyranosyl)oxy-5β-pregnane 21-carboxylic acid 14,21-lactone (20)

The stereochemistry at C-17 and C-20 was confirmed by the observation of NOEs from the C-13 methyl to the low field C-20 proton (4.1%) and from the low field C-20 proton to the C-13 methyl group (4.5%). Only a relatively small NOE (<2%) was observed from the C-13 methyl group to H-17, further confirmation of β stereochemistry for the C-17 sidechain.

21-Nitro-3β-(α-L-rhamnopyranosyl)oxy-5β-pregnane-14β,20(R)-diol (21)

The value for $^3J(17,20)$ is very small (*ca.* 1 Hz) indicating a *gauche* arrangement of H-17 and H-20. Irradiation of the C-13 methyl showed NOEs to H-20 (8.8%), H-8 (3.4%) and H-12β (1.9%) and indicates a β stereochemistry for the C-17 sidechain.

20(R)-(*tert*-Butyldimethylsiloxy)-21-nitro-3β-(tri-O-benzoyl-α-L-rhamnopyranosyl)oxy-5β-pregn-14β-ol (22)

A value of 1.5 Hz for $^3J(17,20)$ indicates a *gauche* arrangement of H-20 and H-17. Irradiation of H-20 resulted in a 1.6% NOE of the C-13 methyl group, while irradiation of the C-13 methyl group resulted in a 5.5% NOE of H-20, clearly indicating that H-20 is *anti* to C-16 as opposed to *anti* to C-13. Irradiation of the C-13 methyl also

resulted in a 2.4% NOE of the low field C-20 $SiCH_3$. Irradiation of the low field $SiCH_3$ resulted in a 0.9% NOE of the C-13 methyl. The NOEs observed between the C-13 methyl and the C-20 SiCH−3 indicate that the C-20 $OSiMe_2Bu^t$ group must be *anti* to H-17. With the location of H-20 already established, this is sufficient to determine the C-20 stereochemistry as R. Note that this sample was run in deuterated benzene - in order to separate the sidechain H shifts.

20(R)-Methoxy-21-nitro-3β-(α-L-rhamnopyranosyl)oxy-5β-pregnane-14β-ol (23)

A value of 1.5 Hz was observed for $^3J(17,20)$. Irradiation of the C-13 methyl resulted in NOEs to H-20 (13.5%) and the C-20 methoxyl (3.65%). Irradiation of the C-20 methoxyl resulted in NOEs to H-20 (6.1%) and the C-13 methyl (1.5%). These data establish that H-20 is *anti* to C-16 and that the C-20 methoxyl is *anti* to H-17. The C-20 stereochemistry is thus R. NOE measurements involving the C-21 protons were not possible owing to overlap with the solvent peak.

21-Nitro-3β-(tri-O-benzoyl-a-L-rhamnopyranosyl)oxy-5β-pregn-20,21-en-14β-ol (24)

The value for $^3J(20,21)$ is 13.4 Hz, closer to that expected for *trans* rather than a *cis* arrangement of H-20 and H-21. This was confirmed by the absence of any detectable NOE between the two protons. In a *cis* arrangement of H-20 and H-21, a substantial NOE would be expected as the protons are separated by approximately 2.4 Å, with few other competing relaxation mechanisms.* Irradiation of H-21 did result in a 1.7% NOE to H-17, while irradiation of the C-13 methyl group resulted in a 4.2% NOE to H-20. These data, along with a $^3J(17,20)$ of 11.5 Hz suggest that the C-17 sidechain adopts a conformation in which H-17 is *anti* to H-20.

*See section 4.2.2.

14β-Hydroxy-3β-(a-L-pyranorhamnosyl)oxy-5β-androstan-17β-acrylic acid (25)

The 15.5 Hz value for $^3J(20,21)$ and the lack of any observable NOE between these protons clearly indicates a *trans* arrangement of H-20 and H-21. Irradiation of H-21 resulted in a 3% NOE to H-17 while irradiation of H-17 resulted in a 7.4% NOE to H-21. Irradiation of the C-13 methyl group resulted in a 7.5% NOE to H-20. $^3J(17,20)$ is 10.7 Hz. This coupling and the NOE data suggest that the sidechain adopts a conformation in which H-17 is *anti* to H-20.

3.1.2 C-17 Side-chain Conformation in Naturally Occurring Cardiac Glycosides and their Genins

Although there are no stereospecific proton-proton couplings which can be used to establish the conformation of the cyclic lactone sidechain, three-bond carbon proton couplings follow a similar Karplus-like function with dihedral angle.[37–39] Two such couplings are available in this case: ^3J(H-17–C-21) and ^3J(H-17–C-22). These values are reported in Table 3.2 for digoxigenin, digitoxigenin and its 3-acetate, digoxin and digitoxin. The values were obtained from a direct first order analysis of the fully coupled ^{13}C specta, examples of which are shown in Figures 3.2 and 3.3.

Difference NOE data obtained by irradiation of H-21 and the C-21 protons are presented for the genins in Table 3.2. Difference NOE measurements were not possible for the glycosides because of the overlap of the C-21 proton signals with those of the C-3 sugar groups. Attempts to obtain NOE data for the glycosides from NOESY spectra were unsuccessful, probably because their high molecular weight resulted in vanishingly small NOEs.[†] ROESY spectra did produce useful data, and examples of ROESY spectra for digoxin and digitoxin are shown in Figures 3.4, 3.5 and 3.6. The numbers reported in Table 3.2 are the two-dimensional integrals (volumes) of the

[†]See section 1.1.1.

cross peaks presented as percentages of the corresponding diagonal peak integral.

Digoxigenin

NOEs are observed from H-22 to H-16β[‡] (0.8%), H-17 (2.2%) and the C-13 methyl protons (0.8%). These data suggest that the lactone ring adopts a conformation in which H-22 eclipses H-17 (the so-called 14/21 conformer, as shown in Figure 1.12[150]). However, the C-21 protons also show significant NOE to H-17. A conformation with H-22 eclipsing H-17 places the C-21 protons too far (4.0 Å)[§] from H-17 for the expected NOE, and a conformation with the C-21 protons adjacent to H-17 (the so-called 14/22 conformer[150]) places H-22 too far (3.9 Å) from H-17 for the expected NOE. The most plausible explanation for these inconsistent data is the existence of an equilibrium mixture of the two conformers. Other conformers, such as those where the plane of the lactone ring is perpendicular to the C-17–C-20 bond, are inconsistent with the finding that both H-22 and the C-21 protons show NOEs to the C-13 methyl protons.

Examination of the three-bond couplings between H-17 and the C-21 and C-22 carbons gives further support to a conformational equilibrium. The 14/21 conformation places C-21 *anti* and C-22 *syn* to H-17 with an expected value for ^3J(H-17–C-21) of 8 to 10 Hz and an expected value for ^3J(H-17–C-22) of 4 to 5 Hz.[38] In the alternative 14/22 conformation C-22 is *anti* and C-21 is *syn* to H-17, and the expected couplings would therefore be reversed. *Gauche* couplings lie in the range of 1 to 3 Hz. The observed values for these couplings are ^3J(H-17–C-21)=6.33 Hz and ^{J}(H-17–C-22)=5.43 Hz. These values lie between the expected *syn* and *anti* couplings and are out of the range expected for any conformer placing the coupled nuclei *gauche*. It must be concluded, therefore, that the lactone ring exists as an equilibrium of the 14/21 and 14/22 conformers. These findings contradict an earlier report where

[‡]It appears that the H-16α and H-16β assignments reported by Drakenberg *et al*[216] may be reversed.

[§]The internuclear distances were estimated using the Spartan[220] molecular modelling package.

digoxigenin was observed to exist almost exclusively in the 14/21 conformation.[150] For comparison, the rigid *anti* coupling between H-22 and C-21 is 8.5 Hz while the rigid *gauche* coupling between the C-21 protons and C-22 is 3.0 Hz.

Digitoxigenin and Digitoxigen-3-acetate

The carbon-proton coupling constants for digitoxigenin and its 3-acetate are identical within experimental error to those observed in digoxigenin. The NOE values are also similar and follow an identical pattern to those of digoxigenin. The similarity of the couplings and NOE values leads to the conclusion that these molecules also exist as a mixture of the 14/21 and 14/22 conformers, and that the relative population of the two rotamers is similar in all three molecules. These findings contradict an earlier report[150] where the 3-acetate was observed to exist in the 14/21 conformation while digitoxigenin was observed to exist as a mixture of 14/21 and 14/22 conformers.

Digoxin and Digitoxin

The stereospecific three-bond couplings between H-17 and the C-21 and C-22 carbons are identical within experimental error to those observed in the genins. The ROESY cross-peak volumes, although not directly comparable to the NOE difference values reported for the genins, also follow a similar pattern; i.e. ROESY cross-peaks are observed between H-17 and both H-21 and the C-21 protons and between the C-13 methyl protons and both H21 and the C-21 protons. These data indicate that the lactone side-chain in digoxin and digitoxin exists as a mixture of the 14/21 and 14/22 conformers and that no detectable difference in rotamer populations exists between the genins and the glycosides. Furthermore, since the data for digoxin and digitoxin are essentially identical, it must also be concluded that the presence of the C-12β hydroxyl group has no effect on the C-17 side-chain conformation.

Table 3.2: Coupling constants, NOE values and rotating frame NOE values for some naturally occurring cardiac glycosides and their aglycones.

Parameter		Digoxigenin	Digitoxigenin	Digitoxigenin 3-OAc	Digoxin	Digitoxin
^3J(H-17–C-22)		5.43	5.49	5.40	5.54	5.43
^3J(H-17–C-22)		6.33	6.48	6.47	—[a]	6.44
N(R)OE:[b]						
H-22 to:	H-16β	0.8	1.0	0.8	0.3	0.3
	H-17	2.2	2.5	2.8	1.1	1.5
	C-13 CH_3	0.8	1.0	0.9	0.3	0.3
H-21A to:	H-17	1.3	1.0	0.7	0.8	0.7
	C-13 CH_3	1.9	2.4	1.8	1.0	1.3
	H-21B	18	20	15	—[a]	7.5
H-21B to:	H-16	2.1	3.5	3.1	2.0	—[a]
	H-17	0.8	0.6	0.6	0.5	0.4
	C-13 CH_3	1.2	0.8	0.7	0.9	0.7
	H-21A	20	22	23	—[a]	7.2

[a] Not observable because of overlap with other peaks.

[b]NOEs as % enhancement are presented for the genins. ROESY cross-peak volumes as % of the diagonal peaks are presented for the glycosides.

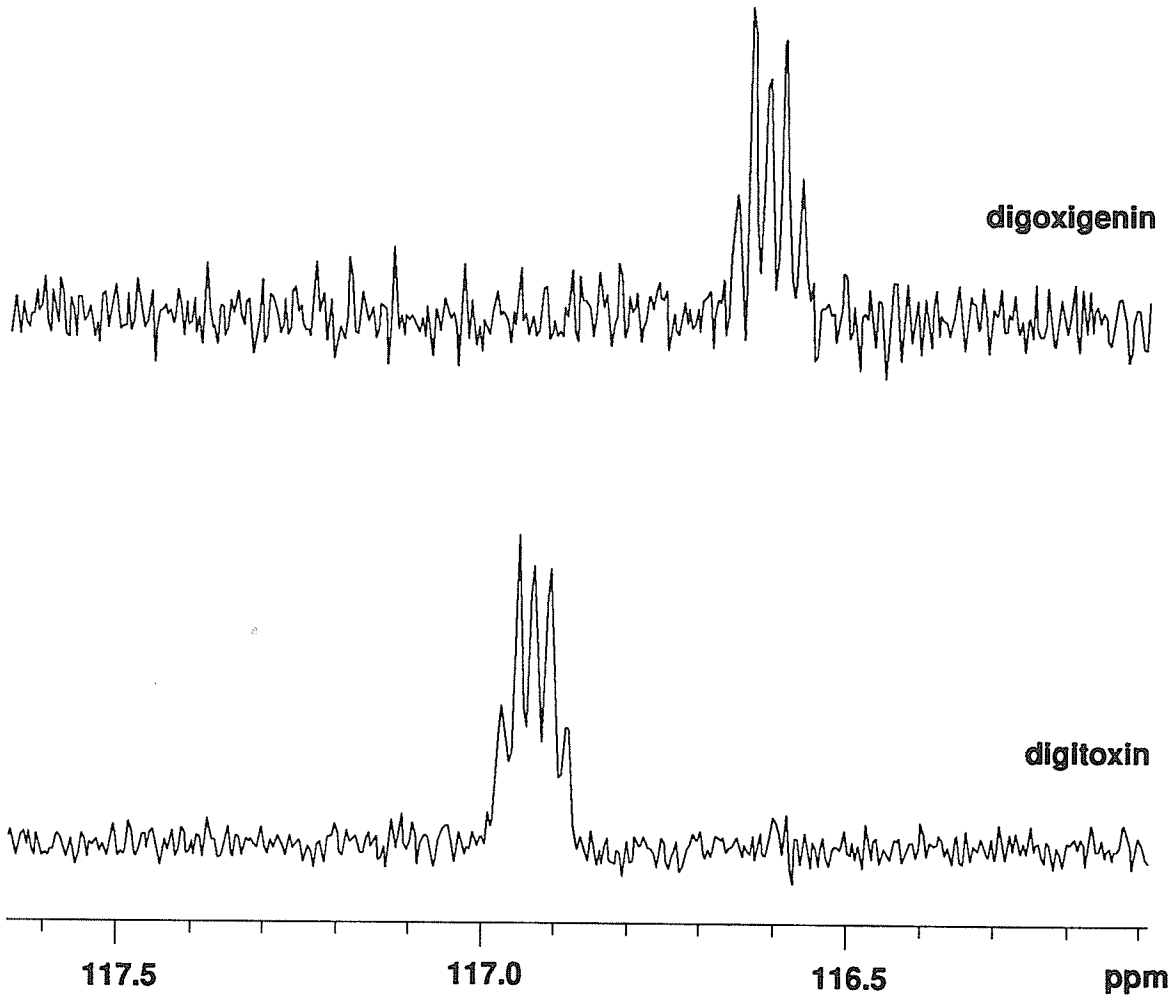

Figure 3.2: Fully coupled ^{13}C spectrum of the C-22 carbon in digoxigenin and digitoxin. Only one half of the symmetric $^{1}J_{CH}$ doublet is shown. The spectra show triplet fine structure (3.0 Hz) due to coupling to the two C-21 protons and a stereospecific doublet coupling (5.4 Hz) from H-17.

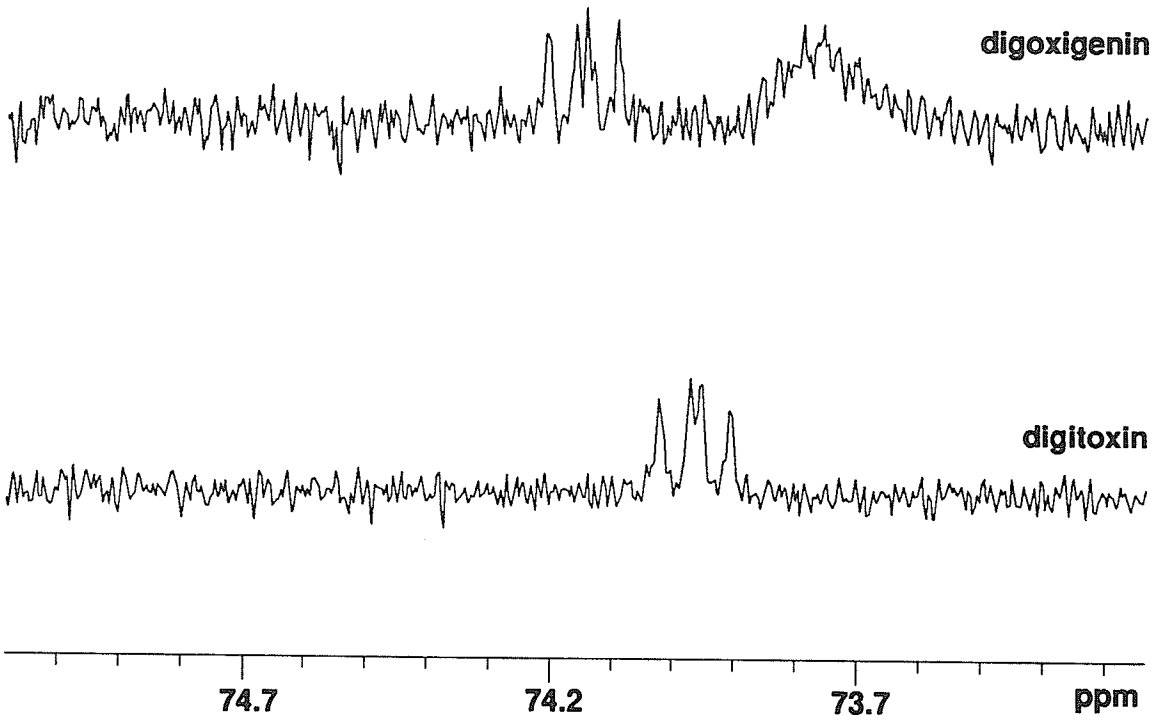

Figure 3.3: Fully coupled ^{13}C spectrum of the C-21 carbon in digoxigenin and digitoxin. Only the low field peak of the symmetric $^{1}J_{CH}$ triplet is shown. The spectra show doublet fine structure (8.5 Hz) due to coupling to the C-22 proton and a stereospecific doublet coupling (6.4 Hz) from H-17.

Table 3.3: ^{13}C Shifts in **1-25** (part 1 of 4)

Compound	Chemical shift (δ ppm)							
number	C-1	C-2	C-3	C-4	C-5	C-6	C-7	C-8
1	30.49	25.10	70.43	30.49	36.88	26.46	20.72	41.52
2	30.51	25.08	70.42	30.51	36.90	26.42	20.62	41.19
3	30.49	25.08	70.48	30.49	36.90	26.48	21.30	41.52
4	30.55	25.10	70.54	30.55	36.97	26.43	21.51	39.81
5	30.52	25.05	70.73	30.52	36.94	26.25	20.54	40.67
6	30.52	25.03	70.52	30.46	36.92	26.36	21.25	40.58
7	30.44	25.01	70.39	30.44	36.80	26.41	20.70	41.24
8	30.41	25.01	70.36	30.41	36.78	26.35	20.95	41.20
9	31.83	27.52	73.60	30.86	38.14	27.90	22.07	42.29
10	31.61	27.47	73.59	30.93	38.05	27.71	21.95	41.83
11	29.69	27.93	66.95	33.30	36.33	26.20	23.69	39.41
12	30.11	28.01	67.00	33.50	36.84	26.79	24.48	40.04
13	30.54	25.12	70.68	30.44	37.23	26.15	23.95	39.78
14	30.51	25.07	70.65	30.43	37.20	26.14	23.92	39.68
15	30.02	24.77	76.24	30.08	36.91	25.82	23.74	39.93
16	30.02	24.78	76.23	30.08	36.91	25.81	23.73	39.55
17	30.03	26.96	73.20	31.51	37.24	26.68	21.40	41.25
18	30.57	27.32	73.10	31.33	37.72	27.55	21.75	41.35
19	30.27	26.60	73.18	29.74	35.92	28.14	24.90	41.91
20	31.29	26.40	73.13	29.69	38.82	26.02	20.68	36.51
21	31.65	27.81	73.64	30.87	38.15	27.49	22.46	41.50
22	30.56	26.52	73.33	29.64	35.39	26.63	21.04	39.90
23	31.66	27.52	73.62	30.89	38.17	27.87	22.14	41.16
24	30.47	26.47	73.22	29.64	35.80	26.52	21.24	41.86
25	31.66	27.54	73.62	30.91	38.24	27.92	22.03	42.66

Table 3.3. continued... (part 2 of 4)

Compound number	Chemical shift (δ ppm)							
	C-9	C-10	C-11	C-12	C-13	C-14	C-15	C-16
1	35.73	35.22	21.28	40.21	47.21	86.15	31.43	24.59
2	35.53	35.22	21.14	40.61	47.26	86.09	32.16	24.79
3	35.69	35.19	20.80	41.67	46.67	85.73	31.72	25.08
4	35.23	35.23	21.07	41.19	47.27	84.42	32.12	20.26
5	35.55	35.18	21.32	41.15	47.64	85.42	32.13	26.47
6	35.46	35.13	21.47	39.98	47.58	84.78	32.52	18.09
7	35.70	35.14	21.24	42.29	47.35	86.04	32.09	25.86
8	35.71	35.14	21.31	41.20	46.82	86.01	31.85	21.41
9	36.88	36.38	22.53	42.54	~50[j]	86.23	32.49	23.59
10	36.88	36.33	22.27	40.42	~50[j]	86.35	32.95	20.02
11	34.97	35.26	21.93	42.73	47.10	155.45	116.34	34.60
12	35.64	35.49	22.22	42.60	46.96	155.70	117.04	34.96
13	34.97	35.09	21.82	42.80	47.29	155.51	116.29	33.72
14	34.77	35.06	21.61	41.69	46.41	154.81	116.79	33.56
15	34.85	34.98	21.69	41.85	46.78	154.83	116.56	34.10
16	34.96	34.45	21.94	42.27	47.07	154.82	116.60	34.91
17	35.89	35.41	20.91	38.52	~50[j]	85.90	31.51	25.13
18	36.43	36.03	22.18	40.44	~50[j]	85.23	33.05	22.99
19	42.22	35.25	25.16	37.36	56.39	100.32	31.96	33.49
20	35.35	35.35	19.65	32.07	43.70	94.20	30.50	27.48
21	36.70	36.36	22.06	40.61	~50[j]	85.74	19.62	33.14
22	36.55	35.32	21.56	40.93	47.24	83.95	32.24	19.41
23	36.42	36.36	22.63	41.13	~50[j]	85.59	33.39	20.26
24	35.29	36.45	20.78	38.26	50.04	85.92	32.85	26.83
25	36.90	36.40	22.50	39.93	50.48	86.92	28.05	33.00

Table 3.3. continued... (part 3 of 4)

Compound number	Chemical shift (δ ppm)							
	C-17	C-18	C-19	C-20	C-21	C-3 OAc	C-3 OAc	
1	52.06	13.69	23.74	86.80	20.34	21.53	170.67	—
2	54.38	16.02	23.76	87.71	21.26	21.53	170.65	—
3	54.31	15.15	23.75	74.28	19.29	21.50	170.63	*a*
4	54.14	14.56	23.79	71.58	18.92	21.51	170.66	*b*
5	56.61	16.31	23.76	71.89	23.32	21.49	170.66	—
6	56.20	14.88	23.75	65.59	22.04	21.47	170.64	—
7	55.05	16.39	23.56	49.36	20.23	21.26	170.60	*c*
8	54.27	13.94	23.58	46.33	19.35	21.46	170.60	*d*
9	54.95	15.94	24.37	51.24	17.32	—	—	*e*
10	55.63	15.40	24.31	47.74	19.85	—	—	*e*
11	58.69	13.95	23.47	46.49	19.30	—	—	*f*
12	58.96	17.03	23.57	47.14	21.40	—	—	*g*
13	58.69	17.55	23.77	69.49	23.58	21.52	170.65	—
14	60.38	17.33	23.63	69.18	23.55	21.50	170.65	—
15	58.19	16.92	23.38	47.90	21.12	—	—	*h*
16	58.20	17.35	23.38	27.61	20.74	—	—	*i*
17	48.27	14.09	23.66	80.78	—	—	—	
18	52.30	15.22	24.34	63.05	—	—	—	
19	43.28	18.77	22.81	35.62	177.14	—	—	
20	42.14	14.63	23.78	31.29	171.97	—	—	
21	53.69	15.21	24.38	68.84	81.68	—	—	
22	52.68	14.90	23.87	39.90	79.12	—	—	
23	53.58	15.25	24.39	79.75	78.03	—	—	
24	49.72	15.82	23.80	148.35	137.73	—	—	
25	55.52	16.57	24.41	157.22	120.11	—	—	

Table 3.3. continued... (part 4 of 4)

[a] C-20 OCO*C*H$_3$: 21.62 ppm; C-20 O*C*OCH$_3$: 170.38 ppm.

[b] C-20 OCO*C*H$_3$: 21.44 ppm; C-20 O*C*OCH$_3$: 169.56 ppm.

[c] C-20 NHCO*C*H$_3$: 23.69 ppm; C-20 NH*C*OCH$_3$: 169.60 ppm.

[d] C-20 NHCO*C*H$_3$: 23.66 ppm; C-20 NH*C*OCH$_3$: 170.25 ppm.

[e] In CD$_3$OD.

[f] C-20 NHCO*C*H$_3$: 23.70 ppm; C-20 NH*C*OCH$_3$: 168.59 ppm.

[g] C-20 NHCO*C*H$_3$: 22.55 ppm; C-20 NH*C*OCH$_3$: 170.99 ppm.

[h] C-3 OCO*C*F$_3$: 115.85 ppm (q, J = 288.0 Hz); C-3 O*C*OCF$_3$: 155.94 ppm (q, J = 37.7 Hz); C-20 OCO*C*F$_3$: 114.64 ppm; (q, J = 285.7 Hz); C-20 O*C*OCF$_3$: 156.98 ppm (q, J = 29.6 Hz).

[i] C-3 OCO*C*F$_3$: 115.84 ppm (q, J = 288.0 Hz); C-3 O*C*OCF$_3$: 155.94 ppm (q, J = 37.8Hz); C-20 OCO*C*F$_3$: 113.02 ppm; (q, J = 286.8 Hz); C-20 O*C*OCF$_3$: 162.04 ppm (q, J = 30.4 Hz).

[j] Obscured by solvent peaks.

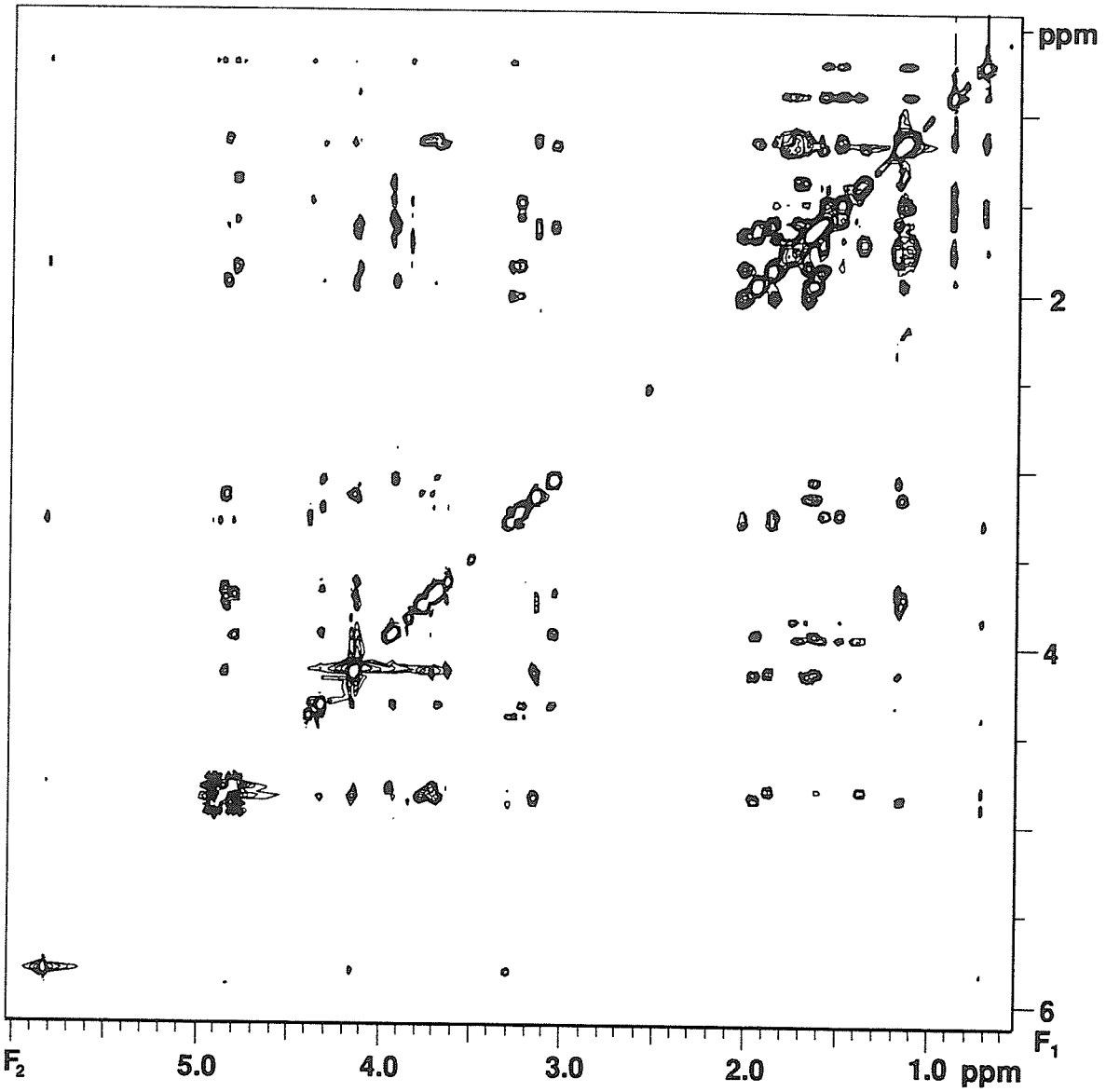

Figure 3.4: ROESY spectrum of digoxin in a 1:1 mixture of $CDCl_3$ and DMSO-d_6 at 313K. A 300 ms mixing time was used. Note the large number of cross-peaks that can be observed. Baseline corrections in F_1 and F_2 have been employed but no symmeterization or other beautification techniques were used.

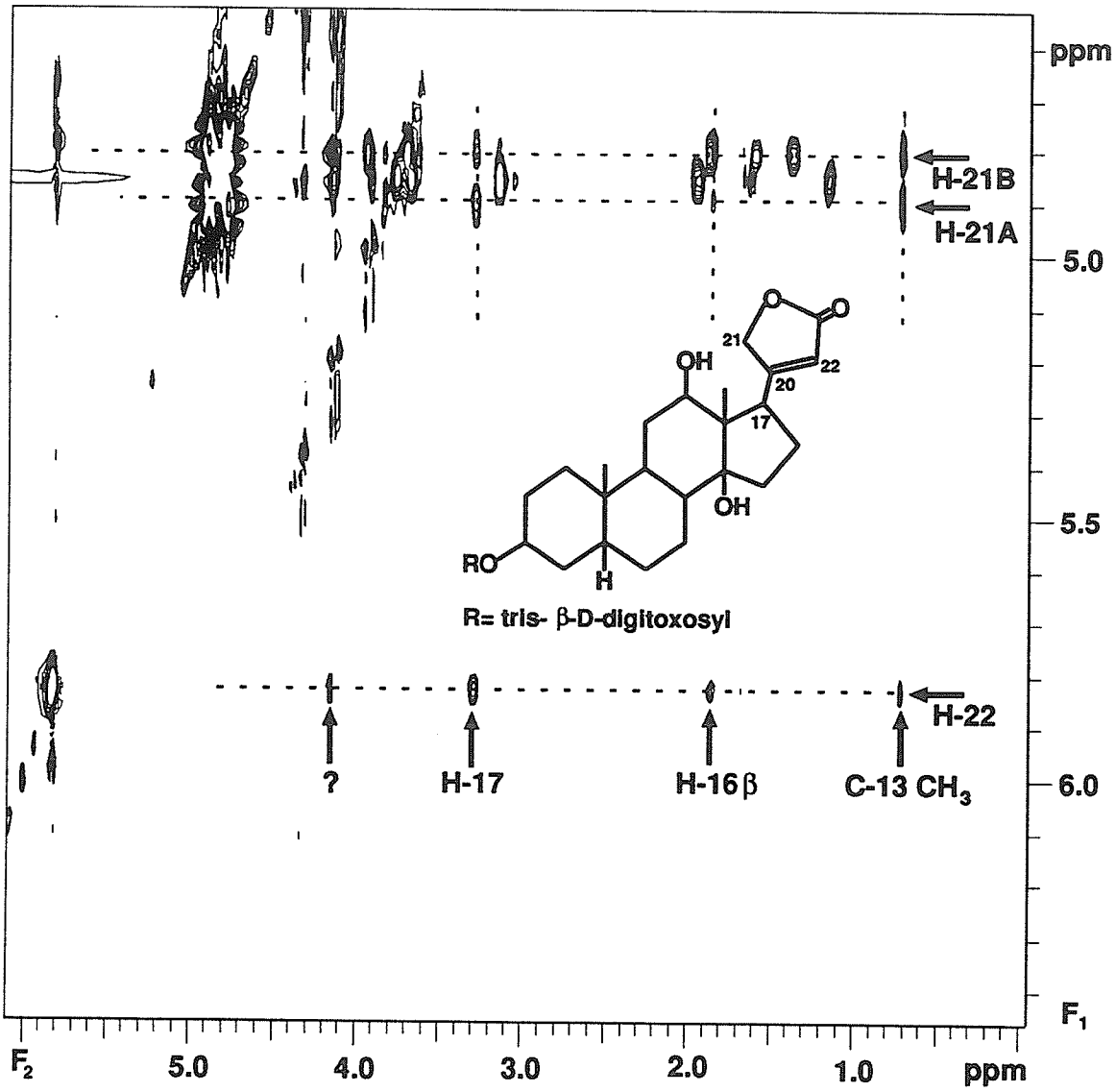

Figure 3.5: Expanded ROESY spectrum of the C-21 and C-22 protons in digoxin in a 1:1 $CDCl_3$ DMSO-d_6 mixture. A 300 ms mixing time was used and the sample temperature was 313K. Other signals in the region of H-21A and H-21B are from the sugar protons.

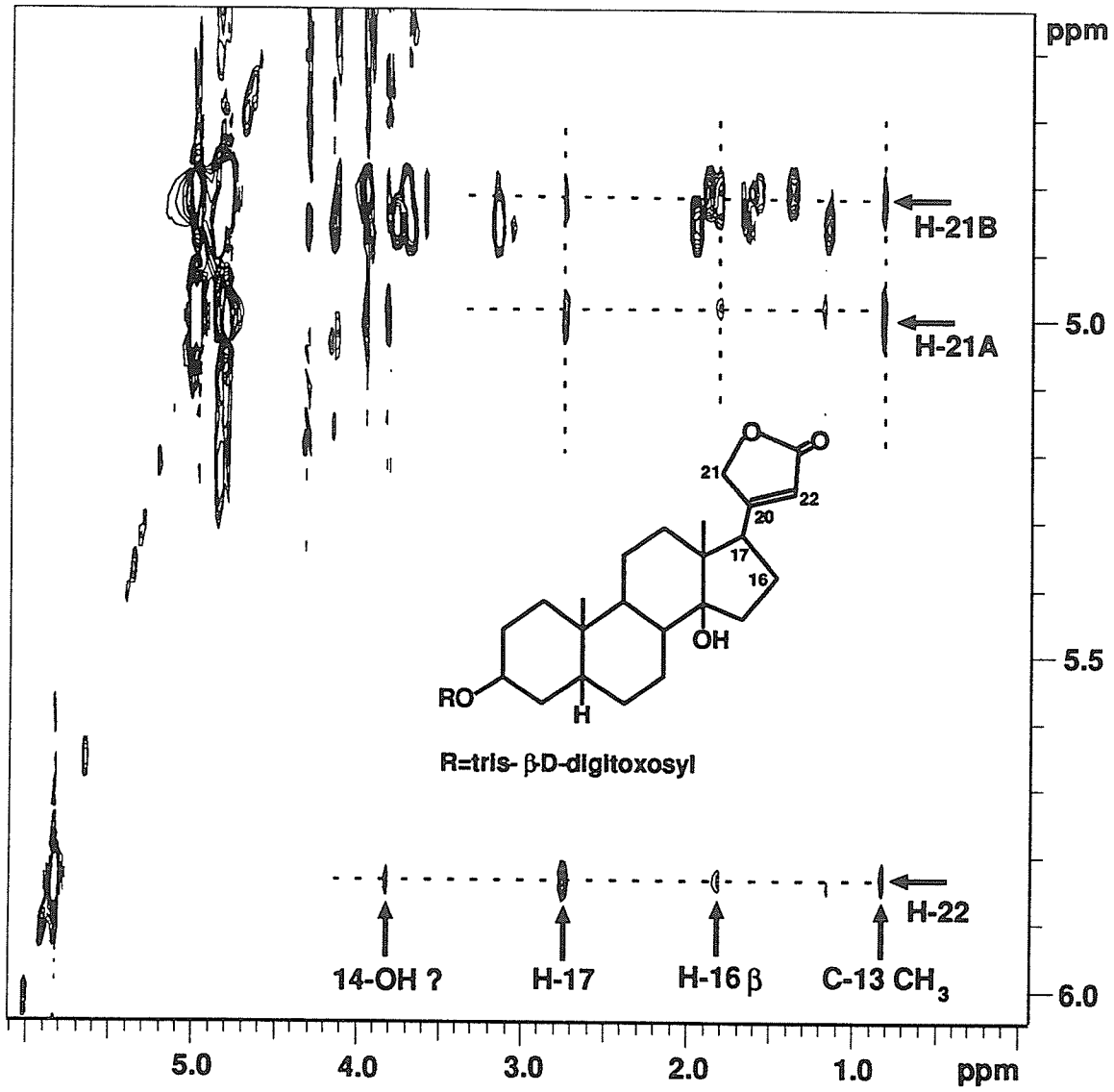

Figure 3.6: ROESY spectrum of the C-21 and C-22 protons in digitoxin a 1:1 $CDCl_3$ DMSO-d_6 mixture. A 300 ms mixing time was used and the sample temperature was 313K. Signals from the sugar protons overlap the H-21A and H-21B signals.

3.1.3 C-17 Side-chain Conformations Predicted by Molecular Mechanics and Semi-Empirical Molecular Orbital Methods

Molecular mechanics calculations at the MM2 and MM3 level were performed on selected compounds in the cardiotonic pregnane (**1** - **10**), pregn-14-ene (**11** - **16**) and 21-norpregnane series(**17** and **18**). Acetyl, acetamido, and trifluoroacetyl groups were avoided because of the large number of conformational possibilities arising from rotation about the C-20–X bond. The results of these calculations and comparisons with the experimentally derived conformers are shown in Table 3.4. AM1 level calculations were also performed on the aglycones digoxigenin and digitoxigenin.

C-20 Substituted Pregnanes and 21-Norpregnanes

Molecular mechanics calculations at the MM3 level predict in the (R)-nitro compound **1** that the nitro group occupies a position *anti* to C-16. AM1 level semi-empirical calculations predict a similar result, with a minor conformation where the nitro group is *anti* to C-13. These findings agree with the experimentally determined conformations shown in Figure 3.1. In the S-epimer, however, MM3 calculations agree with experiment in having the nitro group *anti* to C-13 while AM1 insists on having the substituent *anti* to H-17.

For the C-20 alcohols **5** and **6**, MM2, MM3 and AM1 calculations predict conformations where the hydroxyl lies *anti* to H-17 for both epimers – in agreement with the experimental finding.

Molecular mechanics (MM2 and MM3) predicts that the amino group in **9** should adopt a conformation *anti* to C-16, in clear disagreement with the experimental finding showing the amino group *anti* to H-17. AM1 predicts an almost equal mixture of the *anti* C-16 conformation and the *anti* H-17 conformation. Agreement is better for the S-amino epimer **10**, with MM2, MM3 and AM1 calculations all in agreement

Table 3.4: Conformation of C-17 sidechain as predicted by molecular mechanics and semi-emperical molecular orbital methods.

	location of C-17 sidechain[a]			
Compound	MM2	MM3	AM1	experimental
1	—[b]	*anti*C-16	*anti*C-16 (80%)	*anti*C-16
			*anti*C-13 (20%)	
2	—[b]	*anti*C-13	*anti*H-17	*anti*C-13
5	*anti*C-16 (60%)	*anti*H-17	*anti*H-17	*anti*H-17
	*anti*H-17 (40%)			
6	*anti*H-17	*anti*H-17	*anti*H-17	*anti*H-17
9	*anti*C-16	*anti*C-16	*anti*C-16 (55%)	*anti*H-17
			*anti*H-17 (45%)	
10	*anti*H-17	*anti*H-17	*anti*H-17	*anti*H-17
13	*anti*C-16	*anti*C-16	*anti*C-16	*anti*C-16
14	*anti*C-13 (75%)	*anti*C-13 (60%)	*anti*C-13 (65%)	*anti*C-13
	*anti*H-17 (25%)	*anti*H-17 (40%)	*anti*H-17 (35%)	
17	—[b]	*anti*C-13	*anti*C-16	*anti*C-13
18	*anti*H-17	*anti*H-17	*anti*H-17 (70 %)	*anti*H-17
			*anti*C-13 (30 %)	

[a] Defined as the orientation of the C-20 substituent.

[b] Force field parameters not available for this group.

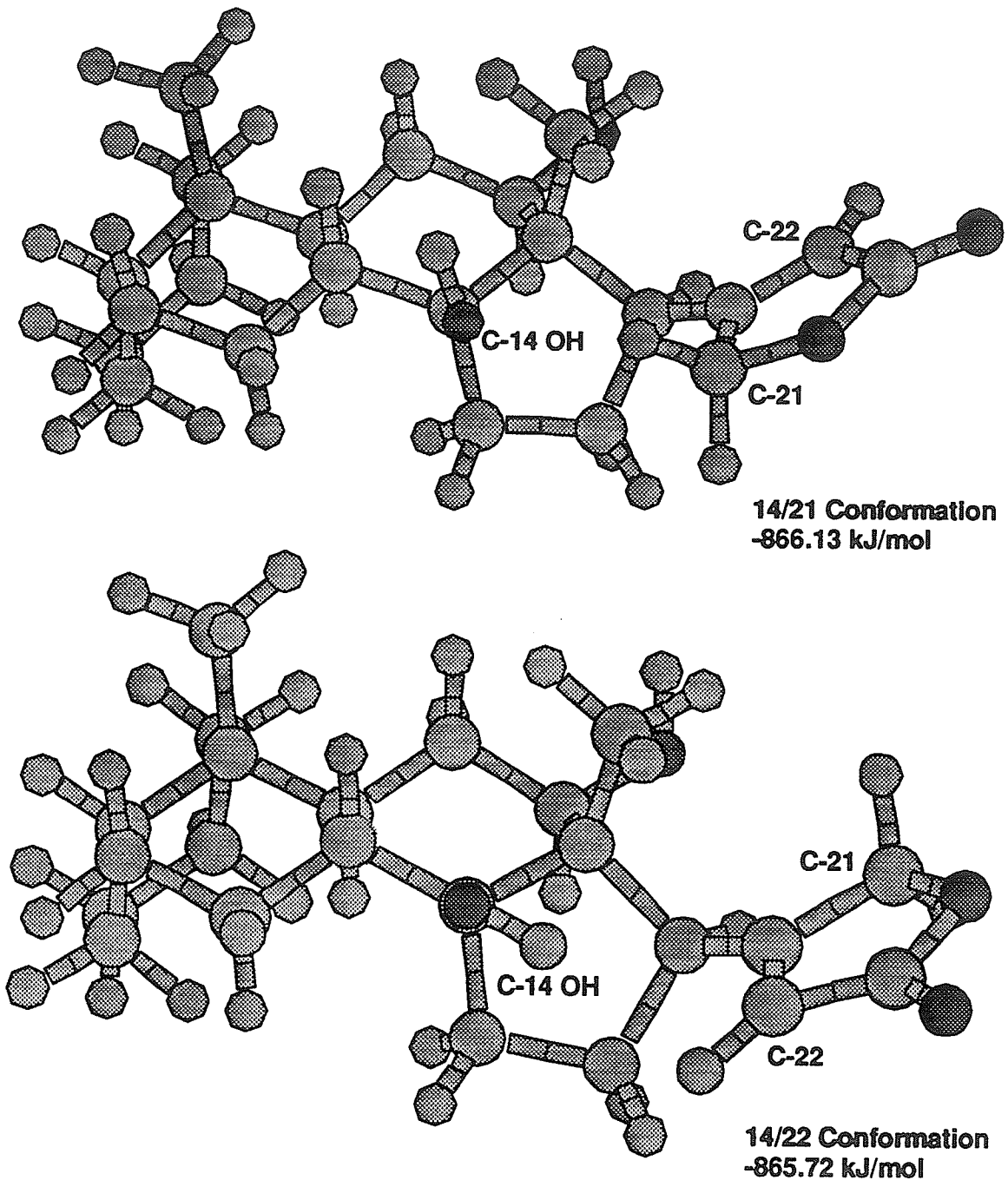

Figure 3.7: Lowest energy conformations of digoxigenin as predicted by AM1 calculations. The two conformers differ by less than one kJ/mol.

with the experimentally determined conformation.

For the Δ^{14} C-20 alcohols **13** and **14** generally good agreement is obtained between the predicted conformations and the experimentally determined conformations. In the S-epimer **14** MM2, MM3 and AM1 all predict a significant population of a rotamer with the hydroxyl *anti* to H-17 (H-20 *gauche* to H-17). The fact that $^3J(17,20)$ drops from 12.3 Hz in **13** to 8.7 Hz in **14** supports this conclusion.

MM3 calculations on the 21-nor nitro compound **17** are in agreement with the experimental finding that the nitro group lies *anti* to C-13 while AM1 calculations predict a conformation where the nitro group is *anti* to C-16.

For the 21-nor alcohol **18** MM2, MM3 and AM1 are all in agreement with the experimental finding that the hydroxyl lies *anti* to H-17.

C-21 Substituted Pregn-20,21-enes (24 and 25)

The Spartan[220] program the did not contain the required MM2 and MM3 force field parameters for **24** and **25**. AM1 calculations predict that a conformation where the polar side-chain approximately eclipes H-17 is lower in energy by 8 kJ/mol in **24** and by 10 kJ/mol in **25**, compared to one where the side-chain is rotated by 180°.

Digoxigenin and Digitoxigenin

The necessary force-field parameters for MM2 and MM3 level calculations for conformational searches about the C-17–C-20 bond were not available in the Spartan program package. Semi-empirical calculations at the AM1 level revealed two probable conformations differing by less than 1 kJ/mol. These are known as the 14/21 and 14/22 conformations and are displayed in Figure 3.7. No significant differences were found between digoxigenin and digitoxigenin, suggesting that the 12β-hydroxyl group has little influence on the C-17 side-chain conformation.

3.2 Cyclosteroids and Cyclopropanosteroids

3.2.1 Determination of Structures

COSY and HSQC spectra were used for a complete assignment of the carbon and proton spectra for each compound. For each compound, all carbons and hydrogens could be assigned. Since the cyclopropyl groups are at quaternary sites (i.e. C-5, C-9 and C-10) and are in some cases (e.g. compounds **32**, **35** and **42**) quaternary themselves, the HMBC experiment was critical in establishing the location of cyclopropyl addition. NOE enhancements from the C-13 CH_3 were used to distinguish the α from the β ring D hydrogens, and to distinguish H-8 from H-9 and H-14. The C-2 protons could be distinguished from the C-1 protons because of the larger geminal coupling of H-2α to H-2β, owing to the presence of the C-3 carbonyl.

19(S)-Bromo-17β-(*tert*-butyldimethylsiloxy)-5β,6β-dibromomethylene-9α,19-cyclo-10α-androstan-3-one (42)

This compound was expected to have a (5,10) dibromocyclopropyl group - the result of a dibromocarbene addition to a (5,10) double bond (Figure 3.8). However, ^{1}H and ^{13}C NMR, mass spectrometry and elemental analysis for C, H and Br did not support this conclusion. There were 3 bromines instead of the expected 2; an unusual broad singlet in the ^{1}H NMR at 2.92 ppm (Figure 3.9); C-6 was found to be methine rather than methylene; C-9 was quaternary; and an extra quaternary carbon was observed in the ^{13}C spectrum. Carbon-proton correlation spectra for this compound are shown in Figures 3.10 and 3.11. These data suggested that this compound had 2 cyclopropyl groups - probably a dibromocyclopropyl at the (5,6) position and a bromocyclopropyl at the (9,10) position. The location of the (9,10) cyclopropyl group was confirmed by the observation in the COSY spectrum (Figure 3.12) of long range (4 bond) coupling between the cyclopropyl proton and H-8, H-1β and H-11β, which also suggests that the cyclopropyl group is α. As further evidence for this conclusion,

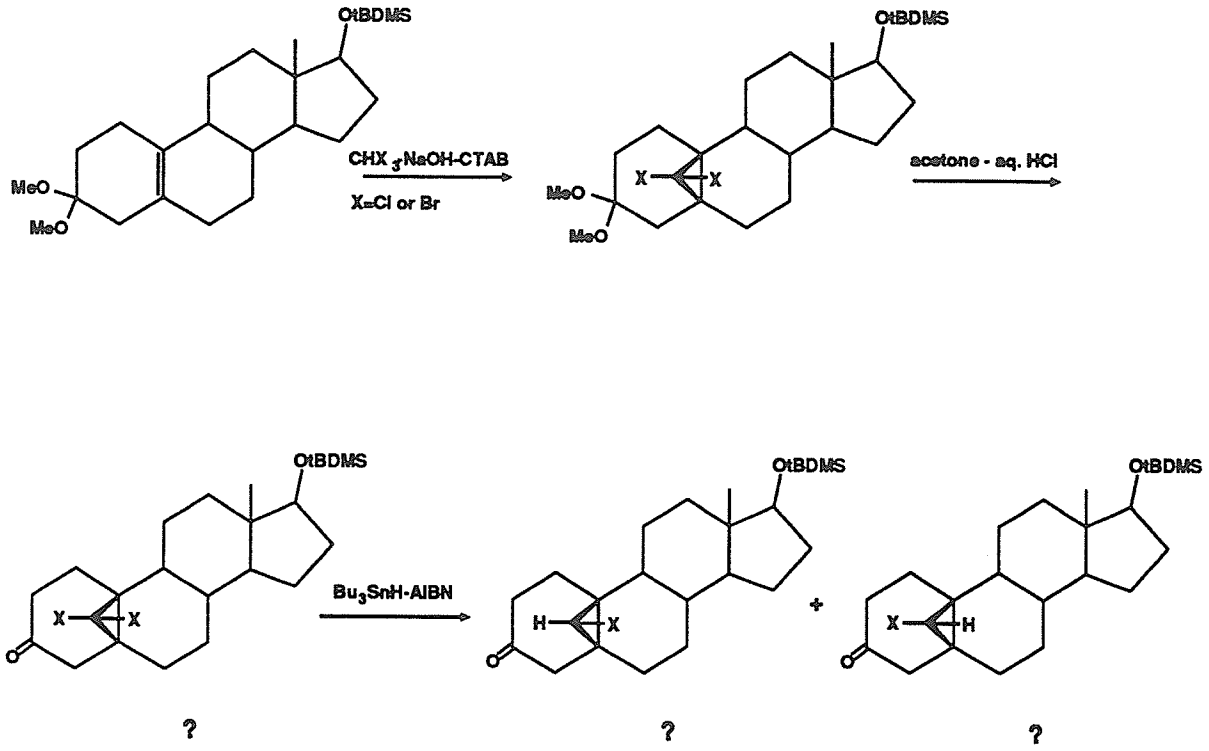

Figure 3.8: Proposed reaction scheme for the synthesis of 19,5- cyclosteroids. The intent was to use a dihalocarbene addition to the 5,10-double bond followed by reduction to the monohalo compound.

H-11α, H-11β and H-8 all lack the usual couplings to H-9, and the expected cross-peaks were observed in the HMBC spectrum. NOEs were observed from the (9,10) cyclopropyl proton to H-7α (4.5%), H-14 (3.8%) and H-4α; and from these data, it was concluded that the cyclopropyl group is on the α side of the steroid with the hydrogen *endo*. The HMBC spectrum confirmed the location of the (5,6) cyclopropyl group, but the stereochemistry of addition could not be determined directly from the NMR data. However, reduction products **18** and **19** both have this cyclopropyl group β.

19(S)-Bromo-5β,6β-[(R)-bromomethylene]-17β(*tert*-butyldimethylsiloxy)-9α, 19-cyclo-10α-androstan-3-one (43) and 19(S)-Bromo-5β,6β-[(S)-bromomethylene]-17β(*tert*-butyldimethylsiloxy)-9α,19-cyclo-10α-androstan-3-one (44)

In **43** and **44** (the reduction products of **42**), NOEs are observed from the (9,10) cyclopropyl proton to H-14 and H-7α. This confirms the location of the cyclopropyl group on the α face of the steroid, with the hydrogen *endo* and the bromine *exo*. In **44**, a strong NOE (12%) is observed from the (5,6) cyclopropyl proton to H-8. The (5,6) cyclopropyl group is thus on the β side of the molecule with the hydrogen *endo* and the bromine *exo*. As further evidence for this conclusion, the coupling patterns clearly indicate that H-6 is equatorial (and thus α) and has a *trans* cyclopropyl coupling (4.3 Hz) to the (5,6) cyclopropyl hydrogen. In **43**, the (5,6) cyclopropyl proton has an NOE to H-4β and a *cis* cyclopropyl coupling (8.1 Hz) to H-6α, clearly indicating that the (5,6) cyclopropyl group is β with the cyclopropyl proton *exo*. Carbon-proton correlation spectra of **43** and **44** are shown in Figures 3.13 and 3.14. NOE difference spectra of **44** are shown in Figures 3.15 and 3.16.

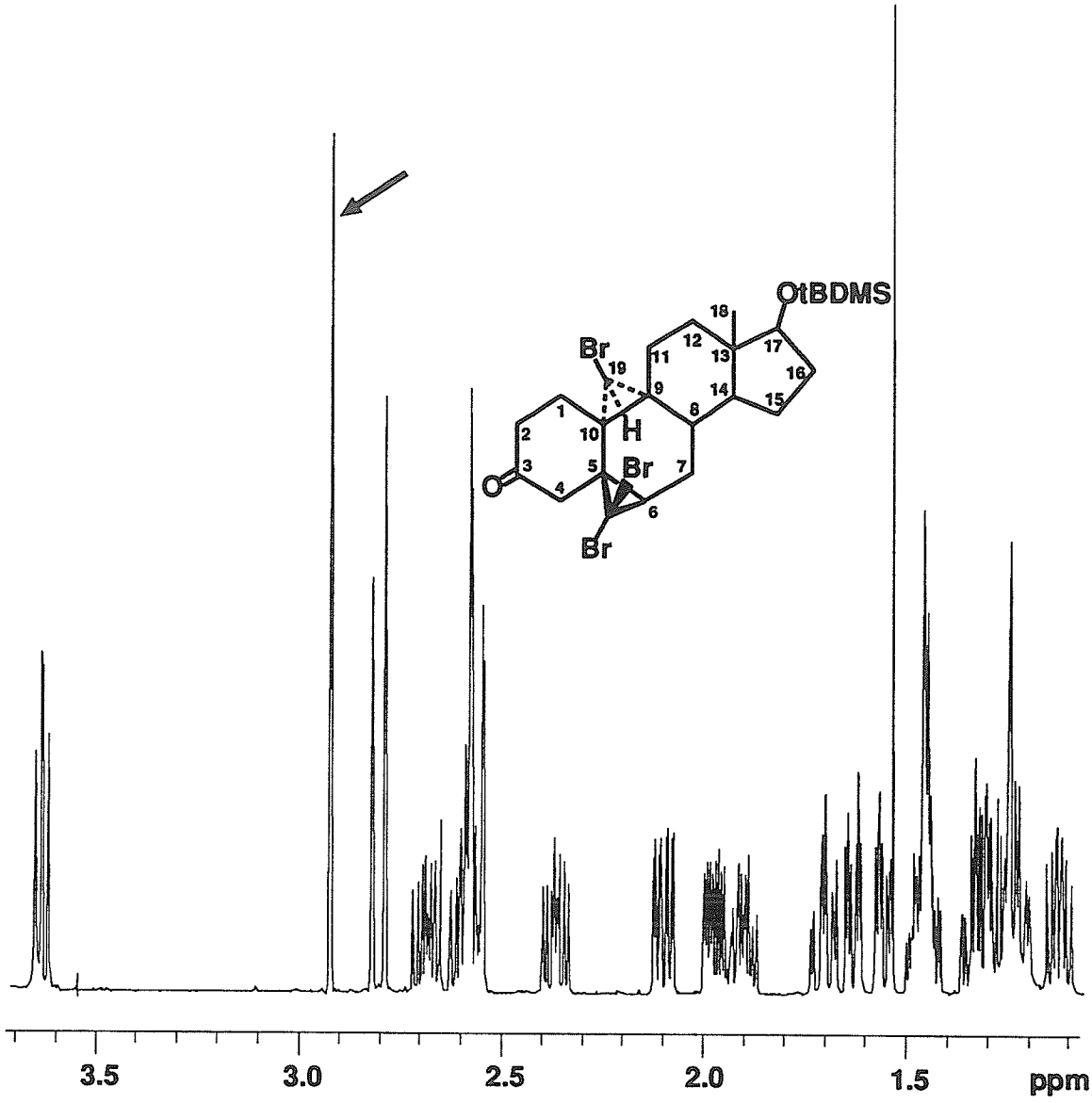

Figure 3.9: Resolution enhanced 500 MHz proton spectrum of **42**. Note the unusual singlet at 2.94 ppm, which cannot be rationalized with the proposed addition of the dibromocarbene to the 5,10 double bond. The correct structure is shown inset at the top of the spectrum.

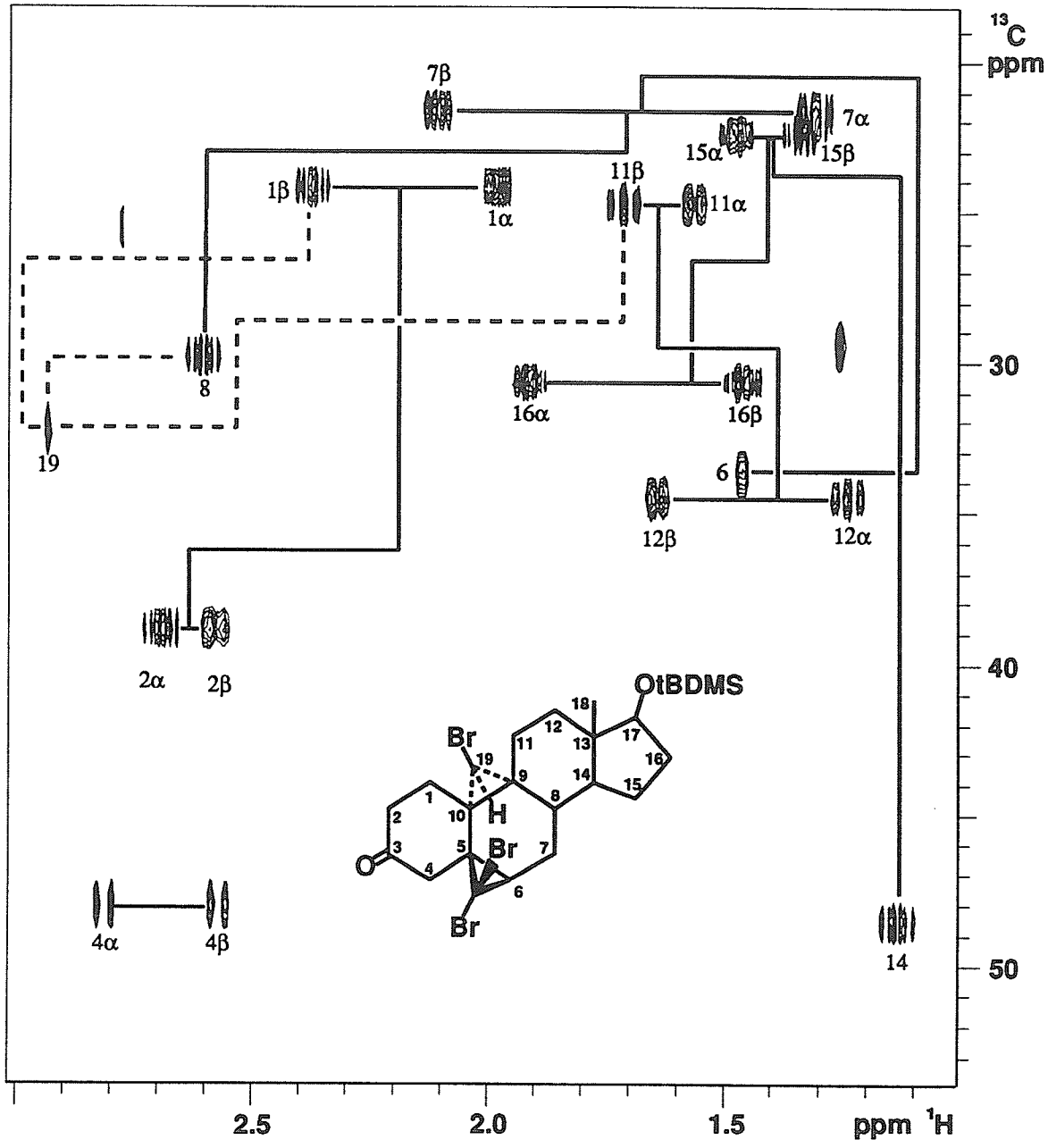

Figure 3.10: Proton detected carbon-proton correlation spectrum of **42**. The lines linking the various cross peaks represent proton-proton couplings obtained from the COSY spectrum. Dashed lines represent probable long range ($J < 1$ Hz) couplings. H-19, the peak originally assigned to position 9, lacks the expected axial couplings to H-8 and H-11β. Only a single H-6 can be observed.

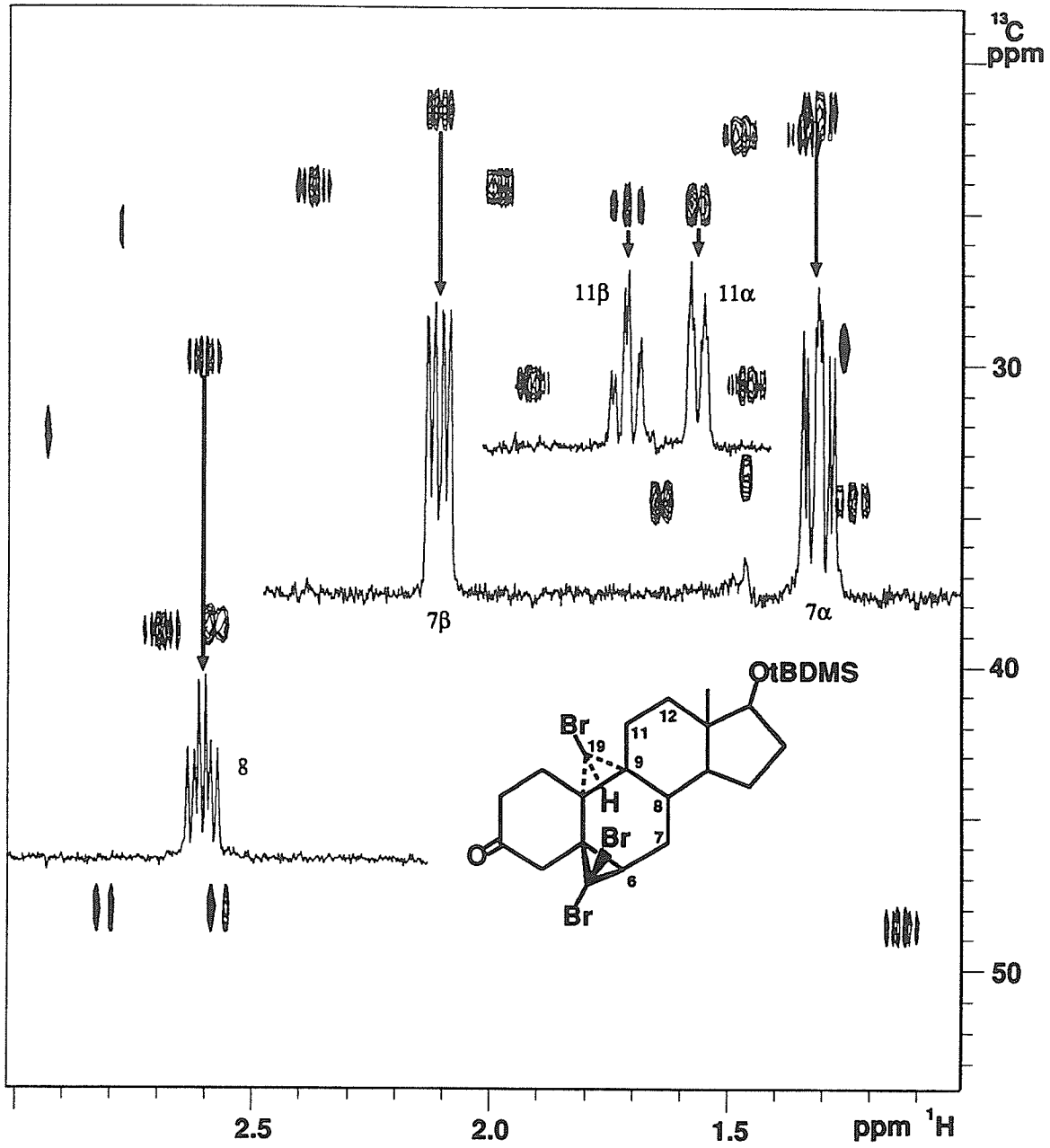

Figure 3.11: Proton detected carbon-proton correlation spectrum of **42** with extracted rows. H-8 has two large couplings rather than the expected three, while H-7α and H-7β lack couplings to the axial H-6 proton; and H-11α and H-11β lack the expected couplings to an axial H-9. Note the clean multiplet patterns that can be obtained with this method.

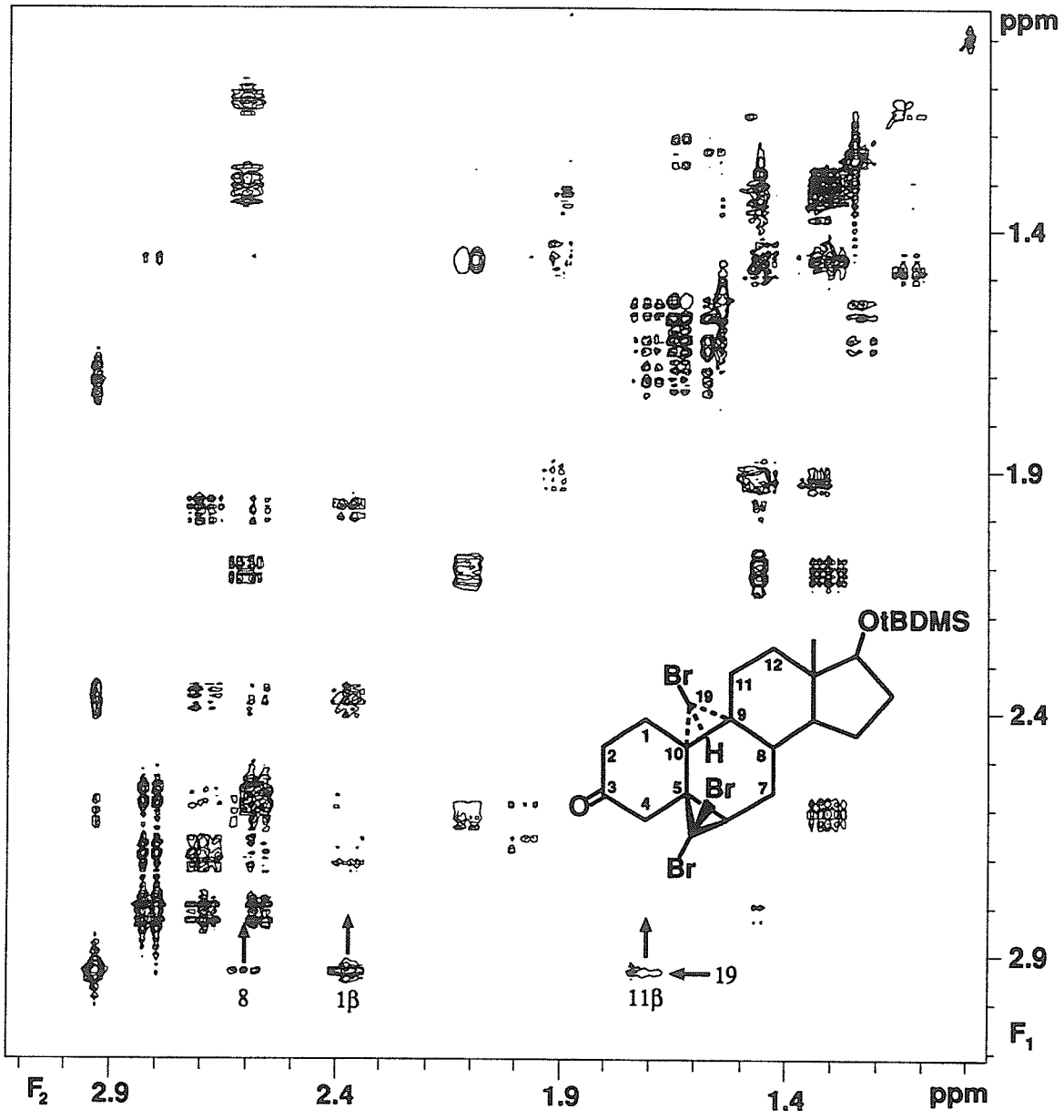

Figure 3.12: COSY spectrum of 42. Long-range couplings have been enhanced by the addition of a 100 ms fixed delay to the evolution time. Note the couplings between the singlet at 2.94 ppm and H-8, H-1β and H-11β. The fact that this singlet is coupled to protons on the β face of the molecule indicates that this proton is on the α face.

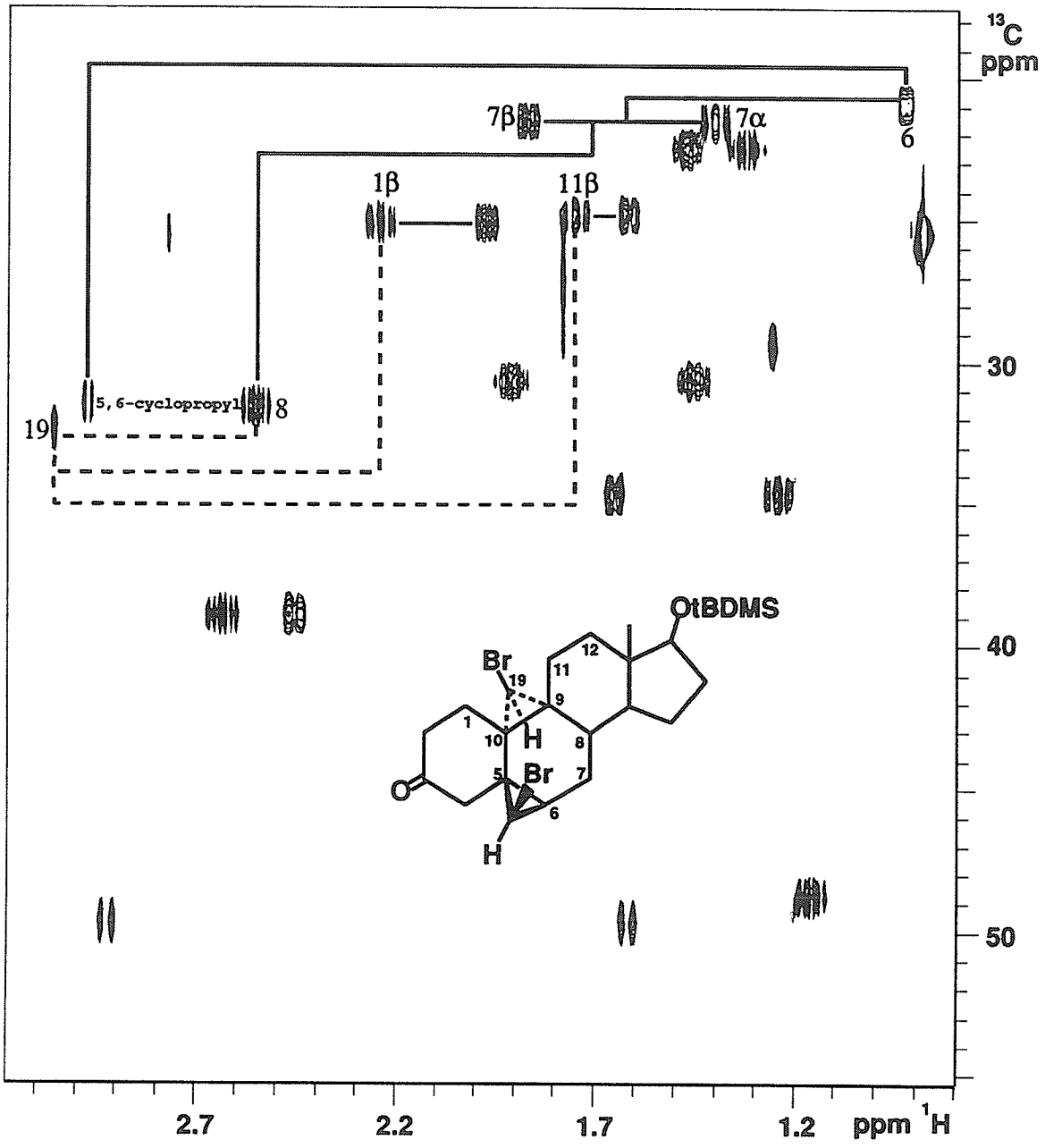

Figure 3.13: Proton detected carbon-proton correlation spectrum of **43**, one of the reduction products of **42**. The unusual singlet, with long range coupling to H-8 and H-11β is still present. A new doublet (J= 8.1 Hz), coupled to H-6, has appeared. The one-bond C-H coupling of the doublet is characteristic of a cyclopropyl group.

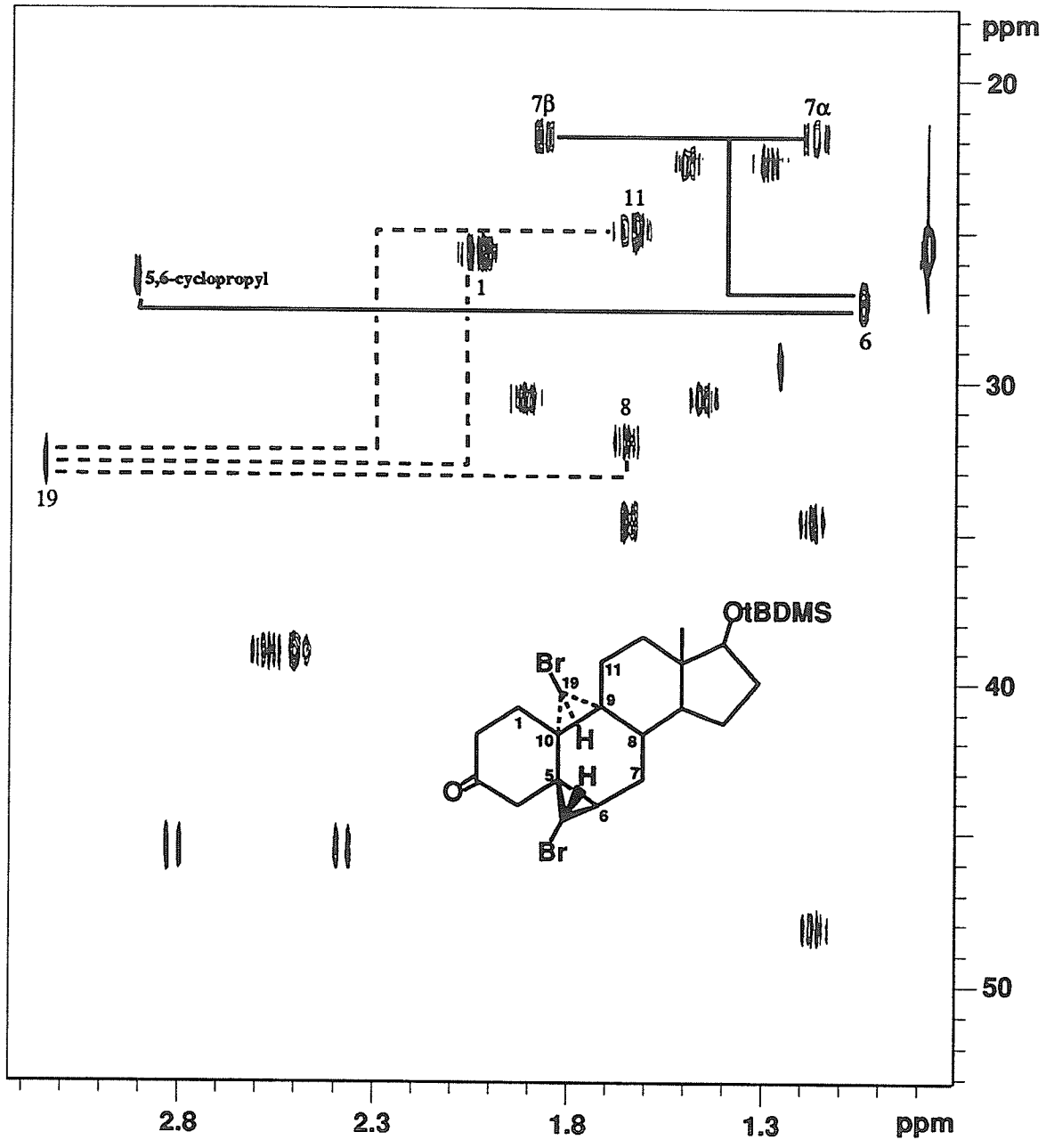

Figure 3.14: Proton detected carbon-proton correlation spectrum of **44**, one of the reduction products of **42**. As with **43**, a new doublet (J= 4.3 Hz) coupled to H-6, has appeared. The size of the doublet couplings in **42** and **43** are characteristic of *cis* and *trans* cyclopropyl couplings.

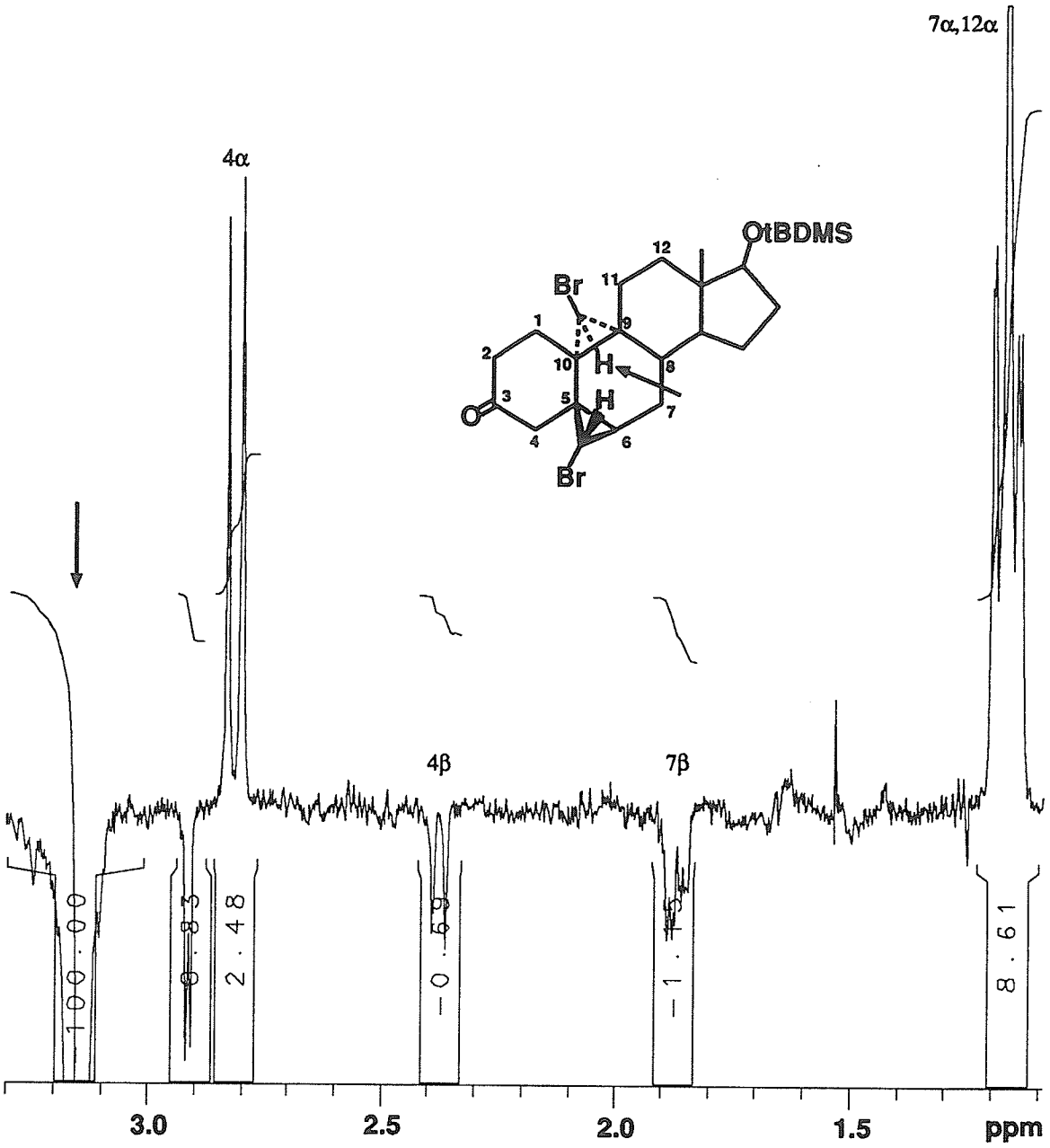

Figure 3.15: Steady-state NOE difference spectrum of 44 while irradiating the C-19 cyclopropyl proton (arrow). Sizable NOEs are observed to protons on the α face of the molecule, confirming α stereochemistry for the 9,10-cyclopropyl group. These NOEs also strongly suggest that the C-19 proton is endocyclic. The negative NOEs observed to H-4β, H-7β and the doublet at 2.90 ppm are three-spin effects (see section 1.1.1).

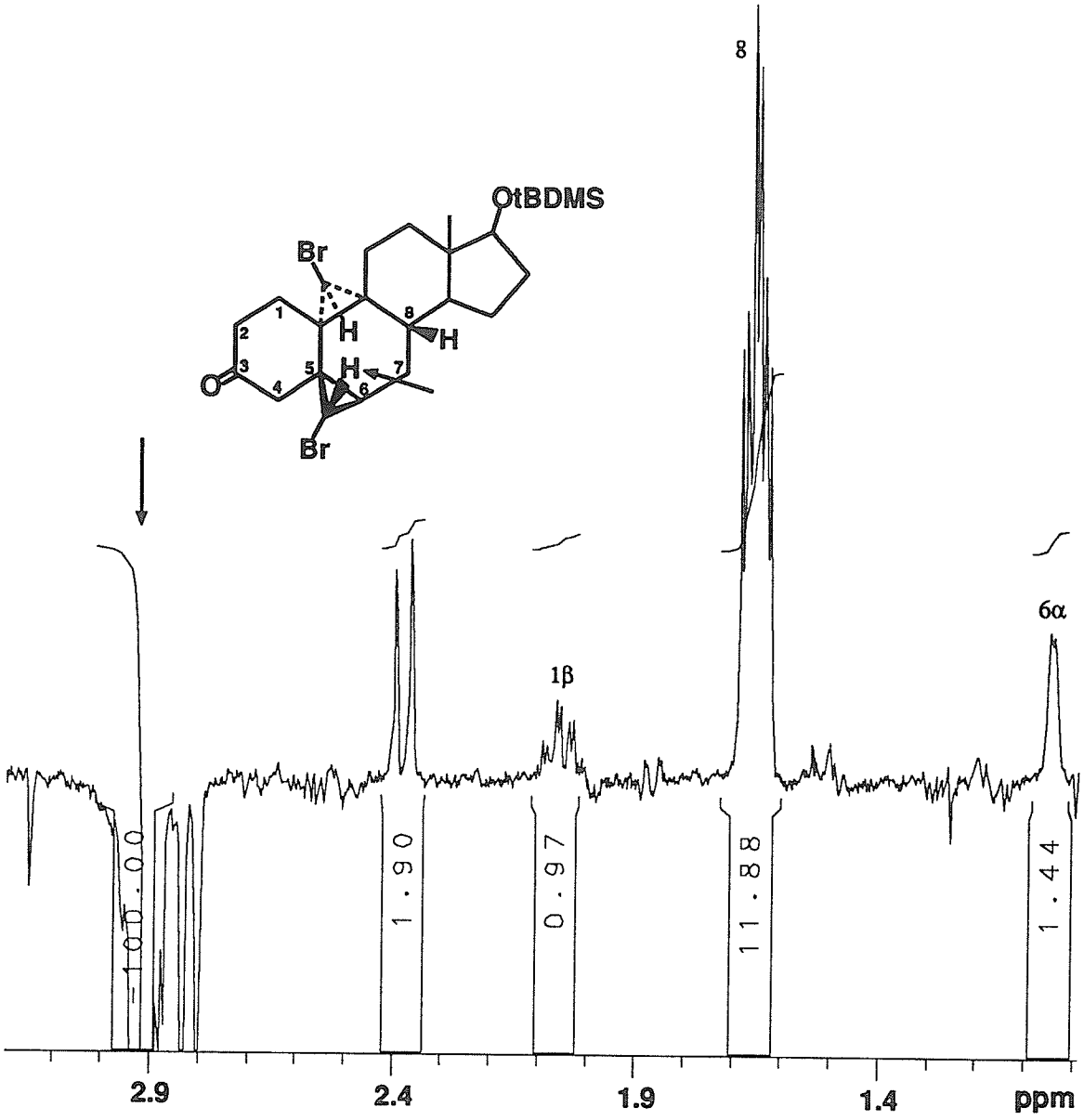

Figure 3.16: Steady-state NOE difference spectrum of 44 while irradiating the 5,6-cyclopropyl proton (arrow). The large NOE observed to H-8 confirms β stereochemistry for the 5,6 cyclopropyl group and shows that the proton is endocyclic.

19(S)-Bromo-5β,6β-17β(*tert*-butyldimethylsiloxy)-9α,19-cyclo-10α-androst-4-en-3-one (45)

The (9,10) location of the cyclopropyl group was confirmed by the observation in the COSY spectrum of long range (4 bond) coupling between the cyclopropyl proton and H-1β and H-11β. These are typical "W" configuration couplings, and also suggest that the cyclopropyl group is on the α face of the steroid. NOE's are observed from the cyclopropyl proton to H-7α (9.2%), H-14 (3.2%), H-2α (0.5%) and H-7β (-1.6%, *via* a 3 spin effect from H-7α). These NOE's further confirm α addition of the cyclopropyl group.

17β-*tert*-Butyldimethylsiloxy-19,19-dichloro-5α,19α-cycloandrostan-3-one (35) and 17β-*tert*-Butyldimethylsiloxy-19,19-dichloro-5β,19-cycloandrostan-3-one (32)

The (5,10) location of the cyclopropyl group was confirmed with the HMBC experiment. The stereochemistry of addition, however, could not be reliably determined from the NMR experiments because of the lack of a proton on the cyclopropyl carbon. Reduction of **35** produced two products, lyz142a and lyz142b, which were confirmed as having the (5,10) cyclopropyl α. Reduction of **32**, on the other hand, produced two products, lyz150a and lyz150b, which were confirmed to have the cyclopropyl group β.

17β-*tert*-Butyldimethylsiloxy-19(S)-chloro-5α,19α-cycloandrostan-3-one (36) and 17β-*tert*-Butyldimethylsiloxy-19(R)-chloro-5α,19α-cycloandrostan-3-one (37)

In lyz142a, a large (9.7%) NOE is observed from the cyclopropyl proton to H-9, and a smaller (3.5%) NOE is observed from the cyclopropyl proton to H-7α, indicating addition of the cyclopropyl group to the α side of the steroid with the cyclopropyl proton under ring B. In lyz142b, a 2.1% NOE is observed from the cyclopropyl proton

to H-4α and a 4.2% NOE is observed to H-2α, confirming alpha addition with the cyclopropyl proton under ring A.

Reduction products 17β-*tert*-Butyldimethylsiloxy-19(S)-chloro-5β,19-cyclo-androstan-3-one (33) and 17β-*tert*-Butyldimethylsiloxy-19(R)-chloro-5β,19-cycloandrostan-3-one (34)

In **33**, a 7.3 % NOE is observed between the cyclopropyl proton and H-8, confirming that the cyclopropyl group is β with the proton over ring-B (S stereochemistry). In **34**, NOEs are observed from the cyclopropyl proton to H-4β(2.9%), H-2β(4.2%), and H-1β(2.3%), confirming β addition of the cyclopropyl group with the cyclopropyl proton over ring A (R stereochemistry).

19(R)-Hydroxy-5β-19-cycloandrostane-3,17-dione (40)

Long range couplings from the cyclopropyl proton to H-9 and H-6α suggest that the cyclopropyl group is at the (5,10) position on the β side of the steroid. NOEs are observed from the cyclopropyl proton to H-4β, H-2β and H-1β, confirming the R stereochemistry at C-19.

3.2.2 Spectral Analysis

The chemical shifts of all protons and carbons in **26-46** were determined from an analysis of 2D homonuclear correlation (COSY) and proton detected heteronuclear correlation (HSQC and HMBC) spectra, and are reported in Tables 3.5 and 3.6. A sample HSQC spectrum of **29** is shown in Figure 3.17.

Protons were identified as to α or β configuration using NOE measurements from substituents with known stereochemistry. Owing to severe overlap with other signals, a 1-D TOCSY experiment was used to isolate the ring-A spectrum in **26-31**. The effectiveness of this technique for isolating the ring A spectrum is demonstrated for **31** in Figure 3.18.

Table 3.5: ^{1}H Shifts in **26-46** (part 1 of 5)

Compound	Chemical shift (δ ppm[a])							
number	H-1α	H-1β	H-2α	H-2β	H-3α	H-3β	H-4α	H-4β
26	—	0.753	—	0.879	1.491	1.952	0.878	1.271
27	1.454	1.916	0.766	—	0.926	—	1.731	1.167
28	1.248	2.447	0.830	—	0.961	—	1.802	1.308
29	0.898	1.996	—	0.780	—	0.831	1.587	1.514
30	0.810	2.063	—	1.060	—	—	1.949	1.671
31	0.548	1.510	1.707	1.850	—	0.784	—	0.357
32	2.156	2.119	2.219	2.282	—	—	2.421	2.789
33	1.959	1.848	2.232	2.284	—	—	2.261	2.568
34	2.020	1.992	2.302	2.150	—	—	2.568	2.496
35	1.991	2.531	2.370	2.160	—	—	2.691	2.378
36	1.710	2.344	2.351	2.138	—	—	2.138	2.562
37	1.971	2.271	2.156	2.301	—	—	2.552	2.468
38	1.981	1.838	2.275	2.258	—	—	2.390	2.253
39	1.996	1.968	2.294	2.184	—	—	2.513	2.537
40	1.986	1.784	2.251	2.113	—	—	2.490	2.331
41	7.27		5.75		—	—	2.49	2.84
42	1.984	2.375	2.692	2.813	—	—	2.813	1.094
43	1.978	2.243	2.633	2.456	—	—	2.922	1.618
44	2.002	2.055	2.575	2.491	—	—	2.815	2.378
45	2.088	2.192	2.667	2.395	—	—	5.84	
46	1.598	—	2.641	2.553	—	—	2.337	2.202

Table 3.5. continued... (part 2 of 5)

Compound number	Chemical Shift (δ ppm[a])								
	H-5	H-6α	H-6β	H-7α	H-7β	H-8	H-9	H-11α	H-11β
26	0.846	1.23	1.26	0.83	1.63	1.38	0.79	1.53	1.36
27	1.055	1.31	1.00	0.82	1.62	1.30	0.50	1.55	1.22
28	1.201	1.28	0.85	0.82	1.64	1.49	0.67	1.66	1.42
29	0.824	1.27	1.11	0.77	1.61	1.23	0.49	1.48	1.26
30	0.793	1.34	1.22	0.82	1.66	1.27	0.49	1.47	1.28
31	0.861	1.49	1.32	0.86	1.67	1.43	0.92	1.53	1.23
32	—	1.90	2.10	0.66	1.48	1.61	1.27	1.77	1.87
33	—	1.69	1.90	0.64	1.35	0.81	1.14	1.80	1.33
34	—	1.69	1.90	0.73	1.46	1.59	0.87	1.73[f]	1.73[f]
35	—	1.52	1.06	1.51	2.06	1.02	1.48	1.72	1.66
36	—	2.06	1.46	0.61	1.55	0.84	1.09	1.87	1.56
37	—	1.86	1.41	1.07	1.55	1.18	1.30	1.61[f]	1.65[f]
38	—	1.90[f]	1.90[f]	0.81	1.51	0.99	1.17	1.48	1.90
39	—	1.71	1.56	0.85	1.54	1.47	1.24	1.43	1.90
40	—	1.66	1.81	0.80	1.52	1.69	1.16	1.89	1.54
41	—	1.88[f]	1.88[f]	0.98	1.53	1.08	1.39	1.35	2.07
42	—	1.46	—	1.32	2.11	2.60	—	1.57	1.71
43	—	0.93	—	1.40	1.86	2.53	—	1.61	1.76
44	—	1.04	—	1.17	1.88	1.65	—	1.63[f]	1.63[f]
45	—	2.42	2.48	0.97	1.48	1.82	—	1.83	1.73
46	2.361	1.74	1.33	1.15	1.96	1.66	1.32	1.31	0.98

Table 3.5. continued... (part 3 of 5)

Compound	Chemical Shift (δ ppm[a])							
number	H-12α	H-12β	H-14	H-15α	H-15β	H-16α	H-16β	H-17
26	1.16	1.73	1.02	1.61	1.26	2.14	1.47	4.58
27	1.11	1.72	1.00	1.60	1.25	2.13	1.46	4.57
28	1.09	1.75	1.00	1.60	1.28	2.14	1.47	4.58
29	1.09	1.69	0.94	1.59	1.25	2.13	1.46	4.57
30	1.17	1.70	0.94	1.58	1.25	2.13	1.46	4.56
31	1.10	1.70	1.02	1.60	1.25	2.13	1.46	4.57
32	1.05	1.74	0.88	1.49	1.25	1.87	1.43	3.58
33	1.07	1.81	0.95	1.51	1.21	1.87	1.43	3.57
34	1.03	1.81	1.23	1.52	1.27	1.87	1.44	3.57
35	1.11	1.84	0.93	1.54	1.22	1.86	1.44	3.57
36	1.02	1.82	0.81	1.53	1.21	1.86	1.44	3.53
37	1.09	1.81	0.98	1.58	1.24	1.87	1.44	3.58
38	1.34	1.88	1.31	1.90	1.50	2.07	2.45	—
39	1.33	1.86	1.28	1.92	1.52	2.08	2.44	—
40	1.30	1.84	1.22	1.89	1.51	2.08	2.45	—
41	1.41	1.89	1.38	1.93	1.53	2.08	2.45	—
42	1.24	1.64	1.14	1.47	1.34	1.92	1.46	3.64
43	1.24	1.64	1.16	1.47	1.34	1.92	1.46	3.65
44	1.17	1.64	1.16	1.50	1.28	1.92	1.46	3.63
45	1.23	1.72	1.23	1.53	1.32	1.94	1.47	3.66
46	1.25	1.80	1.34	1.96	1.55	2.09	2.46	—

Table 3.5. continued... (part 4 of 5)

Compound number	Chemical shift (δ ppm[a]) C-10 CH_3	C-13 CH_3	other	notes
26	0.990	0.790	*endo*: 0.056; *exo*: 0.409	*b*
27	0.665	0.758	*endo*: 0.157; *exo*: 0.425	*b*
28	—	0.801	*endo*: 0.061; *exo*: 0.480	*b,c*
29	0.790	0.758	*endo*: -0.172; *exo*: 0.530	*b*
30	0.826	0.754	*endo*: 0.089; *exo*: 0.842	*b,d*
31	0.812	0.776	*endo*: -0.145; *exo*: 0.618	*b*
32	—	0.738		*e*
33	—	0.739	H-19: 3.22	*e*
34	—	0.739	H-19: 3.10	*e*
35	—	0.730		*e*
36	—	0.703	H-19: 3.23	*e*
37	—	0.740	H-19: 3.19	*e*
38	—	0.916	H-19: 3.88; C-19 OAc: 2.073	
39	—	0.898	H-19: 4.02; C-19 OAc: 2.133	
40	—	0.882	H-19: 3.30	
41	—	0.904	C-19 CH_2: 0.36, 1.16	
42	—	0.764	H-19: 2.93	*g*
43	—	0.780	H-19: 3.06; 5,6-cyclopropyl: 2.97	*g*
44	—	0.781	H-19: 3.14; 5,6-cyclopropyl: 2.91	*g*
45	—	0.833	H-19: 3.37	*g*
46	—	0.880	C-19 OAc: 2.022	

Table 3.5. continued... (part 5 of 5)

[a] Ring A shifts are from the iterative analysis; others were obtained from the HSQC or 1D spectra.

[b] C-17 OAc: 2.02 ± 0.01 ppm

[c] C-19 CH_2: 3.42 ppm (d, J=11.9 Hz); 3.69 ppm (dd, J=11.9, 5.2 Hz)

[d] C-3β OCH_3: 3.23 ppm

[e] C-17 $OSi(CH_3)_2C(CH_3)_3$: 0.876, 0.002, 0.010 ± .004 ppm

[f] Tightly coupled, shifts approximate.

[g] C-17 $OSi(CH_3)_2C(CH_3)_3$: 0.880, 0.014, 0.024 ± .005 ppm

Table 3.6: ^{13}C Shifts in **26**–**46** (part 1 of 3)

Compound number	Chemical shift (δ ppm)							
	C-1	C-2	C-3	C-4	C-5	C-6	C-7	C-8
26	23.58	9.34	23.32	25.28	39.06	28.35	31.55	35.46
27	37.27	10.00	9.03	28.00	42.75	28.59	31.43	35.16
28	30.25	10.24	8.08	27.93	42.57	28.40	31.13	35.87
29	38.94	7.42	9.59	27.57	38.14	29.25	31.46	35.70
30	40.10	17.07	60.63	30.39	39.92	29.27	31.44	35.61
31	32.35	19.40	8.89	14.32	48.70	29.50	31.69	35.36
32	28.12	35.98	210.30	46.95	30.85	29.90	26.28	35.98
33	23.12	36.02	212.62	45.09	24.76	32.64	26.50	35.86
34	28.75	36.06	210.79	48.15	22.48	27.25	26.51	36.71
35	23.34	37.10	210.56	45.62	30.94	25.37	26.73	36.08
36	20.57	37.51	212.77	43.73	26.27	29.35	25.39	38.67
37	23.53	36.22	210.32	46.27	22.42	25.23	25.44	35.23
38	23.12	36.37	212.02	43.10	24.44	31.68	25.70	35.79
39	27.47	36.21	210.66	47.20	21.31	26.60	25.87	36.82
40	27.61	35.63	212.31	47.89	21.18	25.33	26.23	36.83
41	156.18	124.37	196.69	44.90	21.81	32.66	25.51	35.81
42	24.49	39.13	207.76	48.31	32.40	33.95	21.94	30.08
43	25.46	39.21	209.08	49.90	25.50	21.27	21.87	31.85
44	25.97	39.22	208.98	45.78	27.33	27.63	22.17	32.24
45	26.86	35.44	198.83	126.41	162.47	29.60	21.03	36.50
46	17.31	34.64	210.08	43.87	37.93	32.59	30.59	39.01

Table 3.6. continued... (part 2 of 3)

Compound number	Chemical shift (δ ppm)							
	C-9	C-10	C-11	C-12	C-13	C-14	C-15	C-16
26	52.41	34.25	20.59	36.95	42.70	50.88	23.46	27.55
27	56.87	34.35	20.06	37.01	42.51	50.60	23.50	27.50
28	56.83	38.53	21.57	37.33	42.57	50.80	23.44	27.47
29	53.94	34.45	20.23	36.96	42.38	50.76	23.54	27.50
30	53.82	34.99	20.48	36.97	42.43	50.74	23.59	27.54
31	52.87	34.62	20.85	37.09	42.68	50.85	23.52	27.59
32	47.76	32.19	22.27	37.67	44.55	50.38	23.09	30.92
33	45.21	29.87	24.55	36.98	44.00	49.35	23.19	30.86
34	50.46	26.07	22.97	37.69	44.34	47.62	23.29	30.95
35	39.37	31.62	25.82	36.88	43.24	50.53	23.48	30.71
36	47.96	27.21	26.38	37.14	43.29	49.95	23.29	30.80
37	38.00	24.98	24.56	37.00	43.31	50.36	23.66	30.76
38	45.53	27.92	24.10	31.48	48.26	50.26	21.51	35.69
39	46.33	24.75	23.79	31.97	48.46	50.92	21.61	35.74
40	46.47	25.33	24.23	32.20	48.58	51.16	21.19	35.62
41	44.09	27.95	24.73	31.46	48.27	49.94	21.60	35.67
42	33.96	29.51	25.04	34.77	44.05	48.81	22.75	30.93
43	33.17	28.44	25.22	34.96	43.94	49.00	22.81	30.96
44	32.04	29.15	25.24	34.85	43.68	48.31	23.01	30.84
45	33.61	29.71	24.33	34.95	43.77	48.30	22.88	30.91
46	46.14	26.84	21.48	30.94	47.45	50.87	21.54	35.70

Table 3.6. continued... (part 3 of 3)

Compound number	Chemical shift (δ ppm)						
	C-17	C-18	C-19	Cyclopropyl	OAc	OAc	notes
26	82.98	12.08	16.14	8.52	—	—	[a]
27	82.90	12.07	15.00	11.78	—	—	[a]
28	82.82	12.30	61.11	11.16	—	—	[a]
29	82.92	12.17	11.97	11.40	—	—	[a]
30	82.87	12.03	12.23	18.44	—	—	[a,b]
31	82.95	12.20	12.73	12.37	—	—	[a]
32	81.43	11.90	77.93	—	—	—	[c]
33	81.56	11.62	48.82	—	—	—	[c]
34	81.61	11.75	48.48	—	—	—	[c]
35	81.47	11.49	79.04	—	—	—	[c]
36	81.54	11.45	52.82	—	—	—	[c]
37	81.58	11.39	46.39	—	—	—	[c]
38	221.66	14.14	62.13	—	20.53	171.14	
39	220.47	14.09	64.23	—	20.92	170.61	
40	221.22	14.36	63.40	—	—	—	
41	220.18	14.12	31.31	—	—	—	
42	81.15	11.51	32.52	37.71	—	—	[c]
43	81.29	11.47	32.65	31.71	—	—	[c]
44	81.27	11.20	32.92	26.81	—	—	[c]
45	81.31	11.17	34.21	—	—	—	[c]
46	220.26	13.57	56.85	—	20.68	171.19	

[a] C-17 OAc: 21.16, 171.20 ± 0.1 ppm

[b] C-3 OCH_3: 53.44 ppm

[c] C-17 $OSi(CH_3)_2C(CH_3)_3$: -4.5, -4.8, 18.1, 25.8 ± 0.1 ppm

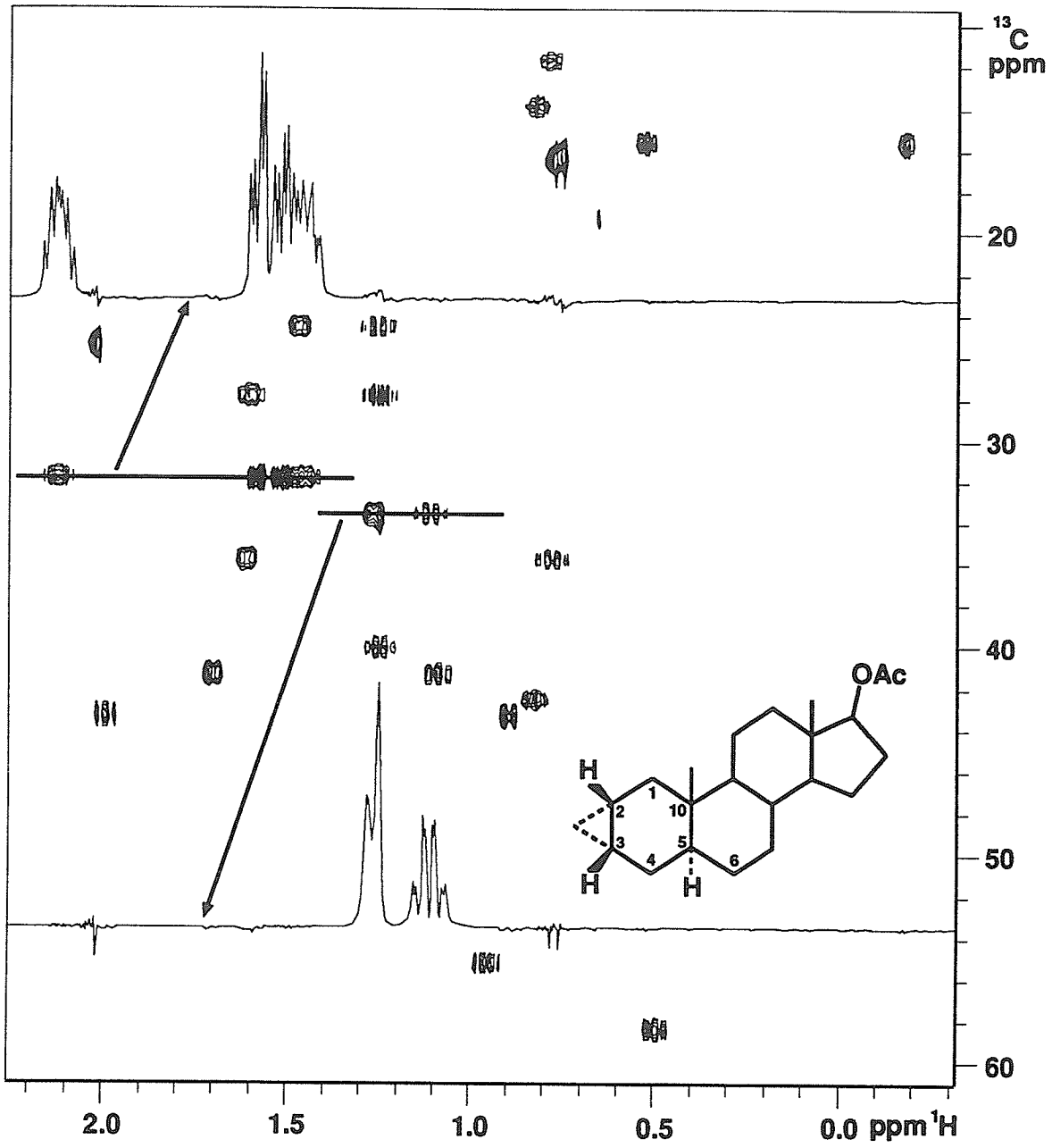

Figure 3.17: Proton detected carbon-proton correlation spectrum of **29**. Note the severe overlap of the ring A protons with other signals. The 1D spectra are rows extracted at the carbon shifts of C-4 and C-6.

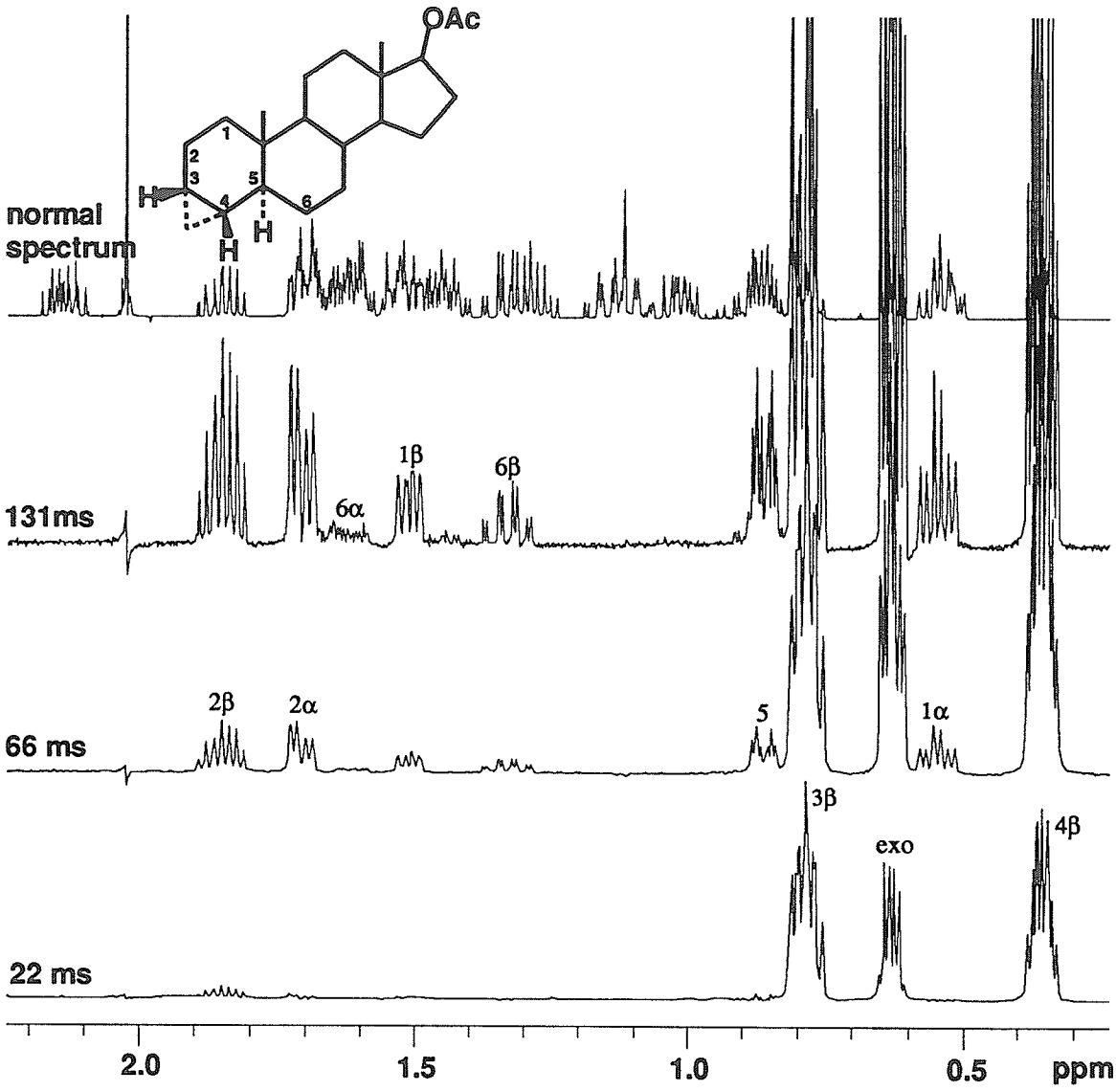

Figure 3.18: 1D TOCSY spectra of **31** at various mixing times with the selective pulse applied to the *endo* cyclopropyl proton at -0.145 ppm. The conventional 500 MHz 1D spectrum is shown at the top. At short mixing times only directly coupled protons are observed while at longer times more remote protons can be seen. Note the excellent suppression of other protons, the faithful preservation of multiplet structure and resolution, and sensitivity equivalent to the conventional spectrum. Each spectrum required approximately twenty minutes of spectrometer time.

In **32-46** the signals from the ring-A protons were sufficiently well separated that analysis could be performed on a resolution enhanced 1-D spectrum, once the shift assignments had been made. Multiplet patterns for ring B, C and D protons, observed directly or *via* the HSQC experiment, were found to be as expected.

Because many instances of tight coupling were observed, the ring A spectra were analyzed by iterative spin simulation, with an example shown in Figure 3.19.

Initial estimates of the shifts and couplings were obtained from rows extracted from the HSQC experiment, but these sub-spectra were not used in the subsequent analysis because they are actually the spectra of the ^{13}C isotopomers with significant isotope shifts. All iterative analyses were therefore performed on regular proton spectra or sub-spectra extracted with the 1-D TOCSY experiment. The simulations for **26 - 31** included all protons in ring-A, plus H-6α and H-6β. The inclusion of the C-6 protons was necessary for the proper analysis of H-5. For **32** to **46** inclusion of the C-6 protons was not necessary because of the break in the spin system at the quaternary C-5. The ring A coupling constants resulting from these analyses are reported in Table 3.7.

3.2.3 Conformational Analysis

In ring fused cyclopropyl compounds such as **26-31** and **46**, the H-C-C bond angles in the cyclopropane ring differ substantially from tetrahedral. An extension of the Karplus equation by Smith and Barfield to include the effects of H-C-C angle[28] has proven to be moderately successful, except at dihedral angles near 180°, where a vicinal coupling of 18 Hz was predicted. A later re-parameterization[31] with new data predicts a more reasonable *anti* coupling of 11.7 Hz, but for a tetrahedral geometry predicts a larger coupling at 0° than at 180°, and is somewhat poorer than the original in predicting known cyclopropane couplings. We have therefore elected to use the original parameters for estimating torsion angles adjacent to the cyclopropane ring in **26 - 31**. The original parameter set predicts a minimum coupling of *ca.* 0 Hz at

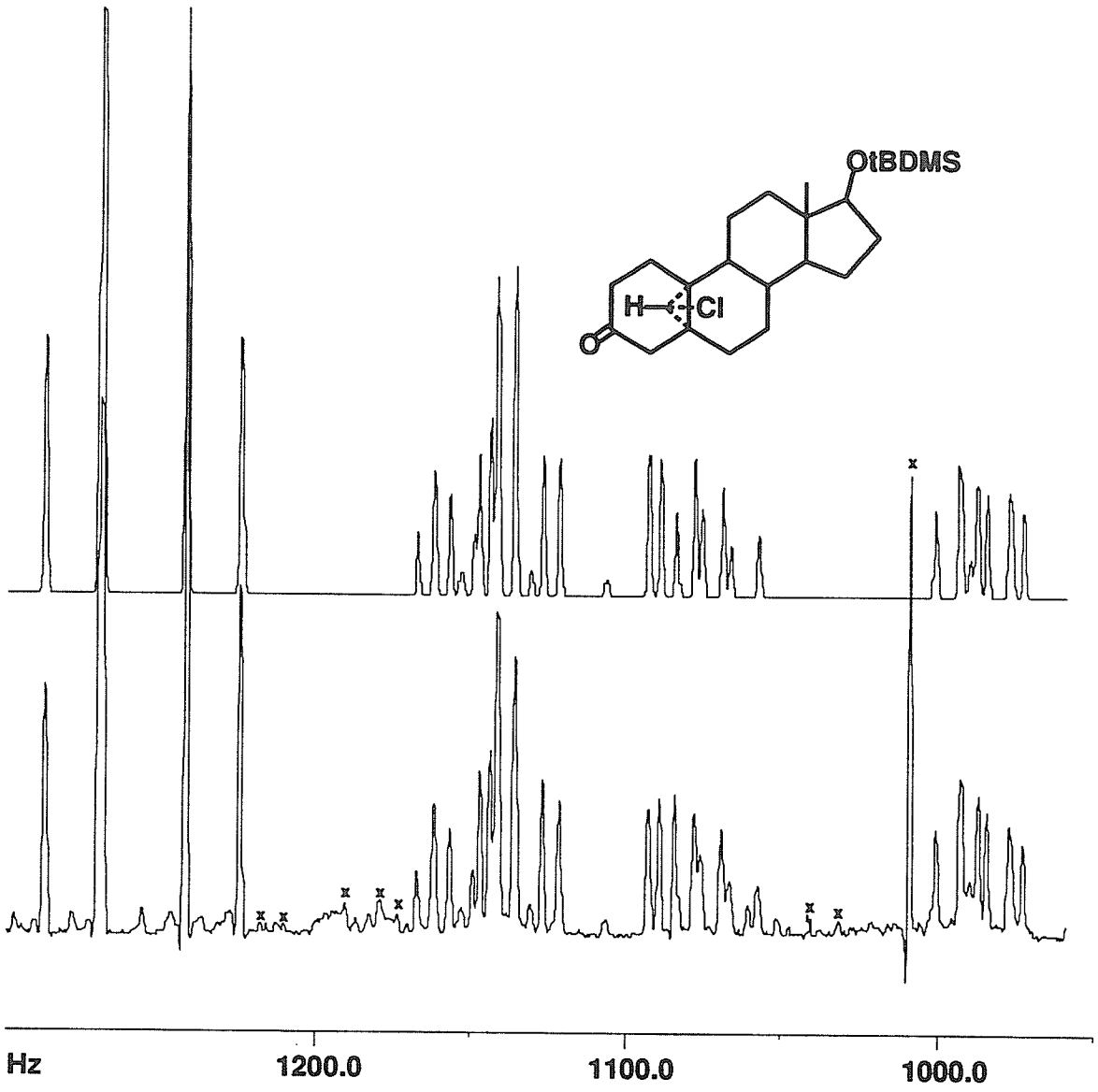

Figure 3.19: Experimental and simulated 500 MHz ring A spectrum of **37**. Top: simulated spectrum. Bottom: resolution enhanced spectrum. Peaks labelled with an "x" are impurities.

Table 3.7: Ring A coupling constants in Hz for **26** - **46** (part 1 of 4)

Compound	Coupling constant (Hz[a])				
number	$^2J(1\alpha,1\beta)$	$^3J(1\alpha,2\alpha)$	$^3J(1\alpha,2\beta)$	$^3J(1\beta,2\alpha)$	$^3J(1\beta,2\beta)$
26	—	—	—	—	8.86(7)
27	-13.87(4)	6.56(5)	—	0.0(3)	—
28	-14.47(3)	5.93(3)	—	0.0(3)	—
29	-13.99(7)	—	2.50(3)	—	9.59(3)
30	-14.17(3)	—	2.44(3)	—	9.75(3)
31	-13.23(5)	5.97(7)	13.16(5)	1.80(5)	6.65(4)
32	-14.53(3)	5.63(6)	2.06(4)	14.18(6)	4.46(4)
33	-14.67(4)	5.97(6)	2.19(5)	13.57(6)	4.50(6)
34	-14.41(3)	6.40(4)	8.91(4)	6.60(5)	6.10(5)
35	-15.50(2)	4.64(3)	14.04(2)	2.31(3)	5.88(2)
36	-15.35(5)	4.13(5)	14.31(4)	2.00(8)	5.74(8)
37	-14.97(5)	6.69(6)	5.14(6)	10.30(6)	5.89(6)
38	-14.70(2)	6.76(4)	3.21(4)	12.22(3)	5.41(4)
39	-14.21(6)	5.58(6)	8.56(5)	7.52(6)	5.75(6)
40	-14.27(2)	6.04(2)	7.63(2)	8.19(2)	5.86(2)
41	—	[b]	—	—	—
42	-14.2(2)	6.9(2)	3.7(2)	11.6(2)	6.2(2)
43	-14.04(5)	6.73(5)	2.70(4)	13.21(4)	4.80(4)
44	-14.01(3)	6.49(3)	3.02(3)	12.85(3)	4.87(3)
45	-13.81(9)	5.09(8)	2.70(9)	14.21(8)	4.43(9)
46	[c]	5.62(2)	1.97(2)	—	—

Table 3.7 continued... (part 2 of 4)

Compound number	Coupling constant (Hz[a])				
	$^2J(2\alpha,2\beta)$	$^3J(2\alpha,3\alpha)$	$^3J(2\alpha,3\beta)$	$^2J(2\beta,3\alpha)$	$^3J(2\beta,3\beta)$
26	—	—	—	1.88(5)	8.85(6)
27	—	9.11(6)	—	—	—
28	—	9.03(4)	—	—	—
29	—	—	—	—	8.45(3)
30	—	—	—	—	—
31	-14.15(3)	—	0.0(3)	—	6.62(6)
32	-17.12(3)	—	—	—	—
33	-17.94(5)	—	—	—	—
34	-18.80(4)	—	—	—	—
35	-18.05(2)	—	—	—	—
36	-18.85(8)	—	—	—	—
37	-19.29(6)	—	—	—	—
38	-17.31(4)	—	—	—	—
39	-18.65(4)	—	—	—	—
40	-18.73(2)	—	—	—	—
41	—	—	—	—	—
42	-15.2(2)	—	—	—	—
43	-14.70(4)	—	—	—	—
44	-14.90(3)	—	—	—	—
45	-17.17(9)	—	—	—	—
46	-18.61(2)	—	—	—	—

Table 3.7. continued... (part 3 of 4)

Compound number	Coupling constant (Hz[a])				
	$^3J(3\alpha,3\beta)$	$^3J(3\alpha,4\alpha)$	$^3J(3\alpha,4\beta)$	$^3(3\beta,4\alpha)$	$^3J(3\beta,4\beta)$
26	-14.35(4)	7.57(6)	12.52(4)	1.47(6)	7.43(4)
27	—	9.78(3)	3.48(4)	—	—
28	—	9.58(4)	2.53(3)	—	—
29	—	—	—	0.0(3)	5.99(6)
30	—	—	—	—	—
31	—	—	—	—	8.68(6)
32	—	—	—	—	—
33	—	—	—	—	—
34	—	—	—	—	—
35	—	—	—	—	—
36	—	—	—	—	—
37	—	—	—	—	—
38	—	—	—	—	—
39	—	—	—	—	—
40	—	—	—	—	—
41	—	—	—	—	—
42	—	—	—	—	—
43	—	—	—	—	—
44	—	—	—	—	—
45	—	—	—	—	—
46	—	—	—	—	—

Table 3.7. continued... (part 4 of 4)

Compound number	Coupling constant (Hz[a])				
	$^3J(4\alpha,4\beta)$	$^3J(4\alpha,5)$	$^3J(4\beta,5)$	$^3J(5,6\alpha)$	$^3J(5,6\beta)$
26	-14.66(4)	3.0	12.75(6)	2.38(4)	13.47(4)
27	-14.97(3)	4.58(2)	12.32(3)	2.63(3)	12.36(3)
28	-13.83(4)	5.13(4)	12.70(3)	3.47(3)	12.99(2)
29	-12.93(2)	4.60(6)	12.48(7)	4.64(4)	13.35(4)
30	4.66(2)	13.10(2)	4.47(6)	13.75(6)	
31	—	—	4.05(4)	3.95(6)	12.79(6)
32	-17.20(2)	—	—	—	—
33	-16.81(4)	—	—	—	—
34	-17.53(3)	—	—	—	—
35	-16.32(3)	—	—	—	—
36	-16.17(4)	—	—	—	—
37	-17.69(4)	—	—	—	—
38	-16.46(2)	—	—	—	—
39	-17.59(4)	—	—	—	—
40	-17.06(2)	—	—	—	—
41	-18.43(5)	—	—	—	—
42	-15.2(2)	—	—	—	—
43	-14.70(4)	—	—	—	—
44	-15.38(3)	—	—	—	—
45	—	—	—	—	—
46	-18.38(3)	7.78(2)	11.91(3)	3.34(3)	12.23(4)

[a] Numbers in parentheses are twice the standard deviation in the least significant digit.

[b] $^3J(1,2)$=10.16(5) Hz.

[c] $^3J(1\alpha,19)$=7.43(2) Hz.

Table 3.8: Cyclopropane fragment coupling constants in **26-31** and **41**

Compound	Coupling constant (Hz[a])				
number	$^2J(exo, endo)$	$^3J(exo, A)$[b]	$^3J(exo, B)$	$^3J(endo, A)$	$^3J(endo, B)$
26	-4.81(3)	8.90(3)	8.95(3)	5.83(3)	4.93(3)
27	-4.56(2)	9.17(2)	9.16(2)	6.01(2)	4.54(3)
28	-4.71(2)	9.04(2)	9.07(2)	5.87(2)	4.64(2)
29	-4.39(4)	8.79(5)	8.81(3)	4.84(5)	5.43(2)
30	-5.18(5)	10.70(5)	—	5.98(5)	—
31	-4.37(3)	8.80(4)	8.69(4)	5.93(4)	4.41(3)
41	-4.33(5)	—	—	—	—

[a] Numbers in parentheses are twice the standard deviation in the least significant digit.

[b] A and B refer to the protons on the higher and lower numbered carbon positions, respectively.

a dihedral angle of 85° while the newer parameter set predicts a minimum coupling of *ca.* 1.0 Hz at a dihedral angle of 95°. The fact that many near zero (certainly less than 0.5 Hz) vicinal couplings were observed was further impetus for us to use the original parameter set. This formulation makes no allowance for the effects of substituent electronegativity on couplings, but this is not a problem in **26** - **31**, which lack electronegative substituents near stereospecific couplings.

The equation of Haasnoot *et al*[29] was used for the estimation of all other torsion angles derived from vicinal couplings. This relationship is shown in Figure 1.2 and is given formally by:

$$^3J = P_1 \cos^2\phi + \sum_i \Delta\chi_i\{P_3 + P_4 \cos^2(\zeta_i\phi + P_5|\Delta\chi_i|)\} \qquad (3.1)$$

where P_1 to P_5 are empirically determined parameters, $\Delta\chi_i$ are the substituent Huggins group electronegativities relative to hydrogen and ζ_i is ± 1, depending on the orientation of the substituent. ϕ Is the dihedral angle between the coupling protons.

For the 3-one steroids **32-46**, the C-2–C-3 and C-3–C-4 torsion angles were estimated from the geminal proton couplings at C-2 and C-4 by the valence bond method originally proposed by Barfield and Grant.[4,5,42,41] A molecular orbital theory of geminal couplings,[46,47] however, and some experimental evidence,[48] suggest a positive contribution to ^2J at C–C torsion angles in the vicinity of 90° rendering the Barfield-Grant equation unreliable in this region. Fortunately, such torsion angles are rarely encountered in 6 membered rings. A maximum in the magnitude of the geminal coupling of -18.5 Hz is predicted when the C=O bond bisects the H–C–H angle (C–C torsion angle of 0). However, abnormally large geminal couplings were observed between protons that are not adjacent to a formal π bond but are adjacent to a cyclopropyl group, for example, $^2J(1\alpha, 1\beta)$ in **32-40**. This implies that there may be a substantial contribution to the geminal coupling from the π-like character of the cyclopropyl group. From the data in Table 3.7 it can be seen that the effect on ^2J can be as large as -2 Hz, but no clear relationship between the orientation of

the cyclopropyl group and the magnitude of the effect can be inferred. The use of $^2J(4\alpha, 4\beta)$ for the estimation of the C-3–C-4 torsion angle in **32-41** was therefore complicated by the presence of the 5,10-cyclopropane ring as it is difficult to separate the contribution of the cyclopropane ring and the C-3 carbonyl. Unusually large $|^2J|$s adjacent to cyclopropane rings have been reported previously,[221] but without any comment.

It was decided, therefore, to apply as a correction to $^2J(4\alpha, 4\beta)$ the magnitude of the effect observed on $^2J(1\alpha, 1\beta)$. Although the geminal protons on C-1 have a similar relationship to the cyclopropane ring as those on C-4, this correction must be regarded as an approximation because of the unknown and probably stereospecific nature of the effect. Nevertheless, when combined with other data the torsion angle estimated from the corrected $^2J(4\alpha, 4\beta)$ is sufficiently accurate for the determination of the ring A conformation.

Ring A Cyclopropanosteroids (26 - 31)

Dreiding models predict that the hydrogens at the junction of the cyclopropane and cyclohexane rings could exist in two probable situations. If the axial cyclohexyl proton on the adjacent carbon is *anti* to the cyclopropane ring the dihedral angles between the ring-junction cyclopropyl proton and the adjacent cyclohexyl protons will be approximately 35° to the axial proton (^3J *ca.* 7.5 Hz) and 80° to the equatorial proton (^3J *ca.* 0 Hz). Vicinal couplings of < 0.5 Hz are observed between ring-junction cyclopropyl protons and adjacent equatorial protons in **27**, **28**, **29** and **31**. The couplings to the corresponding axial protons are in the range of 5.9-6.5 Hz, slightly lower than the value predicted by the Barfield-Smith equation but still within reasonable agreement. If the axial proton on the adjacent carbon is *syn* to the cyclopropane ring, then the dihedral angles will be approximately 0° to the equatorial proton (^3J *ca.* 11 Hz) and 110° to the axial proton (^3J *ca.* 3 Hz). The corresponding observed couplings are 8.85 to 9.59 Hz and 1.88 to 3.48 Hz, respectively.

In 1α,2α-methylene-5α-androstan-17β-ol acetate (**26**), the couplings from H-2β to H-3α and H-3β correspond to a conformation with H-3α axial, with $^3J(2\beta,3\beta)$ somewhat smaller than the predicted value of 11 Hz. A 4.1% NOE was observed from the *endo* cyclopropyl proton to the axial C-3 proton, identifying it as H-3α. A 5.9% NOE was observed from the C-10 methyl to H-1β. The couplings between the protons at C-3, C-4 and C-5 are typical of a cyclohexane in a chair conformation, with the overall ring-A conformation being a 4β,5α half-chair (Figure 3.21.)

In 2β,3β-methylene-5α-androstan-17β-ol acetate (**27**) and 2β,3β-methylene-5α-androstan-17,19-diol 17-acetate (**28**), a characteristic zero coupling between H-1β and H-2α implies that H-1α must be axial and *anti* to the cyclopropane ring. $^3J(1\alpha,2\alpha)$ is 6.56 Hz and 5.93 Hz in **27** and **28** respectively (Table 3.7.) Although these couplings are slightly lower than the predicted 7.5 Hz, they are still consistent with an axial H-1α. The H-1β assignment was confirmed by the observation in **27** of a 3.1% NOE from the C-10 methyl and H-1β. Irradiation of H-1β resulted in NOEs of 7.9% to H-11α, 3.7% to the C-10 methyl, 1.5% to the *endo* cyclopropyl proton, 2.6% to H-2α, 20% to H-1α, and -1.0% to H-9. The negative NOE to H-9 is the result of a three-spin effect involving H-1β, H-1α and H-9 and indirectly indicates close proximity of H-1α and H-9, which is further confirmation of the 1,3 diaxial relationship of these protons (Figure 3.20).

$^3J(3\alpha,4\alpha)$ and $^3J(3\alpha,4\beta)$ suggest an axial H-4β, as does $^3J(4\beta,5)$. A 3.6% NOE was observed from the C-10 methyl to the axial C-4 proton in **27** while in **28** a 5.1% NOE was observed from the high-field C-19 proton to the axial C-4 proton, supporting this conclusion. A comparison of the ^{13}C shifts in **27** and **28** shows that the shift of C-5 is almost unaffected by hydroxyl substitution at C-19, while C-1 is shielded by 7 ppm. This is most easily explained as a γ-*gauche* effect[222,223] resulting from the C-19 hydroxyl lying *anti* to C-5. The ring A conformation in **27** and **28** is best described as a 5α,10β half-chair (Figure 3.21), with no significant conformational changes induced by the C-19 hydroxyl group.

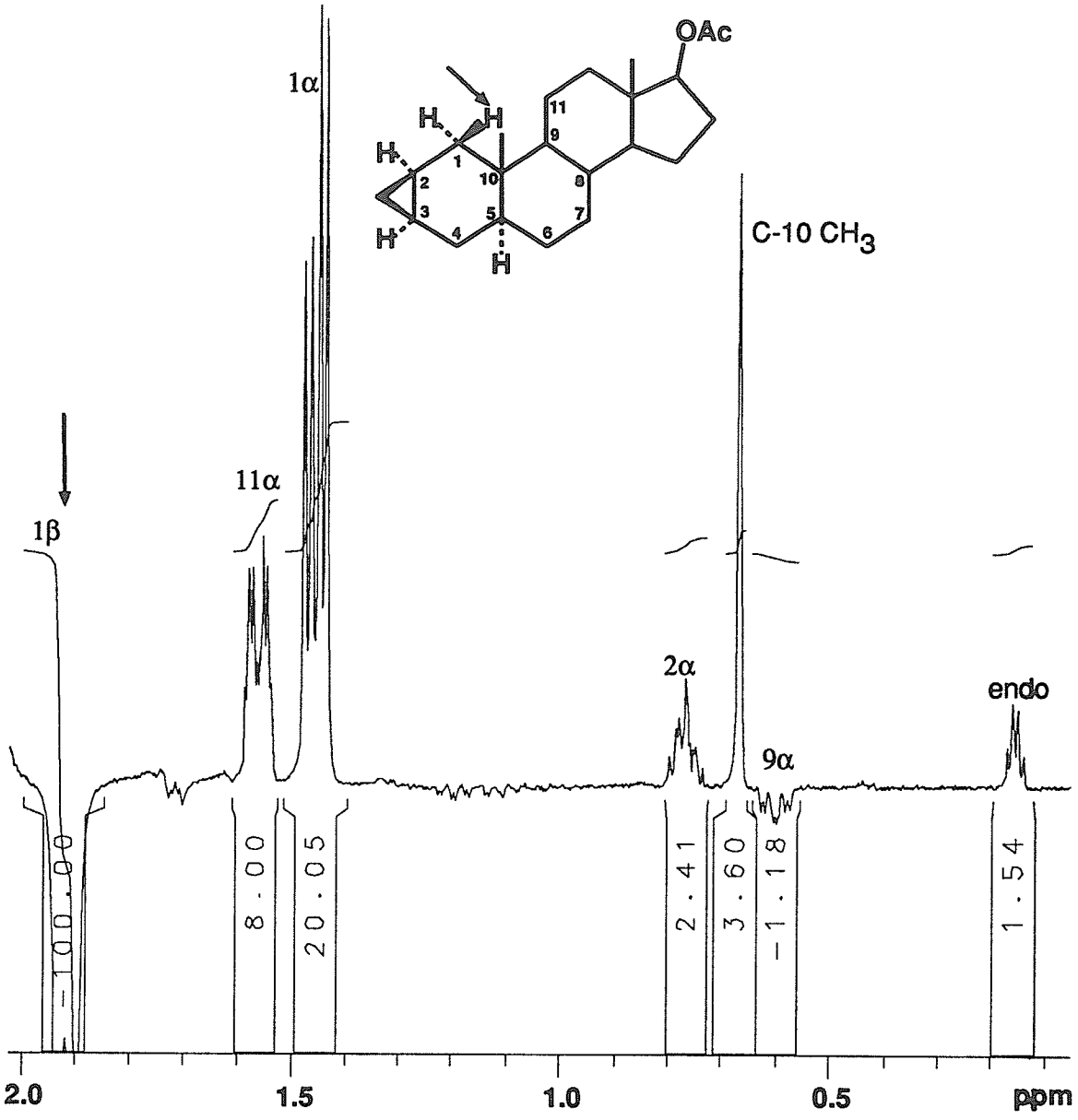

Figure 3.20: Steady state NOE difference spectrum of **27** irradiating H-1β. The geminal NOE from H-1β to H-1α results in an indirect negative NOE (three spin effect) to H-9α from H-1α. This strongly suggests a 1,3-diaxial relationship for these protons.

2α,3α-Methylene-5α-androstan-17β-ol acetate (**29**) and 3β-methoxy-2α,3α-methylene-5α-androstan-17β-ol acetate **30** exist in essentially the same half-chair conformation as **27** and **28**. However, the axial H-1α is *syn* while the axial H-4β is *anti* to the cyclopropane ring. In **29**, $^3J(3\beta,4\alpha)$ is 0 Hz while $^3J(3\beta,4\beta)$ is 5.99 Hz, consistent with an axial H-4β. Axial coupling is observed between H-4β and H-5 in both molecules. NOEs were observed from the *endo* cyclopropyl proton to H-1α (4.9%), H-5 (6.9%) and to the *exo* cyclopropyl proton (32%). A 5% NOE from the C-10 methyl group to the equatorial C-1 proton in **29** confirmed the assignment of this proton as H-1β. $^3J(1\alpha,2\beta)$ and $^3J(1\beta,2\beta)$ are consistent with a C-1–C-2 endocyclic torsion angle of *ca.* 10°. In **29** $^3J(3\beta,4\alpha)$ and $^3J(3\beta,4\beta)$ are consistent with a C-3–C-4 endocyclic torsion angle of *ca.* 10°.

In 3α,4α-methylene-5α-androstan-17β-ol acetate (**31**), H-1α and H-2β clearly show axial couplings, with the assignment of the protons confirmed by the observation of NOEs from the C-10 methyl group to H-1β (1.8%), H-2β (4.5%) and H-4β (3.9%). A $^3J(2\alpha,3\beta)$ of 0 Hz (dihedral angle *ca.* 80°) and a $^3J(2\beta,3\beta)$ of 6.6 Hz are as expected for an axial H-2β *anti* to the cyclopropane ring, while a $^3J(4\beta,5\alpha)$ of 4.0 Hz is consistent with H-5 axial and *syn* to the cyclopropane ring. NOEs were observed from the *endo* cyclopropyl proton to H-5 (4.2%) and the *exo* cyclopropyl proton (28%), and from H-4β to H-5 (1.0%), H-6β (3.2%) and the *exo* cyclopropyl proton (2.9%). These data are consistent with a 1α,10β half-chair conformation for ring A (Figure 3.21.)

5β,19β-Cycloandrostanes (32-34, 38-41)

In 17β-*tert*-butyldimethylsiloxy-19,19-dichloro-5β,19-cycloandrostan-3-one (**32**), 17β-*tert*-butyldimethylsiloxy-19(S)-chloro-5β,19-cycloandrostan-3-one (**33**) and 19(S)-acetoxy-5β,19-cycloandrostane-3,17-dione (**38**), which all have a C-19 substituent over ring A, H-1β is axial. A relatively low value for $^3J(1\alpha,2\beta)$ and relatively high values for $^3J(1\alpha,2\alpha)$ and $^3J(1\beta,2\alpha)$ suggest a fair degree of ring flattening. $^2J(2\alpha,2\beta)$ is

consistent with a C-2–C-3 endocyclic torsion angle of 10 to 20 °, while $^2J(4\alpha, 4\beta)$, corrected for the presence of the cyclopropane ring, is consistent with a C-3–C-4 endocyclic torsion angle of 35 to 40 °. These data are consistent with an "inverted boat" conformation (Figures 3.21 and 3.22) with C-1 and C-4 at the bow/stern positions. NOEs are observed from H-4β to H-1β in both **32** (1.7%) and **33** (2.1%), consistent with the proposed conformation. Overlap of the H-4β signal with other signals prevented a similar measurement in **38**. An alternative 2α,3β half-chair conformation requires much lower values for $^2J(2\alpha, 2\beta)$ and $^2J(4\alpha, 4\beta)$ and is inconsistent with the observed NOEs.

The conformation of **33** and **38** is noteworthy in that the ring A conformation places the C-3 carbonyl in a significantly different location than in a 4-en-3-one steroid such as testosterone, the natural substrate for the aromatase enzyme.

In 17β-*tert*-butyldimethylsiloxy-19(R)-chloro-5β,19-cycloandrostan-3-one **34**, NOEs observed from H-19 to H-1β (2.3%), H-2β (4.1%) and H-4β (2.9%) confirmed the assignments of these signals. H-1α and H-2β are axial, although the value for $^3J(1\alpha, 2\beta)$ is considerably lower than expected for a diaxial coupling. Furthermore, the equatorial-equatorial coupling, $^3J(1\beta, 2\alpha)$, is higher than expected, suggesting considerable distortion of the ring or a conformational equilibrium. This is even more pronounced in 19(R)-acetoxy-5β,19-cycloandrostane-3,17-dione (**39**) and 19(R)-hydroxy-5β,19-cycloandrostane-3,17-dione (**40**) where there appear to be no clear axial or equatorial environments for the C-1 and C-2 protons. Irradiation of H-19 (the cyclopropyl proton) in **39** resulted in NOEs to H-1β (2.9%), H-2β (4.5%) and H-4β (2.3%); irradiation of H-19 in **40** resulted in NOE's to H-1β (3.2%), H-2β (2.4%) and H-4β (4.1%) . The geminal couplings at C-2 and C-4 indicate a near zero C-2–C-3 torsion angle and a C-3–C-4 torsion angle of *ca.* 40°. These angles are consistent with a boat conformation[215] with H-1α, H-2β and H-4α axial, or an alternative boat conformation with H-1β, H-2α and H-4β axial, as shown in Figures 3.21 and 3.22. An equilibrium between these two conformations is the most reasonable explanation

for the atypical vicinal couplings observed at C-1 and C-2. The NOE (0.9%) observed from H-4β to H-1β in **34** is small compared with that observed in **32** and **33**. This observation, and the relative sizes of $^3J(1\alpha, 2\beta)$ and $^3J(1\beta, 2\alpha)$, suggests that in **34** the conformer with H-1α and H-4α axial is predominant. Spectral overlap prevented NOE measurements from the C-4 protons in **39** and **40**, however, the relative sizes of $^3J(1\alpha, 2\beta)$ and $^3J(1\beta, 2\alpha)$ suggest that the two possible conformations must have comparable energies.

The only stereospecific coupling in 5β,19-cycloandrost-1-ene-3,17-dione (**41**) is $^2J(4\alpha, 4\beta)$, and the relatively high value indicates a very low C-3–C-4 torsion angle, consistent with the expected near planarity of ring A.

5α,19α-Cycloandrostanes (35-37)

In 17β-*tert*-butyldimethylsiloxy-19,19-dichloro-5α,19α-cycloandrostan-3-one **35**, H-1α can be inferred to be axial because of a 6.1% NOE observed from the equatorial H-1β to H-11β. Unfortunately, overlap of the H-1β and H-2α resonances prevented a similar measurement in 17β-*tert*-butyldimethylsiloxy-19(S)-chloro-5α,19α-cycloandrostan-3-one **36**. The values for $^3J(1\alpha, 2\alpha)$ and $^3J(1\beta, 2\beta)$ are suggestive of a C-1–C-2 torsion angle of *ca.* 50°. $^2J(2\alpha, 2\beta)$ indicates C-2–C-3 torsion angle of less than 20°, while $^2J(4\alpha, 4\beta)$ indicates a C-3–C-4 torsion angle of *ca.* 50°. NOEs are observed from H-4α to H-1α in both **35** (3.1%) and **36** (3.7%). These 1,4 diaxial NOEs are normally only observed in boat conformations. The only conformation consistent with these data is a boat conformation with H-1α, H-2β and H-4α axial (Figure 3.22.) An alternative 2β,3α half-chair conformation is also consistent with the vicinal couplings, but would require a $^2J(2\alpha, 2\beta)$ closer to -17 Hz and is inconsistent with the NOE measurements. A recent X-ray structure of **35**[213] is in agreement with the boat conformation proposed above.

In 17β-*tert*-butyldimethylsiloxy-19(R)-chloro-5α,19α-cycloandrostan-3-one **37**, H-1β and H-2α are axial, although $^3J(1\beta, 2\alpha)$ is smaller and $^3J(1\alpha, 2\beta)$ is larger than

expected, suggestive of the conformational equilibrium as postulated above for **39** and **40**. NOEs from H-19 to H-4α (2.1%), H-2α (4.2%) and H-1α (1.3%) confirmed the assignment of these resonances. A 1,4 diaxial NOE of 1.1% was observed from H-4β to H-1β and a 3.9% diaxial NOE was observed from H-4β to H-6β. The extremely large negative value for $^2J(2\alpha, 2\beta)$ clearly indicates a near zero C-2–C-3 torsion angle, while $^2J(4\alpha, 4\beta)$ indicates a C-3–C-4 torsion angle of *ca.* 45°. These data are all consistent with a boat conformation but, in contrast to **35** and **36**, the predominant conformer has H-1β, H-2α and H-4β axial (Figure 3.22.)

9α,19α-Cycloandrostanes (42-45)

In 19(S)-bromo-17β-(*tert*-butyldimethylsiloxy)-5β,6β-dibromomethylene- 9α,19-cyclo-10α-androstan-3-one (**42**), 19(S)-5β,6β-[(R)-bromomethylene]-17β(*tert*-butyldimethylsiloxy)- 9α,19-cyclo-10α-androstan-3-one (**43**) and 19(S)-5β,6β-[(S)-bromomethylene]-17β(*tert*-butyldimethylsiloxy)- 9α,19-cyclo-10α-androstan-3-one (**44**), H-1α and H-2β are axial. The very low values for $^2J(2\alpha, 2\beta)$ and $^2J(4\alpha, 4\beta)$ in **42-44** indicate C-2–C-3 and C-3–C-4 torsion angles of *ca.* 55°. The only conformation consistent with these data is a 2α,3β half-chair (Figure 3.22.)

In 19(S)-5β,6β-17β(*tert*-butyldimethylsiloxy)-9α,19- cyclo-10α-androst-4-en-3-one (**45**) H-1β and H-2α are axial. $^2J(2\alpha, 2\beta)$ suggests a decrease in the C-2–C-3 torsion angle to *ca.* 40°, with ring-A best being described as having a 1β sofa conformation (Figure 3.22.)

19(R)-Acetoxy-1β,19-cyclo-5α-androstane-3,17-dione (46)

From the value of $^3J(4\beta, 5\alpha)$ it can be clearly seen that H-4β is axial. $^2J(4\alpha, 4\beta)$ and $^2J(2\alpha, 2\beta)$ are similar and suggest C2–C-3 and C-3–C-4 torsion angles of *ca.* 10 - 20°. The couplings between H-1 and the C-2 protons are most consistent with an H-2α which is axial and *anti* to the cyclopropane ring. However, $^3J(1\alpha, 2\alpha)$ is slightly smaller and $^3J(1\alpha, 2\beta)$ is larger than expected for this situation, and with

those observed for similar situations in **27** - **29** and **31**; possibly the result of a significant opening of the C-1–C-2 torsion angle.

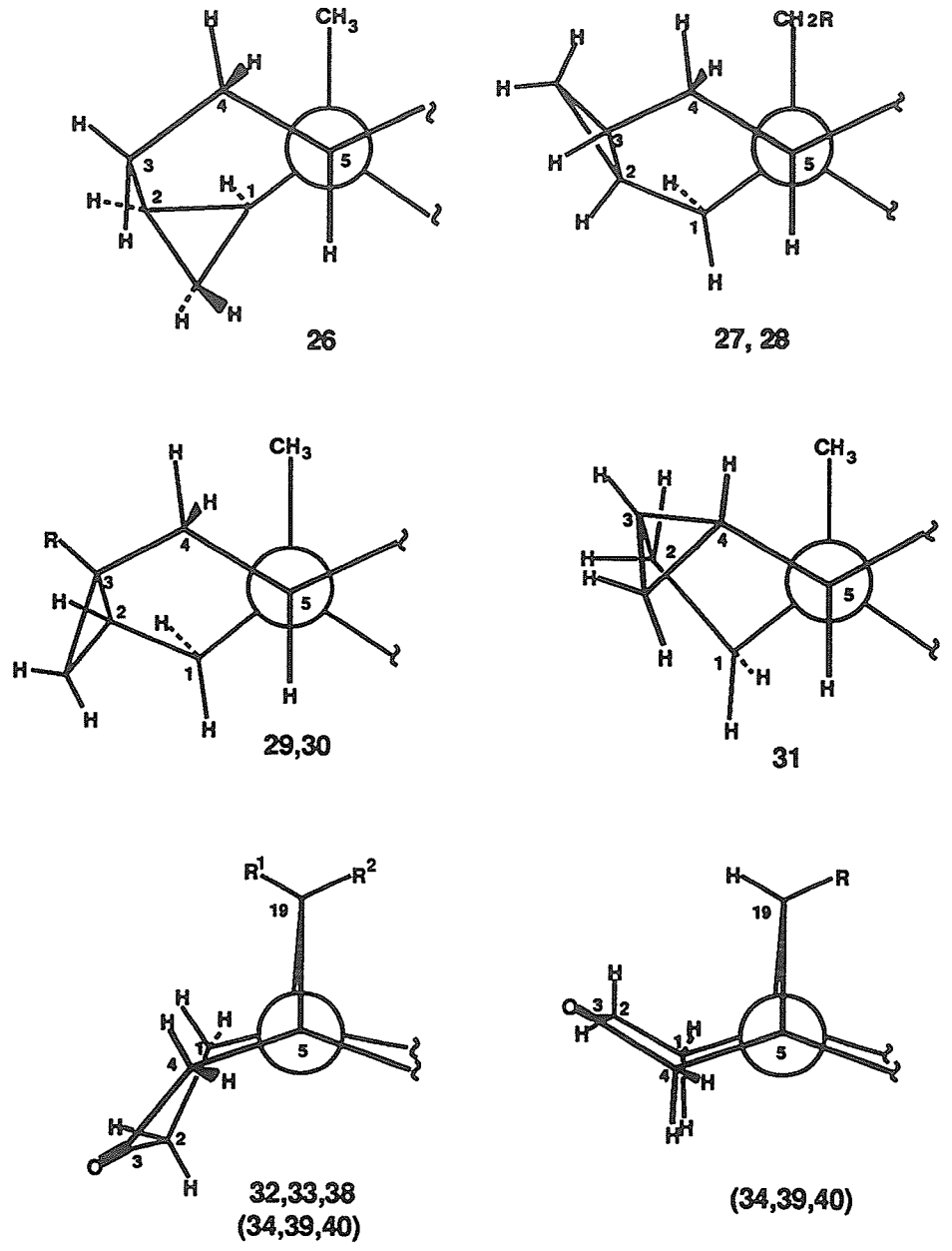

Figure 3.21: Ring A conformations in **26** - **40** viewed along the C-5–C10 bond. Numbers in parentheses indicate the presence of a conformational equilibrium.

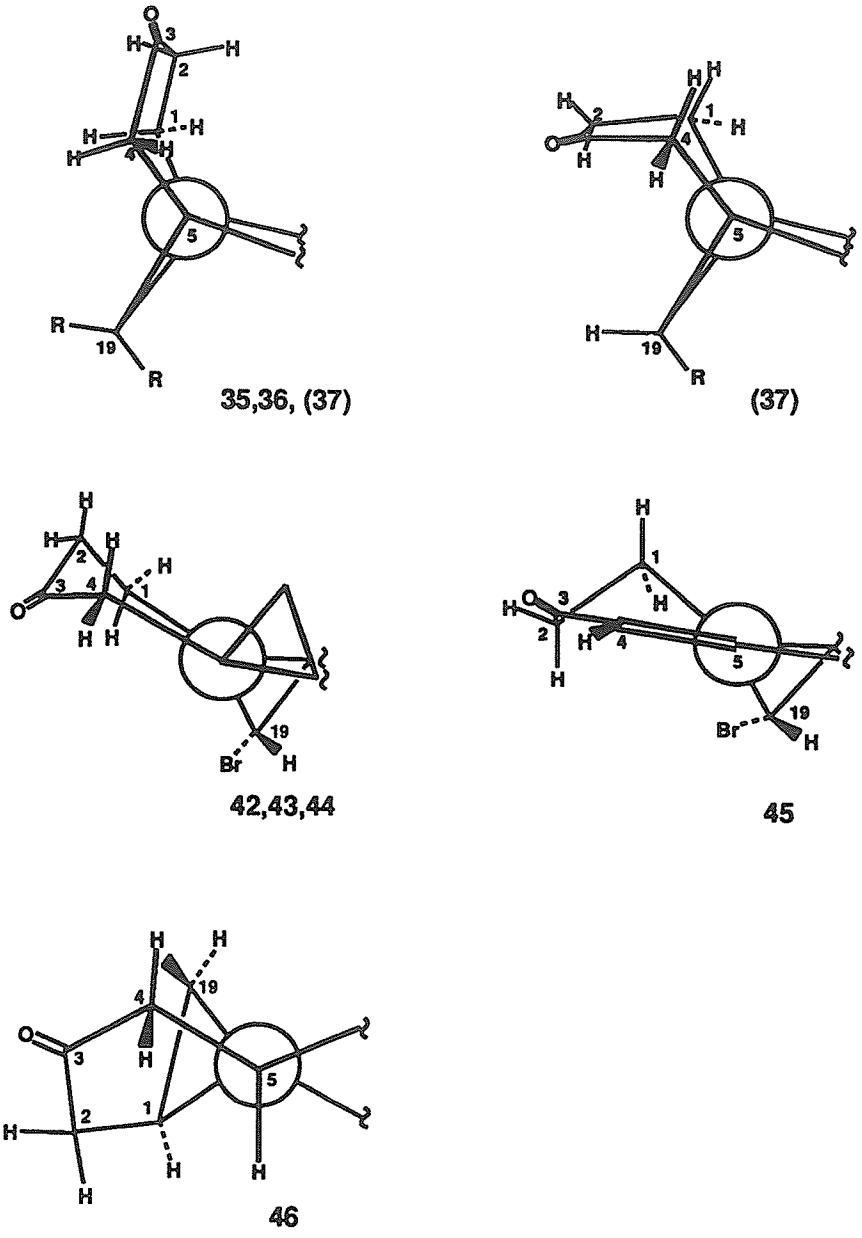

Figure 3.22: Ring A conformations in **35** - **46** viewed along the C-5–C-10 bond. Numbers in parentheses indicate the presence of a conformational equilibrium.

Chapter 4

Discussion

4.1 Cardiotonic Pregnanes

4.1.1 ^{13}C Shifts

Habermehl *et al*[170] have observed that in 20-hydroxy-5β,14β-pregnanes C-16 and C-20 are shielded by 8.4 and 5 ppm, respectively, in the S-epimer compared with the corresponding R-epimer. They attributed these differences to restricted rotation about the C-17–C-20 bond resulting in the C-21 methyl being closer, on average, to the plane of ring D. They suggested that this effect could be a general method for elucidation of C-20 stereochemistry in 20-substituted 14β-pregnanes.

Inspection of the ^{13}C shifts in Table 3.3 shows that this relationship holds true for compounds **3** through **10**, with the shielding of C-16 ranging from 3.6 to 8.4 ppm and the shielding of C-20 ranging from 3.5 to 6.3 ppm. However, in the C-20 nitro-compounds **1** and **2**, C-16 and C-20 are observed to be deshielded in the S-epimer. This exception to the above rule renders it of doubtful value for the determination of C-20 stereochemistry.

The reasons for this exception become clear when the side-chain conformation is taken into account (Figure 3.1). In the S-epimers **4**, **6**, **8** and **10**, both the substituent

and methyl group are *gauche* to C-16. In the corresponding R-epimers **3**, **5**, **7** and **9**, either the substituent or the C-20 methyl group lie *anti* to C-16. C-16 is therefore *gauche* to only one of either the C-20 methyl group or the substituent. Because substituents, including methyl groups, are known to have greater shielding when *gauche* than when *anti*,[224] C-16 in the S-epimers is shielded relative to the corresponding R-epimer. Using published values[224] for the *gauche* and *anti* substituent effects it is possible to calculate a predicted shift difference of 7.2 ppm between the R and S-alcohols **5** and **6**, in good agreement with the observed shift difference of 6.3 ppm (Table 3.3). In the C-20 nitro compounds **1** and **2**, however, H-20 is *gauche* to C-16 in both the R and S-epimers. Shift differences at C-16 must therefore arise primarily from differences in the magnitude of the γ-*gauche* effect between the two groups.* In this case, C-16 in the R-epimer becomes slightly shielded (0.2 ppm) relative to the S-epimer.

The situation for Δ^{14}-compounds **11** - **16** parallels that observed for **1** and **2**. In each case H-20 is *gauche* to C-16, and C-16 is therefore gauche to the methyl group in the R-epimers and *gauche* to the substituent in the S-epimers. The C-16 shift differences are therefore small ($<$ 1 ppm) and are not characteristic of the C-20 stereochemistry.

The shielding of C-20 in the S-epimers **6**, **8** and **10** relative to the corresponding R-epimers **5**, **7** and **9** is most likely a result of steric compression of H-20 and the C-13 methyl group. Such H-H steric interactions are known to cause an upfield shift of the attached carbons. According to the model proposed by Grant,[225] overlapping of the van der Waals radii of closely spaced hydrogens causes a perturbation of the C-H bond which results in a drift of charge towards the carbon. The bonding orbitals at the carbon will thus expand, resulting in an upfield shift of the carbon *via* a change in the paramagnetic shielding term. In the C-20 nitro compounds **1** and **2** and the C-20

*The shielding anisotropies of the N=O bonds in the nitro group are large and, depending on the conformation around the C-N bond, may also influence the shift of C-16.

acetates **3** and **4**, these steric interactions occur in both the R- and S-epimers. In the acetates C-20 is slightly (2.7 ppm) shielded in the S-epimer, suggesting a stronger steric interaction in this epimer. This finding is consistent with the relatively low value of $^3J(17,20)$ (1.9 Hz) in **4** which was earlier postulated to be the result of a twisting of the C-17–C-20 bond away from a fully staggered conformation. In the nitro compounds C-20 is slightly (0.9 ppm) deshielded compared to the R-epimer.

Similar arguments can be made for the shielding of C-18 resulting from steric interaction of the C-18 hydrogen atoms with the H-20. Inspection of the ^{13}C shifts in Table 3.3 shows that the C-18 shifts follow the same trend as the C-20 shifts.

In Δ^{14}-compounds **11** - **16** the C-18 and C-20 shift differences between epimers are generally small (with the exception of the C-18 shifts in **11** and **12**) and are not characteristic of the stereochemistry.

4.1.2 Comparison of Experimentally Determined C-17 Side-chain Conformations with Those Predicted by Molecular Mechanics and Semi-Empirical Molecular Orbital Methods

Cardiotonic Pregnanes

Comparison of the conformations predicted by empirical and semi-empirical methods shown in Table 3.4 with the experimentally determined results reveals a number of differences. In **2**, MM3 calculations predict the correct conformation with the nitro group *anti* to C-13 while an AM1 calculation incorrectly suggests that the nitro group should lie *anti* to H-17. In **5** MM2 incorrectly predicts a major (60 %) conformer with the hydroxyl group *anti* to C-16, while MM3 and AM1 correctly predict that the hydroxyl lies *anti* to H-17. In **9** all three methods of calculation incorrectly insist on placing the amino group *anti* to C-16 rather than *anti* to H-17 as observed experimentally.

In all three of the discrepancies noted above, the experimentally observed conformations have the C-20 methyl *anti* to C-16 and abutting the C-13 methyl. In the calculated conformations, the C-20 methyl is rotated away from the C-13 methyl into a location *anti* to C-13. It seems, therefore, that the calculation may be overestimating the steric interaction of the C-20 and C-13 methyls.

In the 21-nor nitro compound **17**, AM1 predicts that the nitro group lies *anti* to C-16; whereas MM3 agrees with the experimental finding that the nitro group is disposed *anti* to C-13.

Overall, MM3 proved to be the most reliable of the calculation procedures for predicting the side-chain conformation in that it failed to estimate the correct conformation in only one of the cases studied. Surprisingly, the AM1 semi-empirical calculation failed to predict the correct conformation in three of the ten cases investigated.

Digoxigenin

X-ray studies of digoxigenin[176] and its 12β-acetate[179] have shown a mixture of the 14/21 and 14/22 conformers.[†] Molecular mechanics also predicts that the two conformers should have similar energies,[182] as do the AM1 calculations reported earlier. The NMR data reported earlier also suggest a rapidly equilibrating mixture of the two conformers. Hintsche *et al*[150] have proposed an NMR method based on chemical shifts induced in the C-21 and C-22 protons upon formation of the 14-trichloroacetylcarbamate derivatives for the determination of the lactone side-chain conformation. Application of this technique to digoxigenin-3,12-acetate shows exclusively the 14/21 conformer.[150] The reason for the discrepancy is not known, but it is possible that derivatization of the 14-hydroxyl group may influence the conformation.

[†]The 14/22 conformation has the C-22 hydrogens adjacent to the C-14 hydroxyl while the 14/21 conformer has the C-21 hydrogen in this location.[150]

Digoxin

As in digoxigenin, in digoxin the NMR shift method of Hintsche *et al*[150] showed exclusively the 14/21 conformer for the 12-acetate. This is to be expected as differences in substitution in ring-A cannot reasonably be expected to have a significant effect on the C-17 side-chain conformation. Our NMR data, however, show clear evidence of a conformational equilibrium. Again, derivatization of the 14-hydroxyl required by Hintsche's method, or acetylation of the 12β-hydroxyl, may explain the difference.

Digitoxigenin and Digitoxigen-3-acetate

Molecular mechanics methods predict a mixture of the 14/21 and 14/22 conformers for digitoxigenin[147,149,176,182] and its 3β-acetate.[182] The same conformation would presumably also be valid for the glycoside digitoxin, although no calculations have been reported. Our AM1 calculations reported earlier also show little energy difference between the 14/21 and 14/22 conformers, suggesting little influence of the 12β-hydroxyl on the conformation. An x-ray structure for digitoxigenin shows a 14/22 conformation for the lactone ring,[177] while a 14/21 conformation was reported for the 3β-acetate.[178] These differences are possibly the result of crystal packing effects. A rapidly equilibrating mixture of the 14/21 and 14/22 conformers was reportedly observed by the NMR shift method for digitoxigenin, while a 14/21 conformation was observed for the 3β-acetate and sugar peracetylated digitoxin.[150] Molecular mechanics calculations reported by Rohrer *et al*[182] also predict a difference in conformation depending on the 3β-substituent, while our AM1 calculations show no such effect.

AM1 calculations predict a 12 kJ/mol barrier to rotation about the C-17–C-20 bond. A barrier of this magnitude is too small to "freeze-out" the two conformations in a low temperature NMR experiment.

4.1.3 The Relationship between C-17 Side-Chain Structure and Conformation to Biological Activity

The relationship between C-17 side-chain conformation and activity has been the subject of considerable discussion.[140–142,147,112,113,149,114,150,151,153–155] Hintsche *et al*[150] have concluded, based on studies of modified cardenolides with restricted side-chain rotation, that the active conformation is where the lactone carbonyl approximately eclipses H-17 (the 14/22 conformation.) However, the difference in energy between this conformation and one rotated by 180° is small (Section 3.1.2) compared with the energy of interaction of the steroid with the enzyme.[121,140–142] Therefore, conformation is likely to have little influence upon activity in cardenolides with the normal butenolide side-chain. This conclusion does not necessarily hold for the cardiotonic pregnanes and norpregnanes under discussion here because of the additional steric requirements of the sp^3 C-20 and the C-20 methyl group. Others have proposed that the preferred location of the C-23 carbonyl lies between H-17 and C-13.[112,151,114] Because of the uncertainties involved in determining these conformations, the preferred location of the C-23 carbonyl proposed here lies somewhere between C-13 and H-17, as indicated in Figure 4.1.

C-20 Substituted Pregnanes

Inspection of Table 4.1 shows that the 20(R)-epimers have greater cardiac receptor binding affinity (lower IC_{50}) than the corresponding 20(S)-epimers. Typically in these compounds, the C-3 glycosides have much greater binding affinity than the corresponding aglycones.[121] The preferred solution conformation of the polar side-chain substituent is the same in all except the 20-nitro compounds. It seems, therefore, that there is no simple direct relationship between the lowest energy conformation and enzyme binding. The 20(R)-nitro compound **1** shows very high affinity, suggesting that conformations where the polar substituent is *anti* to C-16 (*gauche* to H-17) may also be preferred.

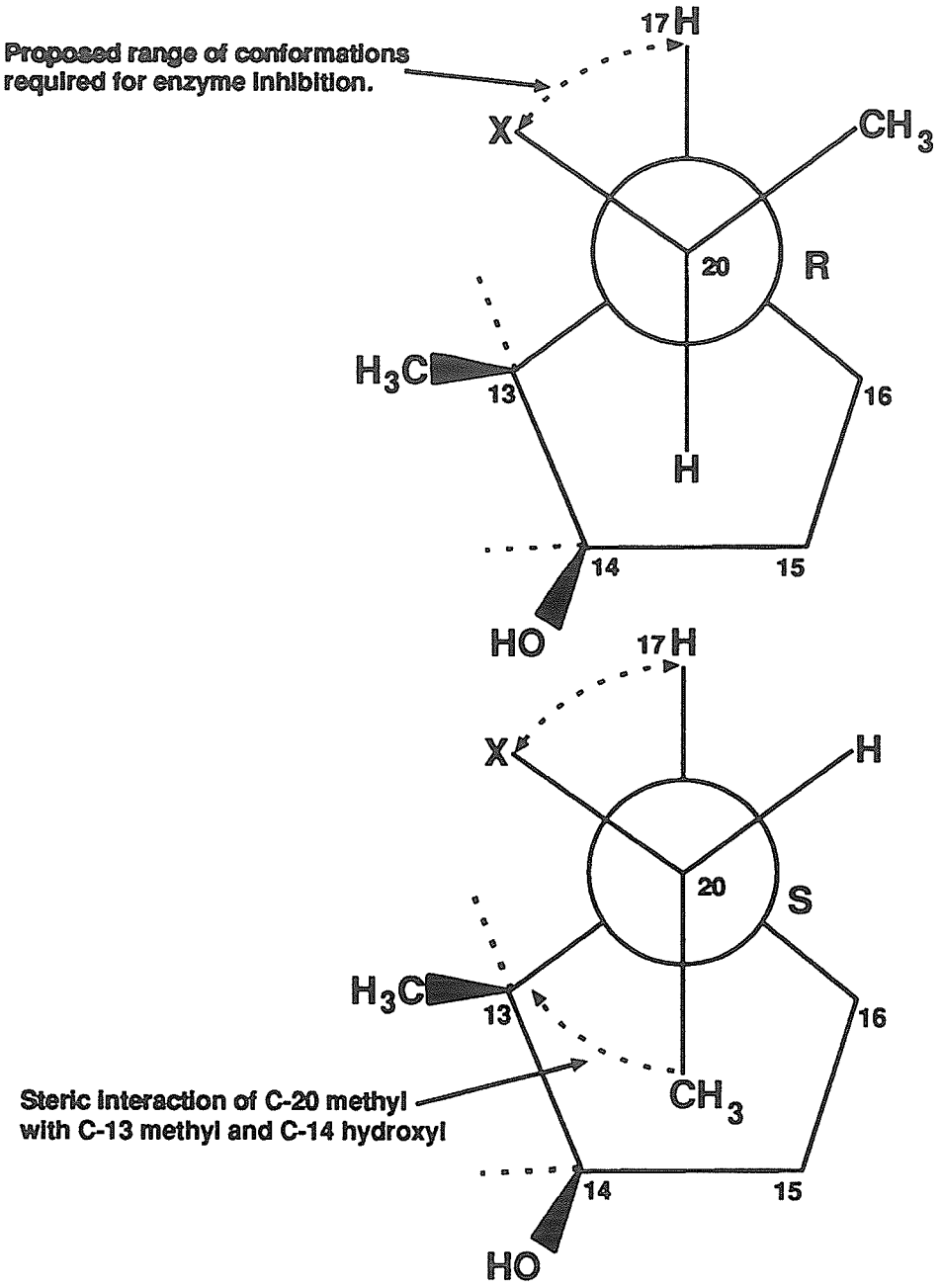

Figure 4.1: Proposed preferred C-17 side-chain locations for enzyme inhibition. The proposed range of conformations varies from having the polar substituent *anti* to C-16 to one where the substituent eclipses H-17. In the 20(S)-epimer rotation of the substituent into this area generates steric interactions between the C-20 methyl and the C-13 and C-14 substituents.

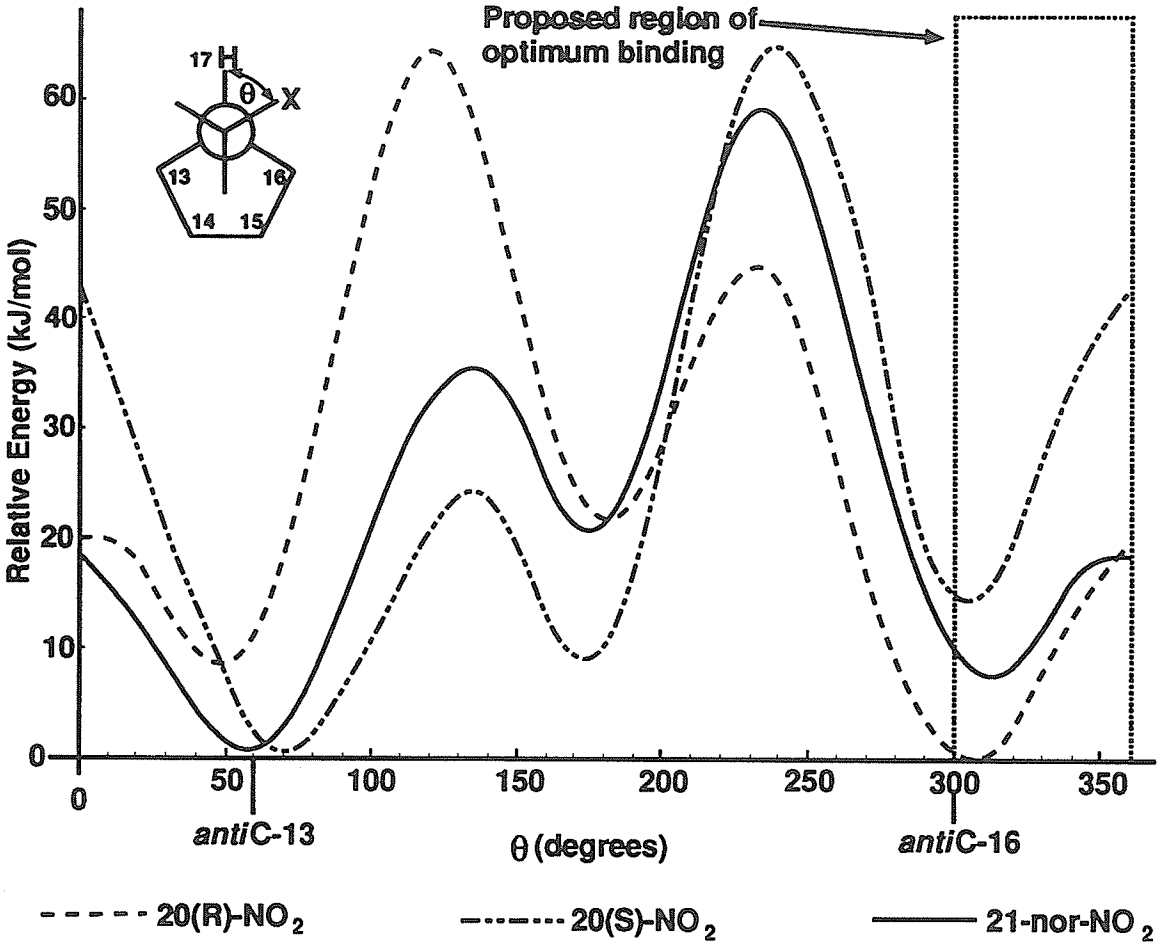

Figure 4.2: Relative MM3 strain energies as a function of rotation angle about the C-17–C-20 bond for nitropregnanes **1** and **2**, and 21-nor-nitropregnane **17**. Calculations were performed at 15° intervals using the Spartan program.[220]

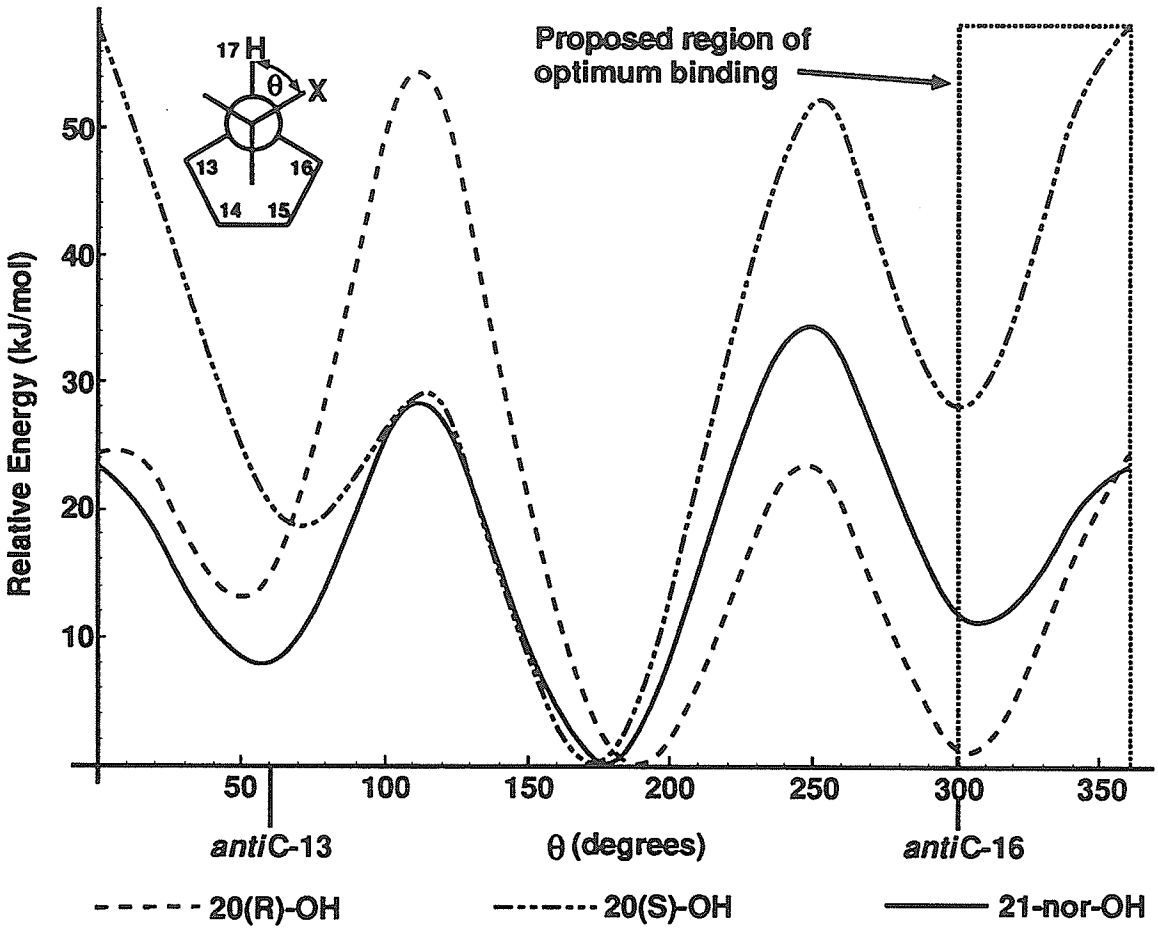

Figure 4.3: Relative MM3 strain energies as a function of rotation angle about the C-17–C-20 bond for hydroxypregnanes **5** and **6**, and 21-nor-hydroxypregnane **18**. Calculations were performed at 15° intervals using the Spartan program.[220]

If binding requires that the polar substituent approximately eclipses H-17, as proposed by Hintsche *et al*,[150] the S-epimers will have the C-20 methyl group abutting the C-13 methyl group while the R-epimers will have the C-20 methyl in a much more sterically favoured location eclipsing C-16. A similar argument can be made for conformations where the substituent is *anti* to C-16. In the R-epimers the C-20 methyl group is in a sterically unhindered location *anti* to C-13, while in the S-epimers the C-20 methyl group is sterically hindered by the C-13 methyl group and the C-14 hydroxyl. It may be, therefore, that the differences in enzyme affinity reflects the ease with which the side-chain can assume a conformation with the polar substituent eclipsing or *gauche* to H-17. The preferred conformation for enzyme binding does not necessarily correspond to the solution conformation, but the energy penalty resulting from the conformational change must be factored into the energetics of the interaction.

AM1 calculations predict for **1** a difference of 12 kJ/mol between a conformation where the nitro group is *anti* to C-16 (*gauche* to H-17) and one where the nitro group eclipses H-17. A molecular mechanics (MM3) calculation (Figure 4.2) of the same energy difference gives 20 kJ/mol. Similar calculations on the S-epimer **2** predict that 25 kJ/mol (AM1) - 42 kJ/mol (MM3) is required to rotate the nitro group into a location eclipsing H-17 while 4 kJ/mol (AM1) - 15 kJ/mol (MM3) is required to rotate it into a position *anti* to C-16. It should be noted that AM1 incorrectly predicts that a conformer with the nitro group *anti* to H-17 is lower in energy by 6.5 kJ/mol compared with the experimentally observed conformation.

C-20 Substituted 21-Norpregnanes

The 21-nor-nitro compound **17** shows very high binding affinity (Table 4.1), comparable to the natural cardiac glycosides, although the preferred solution conformation places the polar nitro group in the same location as the relatively inactive 20(S)-nitropregnane **2** rather than the more active 20(R)-nitropregnane **3**. This would suggest that rotation of the polar substituent into a location suitable for hydrogen

bonding to the enzyme may be critical for high affinity, and that in the 20(S)-nitro compound **2** this rotation is impaired by steric interactions of the C-20 methyl with the C-13 methyl and possibly the C-14 hydroxyl. It is also possible that steric interactions involving the C-20 methyl and the receptor site of the enzyme may play a role in the superior binding affinity of **17** relative to the corresponding 20-nitropregnanes **1** and **2**. An AM1 calculation of the energy required to rotate the nitro group in **17** is problematic in that AM1 incorrectly predicts that the conformer with the nitro group *anti* to C-16 is 12 kJ/mol more stable than the experimentally observed conformation. Furthermore, the conformation where the nitro group eclipses H-17 is predicted to have an energy comparable to the experimentally observed conformation. While the inability of AM1 to predict the correct lowest energy conformer is suspicious, the energies involved in rotating the substituent into the putative positions of optimum binding are lower than those observed for the pregnanes **1** and **2**. Molecular mechanics (MM3) predicts that 18 kJ/mol are required to rotate the nitro group into a location eclipsing H-17 while only 6 kJ/mole are required to rotate the substituent into a location *anti* to C-16. A comparison of the rotational energy barriers for **1**, **2** and **17** based on MM3 calculations is shown in Figure 4.2.

The 21-nor alcohol **18** shows lower binding affinity than the corresponding 20(R)-alcohol **5** (Table 4.1). Both have preferred solution conformations with the hydroxyl *anti* to H-17, possibly hydrogen bonded to the C-14 hydroxyl. If binding of the steroid to the digitalis receptor requires rotation of the polar substituent into a location between C-13 and H-17 (Figure 4.1), then steric interactions between the C-13 and C-20 methyls in **5** may destabilize any hydrogen bonding between the C-20 and C-14 hydroxyls, allowing for easier rotation into the preferred location. Attempts to predict the energy requirements for this rotation using molecular orbital or molecular mechanics methods were inconclusive. AM1 predicts an energy requirement of approximately 24 kJ/mol to rotate the hydroxyl into a location eclipsing H-17 in both **5** and **18**. For rotation to a location *anti* to C-16, AM1 predicts an energy requirement

of 6 kJ/mol for both **5** and **18**. MM3 predicts that only 1.5 kJ/mol are required for rotation to a location *anti* to C-16 in **5**, but that 11 kJ/mol are required in **18**. For rotation to a location eclipsing H-17, the corresponding energies are 24 kJ/mol and 26 kJ/mol.

A comparison of the rotational energy barriers for **5**, **6** and **18** based on MM3 calculations is shown in Figure 4.3.

C-21 Substituted Pregn-20,21-enes (24 and 25)

The C-21 nitro compound **24** and the C-21 carboxylic acid **25** show very strong binding affinity. In both compounds, the NMR results presented earlier clearly demonstrate that the C-17 side-chain and its polar substituent are oriented so that C-21 eclipses H-17. This places the polar C-21 substituent is a similar location to that of the C-23 carbonyl in digoxin-like compounds, and supports the proposal of Hintsche *et al*[150] that optimum receptor binding requires a polar group in this location. AM1 calculations predict that this conformation is 8 kJ/mol lower in energy in **24** and 10 kJ/mol in **25** than one where the C-17–C-20 bond is rotated by 180°. The Spartan program did not have the required force constants to perform MM3 calculations on **24** and **25**.

4.1.4 Suggestions for Further Research

As the C-17 side-chain structure becomes similar to the lactone in the cardiac glycosides, there is a corresponding increase in binding affinity to the cardiac glycoside receptor. For example, the binding affinities of **24** and **25** approach those of digitoxigenin (Table 4.1). However, the overall aim of this work is not to reinvent digitoxin, but to develop safer cardiotonic steroids. It is therefore important to develop a correlation between structure and therapeutic index and not just between structure and binding affinity. It has also been noted that binding does not correlate well with inotropic activity.[135] Once a measure of therapeutic index has been established, the

Table 4.1: Comparison of C-17 sidechain conformation and configuration compared to receptor binding as measured in a [^{3}H]ouabain radioligand binding assay.

		Inhibitory Concentration(IC_{50})[a]		
C-20 substituent	θ[b]	c	d	e
(R)-NO_2 **1**	300	45	10 200	—
(S)-NO_2 **2**	60	940	424 000	—
(R)-OH **5**	180	75	8 000	—
(S)-OH **6**	180	1 600	41 000	—
(R)-NHAc **7**	180	450	1 100	—
(S)-NHAc **8**	180	1 800	14 000	—
(R)-NH_2 **9**	180	72	—	—
(S)-NH_2 **10**	180	115	—	—
21-nor-NO_2 **17**	60	12	—	88
21-nor-OH **18**	180	360	—	610
C-17 side-chain				
(E)-CH=$CHNO_2$ **24**	0	8.3	—	—
(E)-CH=CHCOOH **25**	0	13	—	—

[a] IC_{50} represents the concentration (nM) that inhibits binding of [^{3}H]ouabain by 50 %. Digitoxigenin gives a value of 8 nM. Data were obtained from Templeton *et al.*[163,164]

[b] Most probable H-17–C-17–C-20–X or H-17–C-17–C-20=C-21 torsion angle in degrees as determined from the NMR data presented earlier. A value of 0° indicates X or the double bond eclipsing H-17 while a value of 60° has X or the double bond *anti* to C-13.

[c] 3β-substituent: α-L-rhamnosyl.

[d] 3β-substituent: OAc.

[e] 3β-substituent: tris-β-D-digitoxosyl.

conformational data presented here should be re-evaluated with an aim of establishing such a correlation. The methods described in this thesis for determining the C-17 side-chain conformation and C-20 stereochemistry in C-20 substituted pregnanes are quite general and should be applicable to similar new compounds.

4.2 Cyclosteroids and Cyclopropanosteroids

4.2.1 Cyclopropane Induced Chemical Shifts

Chemical shifts induced by a cyclopropyl group have been used by several groups for conformational studies of steroids.[226,227] From a practical viewpoint, the long range shifts produced by the cyclopropyl group complicate attempts to use popular substituent shift tables for the assignment of steroid spectra. Reports of unusually high field multiplets in steroid spectra have been attributed to long range shielding by cyclopropyl groups,[210,226] but similar multiplets are routinely observed in steroids without a cyclopropyl group and are invariably from axial protons shielded by the steroid framework, typically H-9 or H-7α.

Long range shielding of protons by cyclopropanes can be calculated by the Tori and Kitahonoki[228] modification of the McConnell equation.[229] Application of this equation to the axial C-2 proton in **32-40** predicts an upfield shift of 0.3 ppm when the proton is on the same side of the steroid as the cyclopropyl group. In **34**, the axial 2β hydrogen is shielded by 0.08 ppm compared to the corresponding axial 2α hydrogen in **32** and **33**, in agreement with the proposed boat conformations for these compounds.

Similarly, H-2β in **39** and **40** is 0.1 and 0.17 ppm more shielded than H-2α in **38**. The magnitude of these shifts is considerably lower than the 0.3 ppm predicted above, although in the right direction and in agreement with the conformational differences in these molecules.

This discrepancy may arise from uncertainties in the empirically-derived shielding

parameter used with the McConnell equation, or from changes in the substituent at C-19.

Similar effects can be observed for ^{13}C shifts. For example, the chemical shift of C-19 in the $2\alpha,3\alpha$-methylene compound **29** is almost identical with that of the parent androstane,[9] while a 3 ppm deshielding is observed in the corresponding $2\beta,3\beta$-epimer **27**.

4.2.2 NOEs and Internuclear Distances

In Section 1.1.1 it was shown that no simple relationship exists between steady-state NOE data and internuclear distance. However, for groups of similar molecules a rough $1/r^6$ dependence of NOE on internuclear distance has been observed.[53] A plot of measured % NOE enhancement as a function of $1/r^6$ for two groups of structural isomers in the cyclosteroid series is shown in Figure 4.4. Internuclear distances were calculated with the Spartan program[220] based on AM1 optimized geometries of the experimentally determined conformers. Although there is considerable scatter, the $1/r^6$ relationship can be clearly seen.

One feature of this plot is particularly instructive. The NOEs observed between the geminal cyclopropyl protons are, on average *ca* 20 % larger than those between geminal cyclohexyl protons, although the cyclopropyl protons are on average 0.05 Å further apart. The probable reason for this is that in these compounds the cyclopropyl protons are more isolated from other relaxation sources (i.e. other protons) than are cyclohexyl protons. The cyclopropyl protons will therefore have a greater proportion of dipole-dipole relaxation from their geminal partner than the cyclohexyl protons. The puckering of a cyclohexyl ring results in considerable relaxation from protons on adjacent carbons.

Other generalizations for common situations that can be drawn from Figure 4.4 include: 1,3 diaxial NOEs should range from 4 % to 10 %, 1,4 diaxial NOEs in a boat conformation should range from 1 % to 3 %, axial-equatorial NOEs should range from

3 % to 8 %, while equatorial-equatorial NOEs should range from 2 % to 6 %. NOEs become vanishingly small beyond approximately 3.7 Å. These generalizations should hold for steroids of similar molecular weight in $CDCl_3$ solution at 500 MHz.

4.2.3 The Relationship of Ring A Structure and Conformation to Biological Activity

Assays for inhibition of human placenta microsomal aromatase activity have been obtained for compound **40**, the 17-keto analogs of compounds **33** and **34**, and the 19(S)-isomer of compound **40**.[‡] Unfortunately, none of these compounds showed significant inhibitory activity. The reasons for the lack of activity are not yet understood, although it is possible to speculate on several likely possibilities, based on the model of Oh and Robinson:[205]

1. The ring A conformation of the steroid may not be suitable for hydrogen bonding of the C-3 carbonyl to the Histidine-128 residue of the enzyme. In particular, the predominant inverted boat conformations observed for the 19(S)-isomers **32**, **33**, **38** and **40** (Figures 3.21 and 3.22) places the C-3 carbonyl approximately 1.5 Å[§] from its location in testosterone, the enzyme's natural substrate (Figure 4.5 B). The boat conformation observed for the corresponding R-epimers places the carbonyl approximately 0.2 Å from its location in testosterone.

   If inhibition requires conversion of the substituted cyclopropane into a cyclopropanone as indicated in Figures 1.13,1.15 and 1.16, then it is the S-epimers that are the most likely to show activity. Although the R-epimers have a ring-A conformation closer to that observed for testosterone, the electronegative C-19 substituent is situated on the wrong side of the cyclopropane ring for hydrogen

[‡]Assays were performed by Dr. A. Brodie at the Department of Pharmacology and Experimental Therapeutics, University of Maryland at Baltimore

[§]Estimated by molecular modelling with the Spartan[220] program.

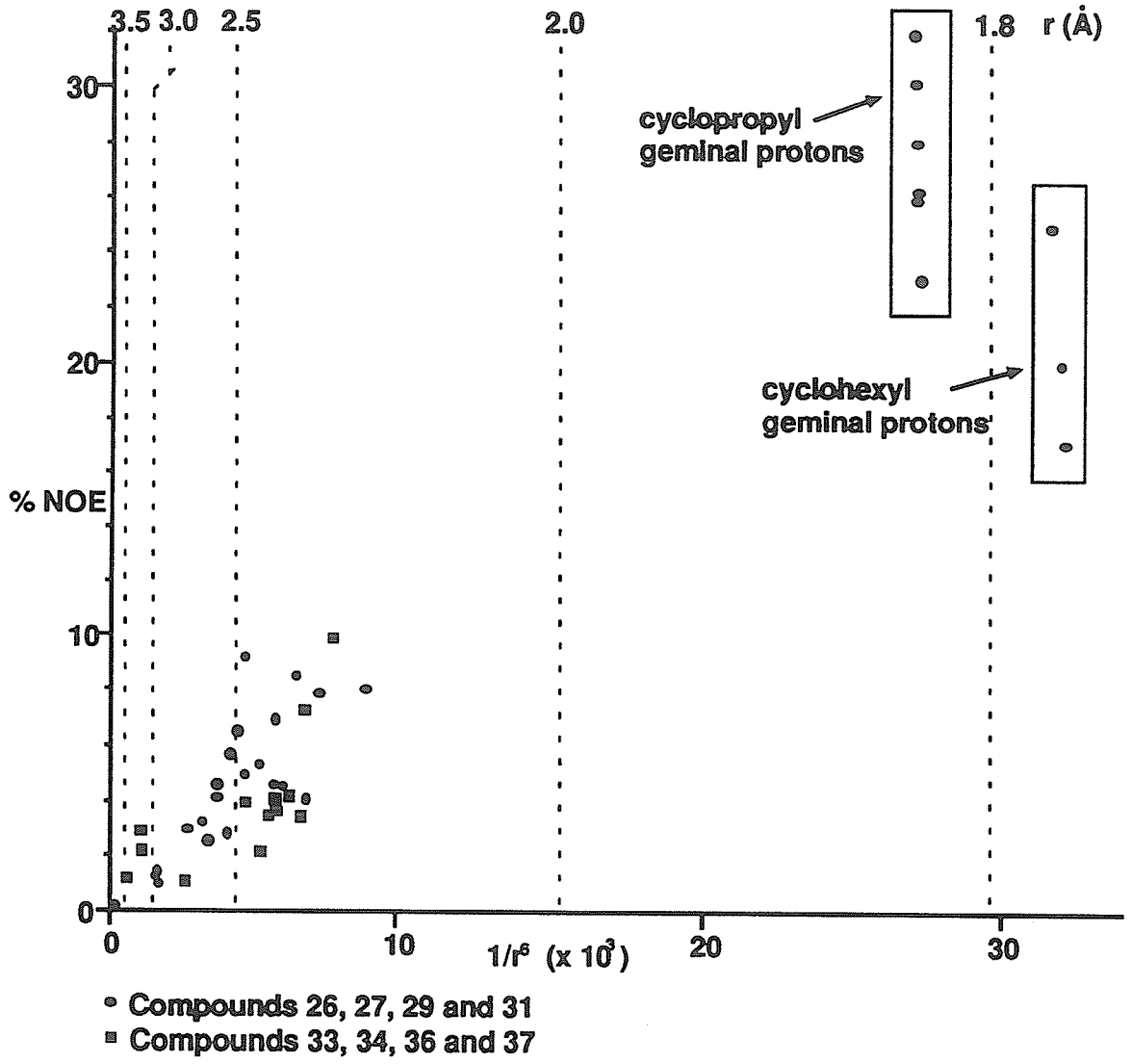

Figure 4.4: A plot of % NOE as a function of $1/r^6$ (in Å) for two series of structural isomers. The NOE values are those reported earlier in Sections 3.2.1 and 3.2.3. The internuclear distances were estimated by molecular modelling methods (Spartan program[220])

bonding to the Glu-128 residue of the enzyme, as shown in Figure 4.5 B. It is conceivable, however, that the R-epimer could be oxidized in the first step of estrogen synthesis (Figure 1.15, followed by elimination of water (or HX) to form the cyclopropanone directly.

2. The aromatization of ring A in testosterone proceeds through two stepwise hydroxylations of C-19 (Figures 1.14, 1.15 and 1.16). At each of these steps rotational freedom of the C-10–C-19 bond is maintained, allowing for optimum orientation of the C-19 substituents. In 5,19-cyclosteroids, however, this rotation is not possible and reactions upon the C-19 substituents may not be possible because a substituent may not be suitably situated close to a necessary group in the enzyme.

3. If enzymatic action upon the cyclosteroid can proceed to the point of producing a cyclopropanone, then irreversible inhibition requires nucleophilic attack by the enzyme upon the ketone thus producing a covalent enzyme-substrate bond (Figure 1.13). However, as shown in Figure 4.5 C and D, the cyclopropanone carbonyl is considerably removed from the location of the carbonyl in the aldehyde intermediate in the third step of estrogen synthesis.

4.2.4 Suggestions for Further Research

Despite the disappointing aromatase inhibition results mentioned above, the idea of using a cyclopropane derivative as a mechanism based enzyme inhibitor has promise. The finding that no significant inhibition of aromatase was noted suggests little or no binding to the enzyme, as binding should result in at least reversible competitive inhibition. This would strongly suggest that the problem lies in the fit of the substrate to the enzyme and not with an inability of the enzyme to act upon the enzyme once bound. A weakly binding inhibitor may be effective, however, if irreversible mechanism-based inhibition inactivates the enzyme faster than the kinetics of enzyme

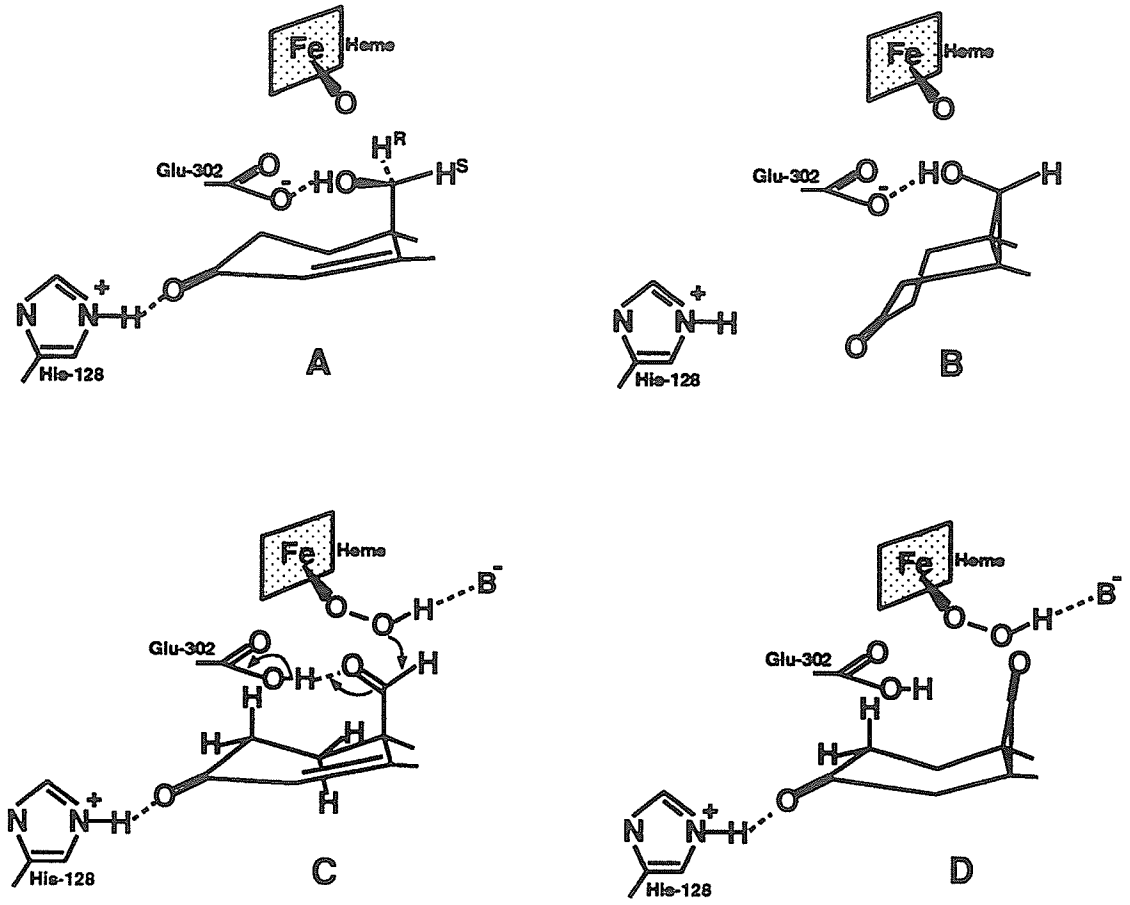

Figure 4.5: Possible difficulties in the binding of a 19(S)-hydroxy-5β,19β-cyclosteroid to aromatase in the model of Oh and Robinson.[205] A: Binding of the natural substrate at the second stage of estrogen synthesis. B: Binding of a 19(S)-hydroxy-5β,19β-cyclosteroid. C: Binding of the natural substrate at the third stage in estrogen synthesis. D: Binding of the cyclopropanone produced by the oxidation of a 5β,19β-cyclosteroid. The ring A conformation shown in D is speculative, but is assumed to be similar to that observed for 19(R)-substituted 5β,19β-cyclosteroid.

synthesis can replenish it.

A flatter ring A, possibly induced by the introduction of unsaturation into the ring, may result in improved enzyme binding as this more closely approximates the ring A conformation of the enzyme's natural substrate. 1,19-Cyclosteroids or steroids with a cyclopropyl group at the $4\beta,5\beta$-position would present a different arrangement of substituents to the enzyme, and may be better suited as aromatase inhibitors. Cyclopropane rings at these positions would also serve to flatten ring A.

The NMR techniques developed in this thesis would all be applicable to conformational studies of these classes of potential inhibitors.

Bibliography

[1] R. F. Zurcher. *Helv. Chim. Acta.* **44**, 1380, (1961).

[2] R. F. Zurcher. *Helv. Chim. Acta.* **46**, 2054, (1963).

[3] N. S. Bhacca and D. H. Williams. *Applications of NMR Spectroscopy in Organic Chemistry - Illustrations from the steroid field.* Holden-Day, San Francisco, (1964).

[4] K. Marat, J. F. Templeton, and V. P. S. Kumar. *Magn. Reson. Chem.* **25**, 25, (1987).

[5] K. Marat, J. F. Templeton, R. K. Gupta, and V. P. S. Kumar. *Magn. Reson. Chem.* **25**, 730, (1987).

[6] K. Hayamizu, T. Ishii, M. Yanagisawa, and O. Kamo. *Magn. Reson. Chem.* **28**, 250, (1990).

[7] H.-J. Schneider, U. Buchheit, N. Becker, G. Schmidt, and U. Siehl. *J. Amer. Chem. Soc.* **107**, 7027, (1985).

[8] D. N. Kirk, H. C. Toms, C. Douglas, K. A. White, K. E. Smith, S. Latif, and R.W. P. Hubbard. *J. C. S. Perkin Trans. 2* 1567, (1990).

[9] J. W. Blunt and J. B. Stothers. *Org. Magn. Reson.* **9**, 439, (1977).

[10] Y. Letourneux, Q. Khuong-Huu, M. Gut, and G. Lukacs. *J. Org. Chem.* **40**, 1674, (1975).

[11] H. Beierbeck and J. K. Saunders. *Can. J. Chem.* **54**, 632, (1975).

[12] H. Beierbeck and J. K. Saunders. *Can. J. Chem.* **54**, 2985, (1976).

[13] W. B. Smith. *Annual Reports on NMR Spectroscopy, Edited by G. A. Webb* 8 199, (1978).

[14] H. L. Holland and E. M. Thomas. *Can. J. Chem.* **57**, 3069, (1979).

[15] H. Eggert and C. Djerassi. *J. Org. Chem.* **46**, 5399, (1981).

[16] J. M. Coxon and J. R. Gibson. *Aust. J. Chem.* **34**, 1451, (1981).

[17] S. Q. A. Rizvi and J. R. Williams. *J. Org. Chem.* **46**, 1127, (1981).

[18] L. Brown, H. T. Andrew Cheung, R. Thomas, T. R. Watson, and J. L. E. Nemorin. *J. C. S. Perkin I* 1779, (1981).

[19] H.-J. Schneider and W. Gschwentner. *J. Org. Chem.* **47**, 4216, (1982).

[20] T. Iida, T. Tamura, and T. Matsumoto. *Magn. Reson. Chem.* **21**, 558, (1983).

[21] M. D. Gonzalez and G. Burton. *Org. Magn. Reson.* **22**, 586, (1984).

[22] J. C. Gramain and J. C. Quirion. *Magn. Reson. Chem.* **24**, 938, (1986).

[23] H. Duddeck, D. Rosenbaum, M. Hani, A. Elgamal, and M. B. E. Fayez. *Magn. Reson. Chem.* **24**, 999, (1986).

[24] J. B. Lambert. *Acta. Chem. Res.* 4, 87, (1971).

[25] W. Robien, B. Kopp, D. Schabl, and Herbert Schwarz. *Progress in Nuclear Magnetic Resonance Spectroscopy (J. W. Emsley, J. Feeney and L. H. Sutcliffe - editors)* **19**, 131, (1987).

[26] F. H. Allen. In *Molecular structure and biological activity (J. F. Griffin and W. L Duax, editors)* 105, (1982).

[27] M. Karplus. *J. Chem. Phys.* **30**, 11, (1959).

[28] M. Barfield and W. B. Smith. *J. Amer. Chem. Soc.* **114**, 1574, (1992).

[29] C.A. G. Haasnoot, F. A. A. M. de Leeuw, and C. Altona. *Tetrahedron* **36**, 2783, (1980).

[30] W. J. Colucci, S. J. Jungk, and R. D. Gandour. *Magn. Reson. Chem.* **23**, 335, (1985).

[31] W. B. Smith and M. Barfield. *Magn. Reson. Chem.* **31**, 696, (1993).

[32] K. Imai and E. Ōsawa. *Magn. Reson. Chem.* **28**, 668, (1990).

[33] E. Ōsawa, T. Ouchi, N. Saito, M. Yamato, O. S. Lee, and M. K. Seo. *Magn. Reson. Chem.* **30**, 1104, (1992).

[34] M. J. Minch. *Concepts in Magnetic Resonance* **6**, 41, (1994).

[35] C. Altona, R. Francke, R. de Haan, J. H. Ippel, G. J. Daalmans, A. J. A. Westra Hoekzema, and J. van Wijk. *Magn. Reson. Chem.* **32**, 670, (1994).

[36] Wolfram Research, Inc., P.O. Box 6059, Champaign, IL, 61826-9902, USA. *Mathematica Program* (1994).

[37] J. L. Marshall. *Carbon-carbon and carbon-proton couplings – applications to organic stereochemistry.* Verlag Chemie International, Deerfield Beach, Florida, (1983). three-bond C-H couplings.

[38] F. W. Wehrli, A. P. Marchand, and S. Wehrli. *Interpretation of Carbon-13 NMR Spectra.* Wiley, Chichester, (1988).

[39] T. Spoormaker and M. J. A. DeBie. *Recl. J. Roy. Neth. Chem. Soc.* **98**, 380, (1979).

[40] B. Zeng, R. M. Pollack, and M. F. Summers. *J. Org. Chem.* **55**, 2534, (1990).

[41] T. C. Wong and G. R. Clark. *J. Chem. Soc. Chem. Commun.* 1518, (1984).

[42] M. Barfield and D. M. Grant. *J. Amer. Chem. Soc.* **85**, 1899, (1963).

[43] R. C. Cookson and T. A. Crab. *Tetrahedron* **28**, 2139, (19720.

[44] R. Cahill, R. C. Cookson, and T. A. Crabb. *Tetrahedron* **25**, 4681, (1969).

[45] R. Cahill, R. C. Cookson, and T. A. Crabb. *Tetrahedron* **25**, 4711, (1969).

[46] J. A. Pople and A. A. Bothner-By. *J. Chem. Phys.* **42**, 1339, (1965).

[47] G. E. Maciel, Jr. J. W. McIver, N. S. Ostlund, and J. A. Pople. *J. Amer. Chem. Soc.* **92**, 4151, (1970).

[48] D. Montecalvo and M. St-Jacques. *J. Org. Chem.* **40**, 940, (1975).

[49] R. Davies and J. Hudec. *J. Chem. Soc. Perkin. Trans. II* 1395, (1975).

[50] R. Davies. *J. Chem. Soc. Perkin. Trans. II* 1400, (1975).

[51] A. W. Overhauser. *Phys. Rev.* **92**, 411, (1953).

[52] F. A. L. Anet and A. J. R. Bourn. *J. Amer. Chem. Soc.* **87**, 5250, (1965).

[53] R. A. Bell and J. K. Saunders. *Can. J. Chem.* **48**, 1114, (1970).

[54] R. E. Schirmer, J. H. Noggle, J. P. Davis, and P. A. Hart. *J. Amer. Chem. Soc.* **92**, 3266, (1970).

[55] J. H. Noggle and R. E. Schirmer. *The Nuclear Overhauser Effect - Chemical Applications.* Academic Press, New York, (1971).

[56] I. Solomon. *Phys. Rev.* **99**, 559, (1955).

[57] D. Neuhaus and M. Williamson. *The Nuclear Overhauser Effect in Structural and Conformational Analysis.* VCH Publishers, New York, (1989).

[58] D. Maes, M. Van Cautern, L. Wyns, J. Lisgarten, R. Palmer, D. Lisgarten, R. Willem, M. Biesemans, and F. Kayser. *J. Chem. Soc. Perkin Trans 2* 2179, (1992).

[59] A. Kuliopulos, G. P. Mullen, L. Xue, and A. S. Mildevan. *Biochemistry* **30**, 3169, (1991).

[60] D. M. Doddrell, D.T. Pegg, and M. R. Bendall. *J. Magn. Reson.* **48**, 323, (1982).

[61] G. A. Morris and R. Freeman. *J. Amer. Chem. Soc.* **101**, 760, (1979).

[62] J. N. Shoolery. *J. Nat. Prod.* **47**, 226, (1984).

[63] M. W. Barrett, R. D. Farrant, D. N. Kirk, J. D. Mersh, J. K. M. Sanders, and W. L. Duax. *J. C. S. Perkin II* 105, (1982).

[64] R. D. Farrant, D. N. Kirk, J. D. Mersh, and J. K. M. Sanders. *J. Steroid. Biochem.* **19**, 181, (1983).

[65] J. D. Mersh and J. K. M. Sanders. *J. Magn. Reson.* **50**, 289, (1982).

[66] J. K. M. Sanders and J. D. Mersh. *Progress in NMR Spectroscopy* **15**, 353, (1982).

[67] M. R. Bendall, D. T. Pegg, D. M. Doddrell, and J. Field. *J. Magn. Reson.* **51**, 520, (1983).

[68] R. Freeman, T. H. Mareci, and G. A. Morris. *J. Magn. Reson.* **42**, 341, (1980).

[69] W. P. Aue, J. Karahan, and R. R. Ernst. *J. Chem. Phys.* **64**, 4226, (1976).

[70] L. D. Hall and J. K. M. Sanders. *J. Amer. Chem. Soc.* **102**, 5703, (1980).

[71] L. D. Hall and J. K. M. Sanders. *J. Org. Chem.* **46**, 1132, (1981).

[72] F. Frappier, W. E. Hull, and G. Lukacs. *J. Org. Chem* **46**, 4314, (1981).

[73] V. Rutar and T. C. Wong. *J. Magn, Reson.* **60**, 333, (1984).

[74] T. Facke and S. Berger. *J. Magn. Reson.* **A113**, 114, (1995).

[75] W. P. Aue., E. Bartholdi, and R. R. Ernst. *J. Chem. Phys.* **64**, 2229, (1976).

[76] K. Nagayama, K. Wuthrich, and R. R. Ernst. *Biochem. Biophys. Res. Comm.* **90**, 305, (1979).

[77] K. Nagayama, A. Kumar, K. Wuthrich, and R. R. Ernst. *J. Magn. Reson.* **40**, 321, (1980).

[78] L. Braunschweiler and R. R. Ernst. *J. Magn. Reson.* **53**, 521, (1983).

[79] A. Bax and R. Freeman. *J. Magn. Reson.* **44**, 542, (1981).

[80] S.W. Homans et al. *Proc. Natl. Acad. Sci. USA* **81**, 6286, (1984).

[81] D. W. Hughes. *Magn. Reson. Chem.* **26**, 214, (1988).

[82] A. Bax and D. G. Davis. *J. Magn. Reson.* **65**, 355, (1985).

[83] J. A. Findlay, M. Jaseja, and J.-R. Brisson. *Can. J. Chem.* **65**, 2605, (1987).

[84] A. A. Bothner-By, R. L. Stephens, J.-M. Lee, C. D. Warren, and R. W. Jeanloz. *J. Amer. Chem. Soc.* **106**, 811, (1984).

[85] A. Bax and D. G. Davis. *J. Magn. Reson.* **63**, 207, (1985).

[86] Tsang-Lin Hwang and A. J. Shaka. *J. Amer. Chem. Soc.* **114**, 3157, (1992).

[87] T. Schmittmann, K. Rotscheidt, and E. Breitmaier. *J. Prakt. Chem.* **336**, 225, (1994).

[88] S. Luo, L. Z. Long, G. A. Cordell, L. Xue, and M. E. Johnson. *Magn. Reson. Chem.* **31**, 215, (1993).

[89] A. Bax and G. Morris. *J. Magn. Reson.* **42**, 501, (1981).

[90] H. Kessler, C. Griesinger, J. Zarbock, and H. R. Loosli. *J. Magn. Reson.* **57**, 331, (1984).

[91] A. Bax, R. H. Griffey, and B. L. Hawkins. *J. Magn. Reson.* **55**, 301, (1983).

[92] G. Bodenhausen and D. J. Ruben. *Chem. Phys. Lett.* **69**, 185, (1980).

[93] A. Bax and M. F. Summers. *J. Magn. Reson.* **108**, 2093, (1986).

[94] A. Bax, R. Freeman, and T. A. Frenkiel. *J. Amer. Chem. Soc.* **103**, 2102, (1981).

[95] C. Kruk, A. W. H. Jans, and J. Lugtenburg. *Magn. Reson. Chem.* **23**, 267, (1985).

[96] H. H. Sun, S. S. Cross, M. Gunasekera, and F. E. Koehn. *Tetrahedron* **47**, 1185, (1991).

[97] H. Kessler, H. Oschkinat, C. Griesinger, and W.Bermel. *J. Magn. Reson.* **70**, 106, (1986).

[98] H. Kessler, U. Anders, G. Gemmecker, and S. Steuernagel. *J. Magn. Reson.* **85**, 1, (1989).

[99] L. Emsley and G. Bodenhausen. *J. Magn. Reson.* **82**, 211, (1989).

[100] L. Emsley and G. Bodenhausen. *Chem. Phys. Lett.* **165**, 469, (1990).

[101] O. W. Sorensen, M. Rance, and R. R. Ernst. *J. Magn. Reson.* **56**, 527, (1984).

[102] H. R. Bircher, C. Muller, and P. Bigler. *J. Magn Reson.* **89**, 146, (1990).

[103] W. L. Duax, V. Cody, and J. Hazel. *Steroids* **30**, 471, (1977).

[104] W. L. Duax, V. Cody, J. Griffin, J. Hazel, and C. M. Weeks. *J. Steroid Biochem.* **9**, 901, (1978).

[105] W. L. Duax and P. D. Strong. *Steroids* **34**, 501, (1979).

[106] W. L. Duax, C. M. Weeks, D. C. Rohrer, Yoshio Osawa, and M. E. Wolff. *J. of Steroid Biochem.* **6**, 195, (1975).

[107] M. Bohl, G. Kaufmann, M. Hubner, G. Reck, and R.-G. Kretschmer. *J. Steroid Biochem.* **23**, 895, (1985).

[108] M. E. Wolff, W. Ho, and R. Kwok. *J. Med. Chem.* **7**, 577, (1964).

[109] J. A. Vida. *Androgens and Anabolic Agents.* Academic Press, New York, (1969).

[110] A. Roldan, G. Burton, M. B. Castillo, M. C. Damasco, and C. P. Lantos. *J. Steroid Biochem.* **15**, 467, (1981).

[111] T. Eguchi, M. Yoshida, and N. Ikekawa. *Bioorg. Chem.* **17**, 294, (1989).

[112] D. S. Fullerton, K. Ahmed, A. H. L. From, R. H. McFarland, and J. F. Griffin. chapter 10. Elsevier, Amsterdam, (1986).

[113] D. S. Fullerton, K. Yoshioka, D. C. Rohrer, A. H. L. From, and K. Ahmed. *Mol. Pharmacology* **17**, 43, (1980).

[114] A. A. Ovchinnikov, I. L. Shamovsky, and G. M. Barenboim. *Proc. 3rd. Int. Conf. Biotechnology Biologically Active Products* **3**, 20, (1985).

[115] F. J. Zeelen. *Medicinal Chemistry of Steroids.* Elsevier, Amsterdam, (1990).

[116] P. K. S. Siegel. *J. Cardiovascular Pharmacol.* **8** (suppl. 9), 1986.

[117] J. N. Cohn. *New England J. Medicine* **320**, 729, (1989).

[118] K. Wiesner. *Conf. Biotechnology Biologically Active Products* **1**, 215, (1985).

[119] B. G. Woodcock and N. Rietbrock. *TIPS* **6**, 273, (1985).

[120] N. Dzimiri, U. Fricke, and W. Klaus. *Br. J. Pharmacol* **91**, 31, (1987).

[121] Thomas, P. Gray, and J. Andrews. *Advances in Drug Research* **19**, 313, (1990).

[122] B. M. Anner. *Biochem. J.* **227**, 1, (1985).

[123] K. J. Sweadner. *J. Biol. Chem.* **254**, 6060, (1979).

[124] G. E. Shull, J. Greeb, and J. B. Lingrel. *Biochemistry* **25**, 8125, (1986).

[125] M. M. Shull and J. B. Lingrel. *Proc. Natl. Acad. Sci. USA* **84**, 4039, (1987).

[126] J. Orlowski and J. B. Lingrel. *J. Biol. Chem.* **263**, 10436, (1988).

[127] E. Erdmann, G. Philipp, and H. Scholz. *Biochem. Pharmacol.* **29**, 3219, (1980).

[128] E. Erdmann, K. Werden, and L. Brown. *Eur. Heart. J.* **5**, 297, (1984).

[129] G. Grupp, A. De Power, I. L. Grupp, and A. Schwartz. *Proc. Soc. Exp. Biol. Med.* **175**, 39, (1984).

[130] G. Grupp, I. L. Grupp, T. Hickerson, S. W. Lee, and A. Schwartz In. E. Erdmann, K. Greef, and J. C. Skou, editors, *Cardiac Glycosides 1785-1985*, pages 99–108. Springer-Verlag, New York, (1986).

[131] K. R. H. Repke and J. Weiland. *Pharmacol. Res. Commun.* **20**, 425, (1988).

[132] K. Weisner and T. Y. R. Tsai. *Pure and Appl. Chem.* **58**, 799, (1986).

[133] K. R. H. Repke. *Pharmazie* **27**, 693, (1972).

[134] R. Thomas, J. Boutagy, and A. Gelbart. *J. Pharm. Sci.* **33**, 1649, (1974).

[135] J. F. Templeton, V. P. S. Kumar, D. Cote, D. Bose, D. Elliot, R. S. Kim, and F. S. LaBella. *J. Med. Chem.* **30**, 1502, (1987).

[136] M. Bentfeld, H. Lullmann, T. Peters, and D. Proppe. *Br. J. Pharmacol.* **61**, 19, (1977).

[137] M. Heller. *Biochem. Pharmacol.* **37**, 2293, (1988).

[138] R. A. Gillis and J. A. Quest. *Pharmacol. Rev.* **31**, 19, (1980).

[139] R. A. Gillis and J. A. Quest. In *Cardiac Glycosides 1785-1985* (E. Erdman K. Greef and J. C. Skou, eds.) Steinkopff Verlag, Darmstadt, (1986).

[140] I. M. Glynn. *J. Physiol.* **136**, 148, (1957).

[141] L. F. Hoffmann. *Am. J. Med.* **41**, 666, (1966).

[142] K. R. H. Repke, F. Dittrich, P. Berlin, and H. J. Portius. *Ann. N. Y. Acad. Sci.* **242**, 735, (1974).

[143] L. Brown, R. Thomas, and T. Watson. *Naunyn-Schmied. Arch. Pharmacol.* **332**, 98, (1986).

[144] A. Gelbart and R. Thomas. *J. Med. Chem.* **21**, 284, (1978).

[145] B. K. Naaido, T. R. Witty, W. A. Remers, and Jr. H. R. Besch. *J. Pharm. Sci.* **63**, 1391, (1974).

[146] R. E. Thomas, J. Boutagy, and A. Gelbert. *J. Pharm. Sci.* **63**, 1649, (1974).

[147] D. S. Fullerton, K. Yoshioka, D. Rohrer, A. From, and K. Ahmed. *J. Med. Chem.* **22**, 529, (1979).

[148] M. Bohl, K. Ponsold, and G. Reck. *J. Steroid Biochem.* **21**, 373, (1984).

[149] D. C. Rohrer, D. S. Fullerton, K. Yoshioka, A. H. L. From, and K. Ahmed In. *Computer Assisted Drug Design, ACS Symposium Series 112.* American Chemical Society, New York, (1979).

[150] R. Hintsche, R. Megges, D. Pfeiffer, H. J. Portius, W. Schönfeld, and H. R. H. Repke. *Eur. J. Med. Chem.* **20**, 9, (1985).

[151] R. E. Thomas, J. Boutagy, and A. Gelbart. *J. Pharm. Exp. Ther.* **191**, 219, (1974).

[152] W. Schönfeld, J. Weiland, C. Lindig, M. Masnyk, M. M. Kabat, J. Wicha, and K. R. H. Repke. *Naunyn-Schmeid. Arch. Pharmacol.* **329**, 414, (1985).

[153] M. Bohl and R. Sussmilch. *Eur. J. Med. Chem.* **21**, 193, (1986).

[154] J. Boutagy and R. E. Thomas. *Aut. J. Chem.* **24**, 2723, (1971).

[155] J. Boutagy and R. E. Thomas. *Aust. J. Pharm. Sci.* **NS1**, 67, (1972).

[156] J. Boutagy and R. E. Thomas. *Aust. J. Pharm. Sci.* **NS2**, 9, (1973).

[157] R.S. Kim, E. Chow, G. Queen, and F. S. LaBella. *Proc. Can Fed. Bio. Soc* **21**, 156, (1978).

[158] F. S. LaBella, I. Bihler, J. F. Templeton, R. S. Kim, M. Hnatowick, and D. Rohrer. *Fed. Proc.* **44**, 2806, (1985).

[159] D. Bose, D. Elliot, T Kobayashi, J. F. Templeton, V. P. S. Kumar, and F. S. LaBella. *Brit. J. Pharmacol.* **93**, 453, (1988).

[160] J. F. Templeton, V. P. S. Kumar, D. Bose, and F. S. LaBella. *J. Med. Chem.* **32**, 1977, (1989).

[161] J. F. Templeton, Y. Ling, T. H. Zeglam, K. Marat, and F. S. Labella. *J. Chem. Soc. Perkin Trans. I* 2503, (1992).

[162] J. F. Templeton, V. P. Sashi Kumar, K. Marat, R. S. Kim, F. S. Labella, and D. Cote. *J. Nat. Prod.* **50**, 463, (1987).

[163] J. F. Templeton, P. Setiloane, Kumar V. P. S, Y. Yan, T. H. Zeglam, and F. S. LaBella. *J. Med. Chem.* **34**, 2778, (1991).

[164] J. F. Templeton, Y. Ling, T. H. Zeglam, and F. S. LaBella. *J. Med. Chem.* **36**, 42, (1993).

[165] F. S. LaBella, J. F. Templeton, V. P. S. Kumar, and D. Bose. *Trends Pharmacol. Sci.* **10**, 11, (1989).

[166] J. F. Templeton, V. P. S. Kumar, D. Bose, D. D. Smyth, R. S. Kim, and F. S. LaBella. *Can. J. Physiol. Pharmacol.* **66**, 1420, (1988).

[167] D. D. Smyth, J. F. Templeton, V. P. S. Kumar, Y. Yan, W. Widajewicz, and F. S. LaBella. *Can. J. Physiol. Pharmacol.* **70**, 723, (1992).

[168] J. F. Templeton, Y. Ling, H. B. Xin, and F. S. LaBella. *unpublished work.*

[169] W. R. Benn. *J. Org. Chem.* **28**, 3557, (1963).

[170] G. G. Habermehl, P. E. Hammann, and V. Wray. *Magn. Reson. Chem.* **23**, 959, (1985).

[171] M. Biesemans, G. Van de Woude, and L. van Hove. *Bull. Soc. Chim. Belg.* **94**, 1, (1985).

[172] G. Cooley, D. N. Kirk, R. E. Morgan, and M. L. S. é Melo. *J. C. S. Perkin I* 1390, (1977).

[173] M. S. Maier, A. M. Seldes, and E. G. Gros. *Magn. Reson. Chem.* **29**, 137, (1991).

[174] H. Lee, N. S. Bhacca, and M. E. Wolff. *J. Org. Chem.* **31**, 2692, (1966).

[175] C. H. Robinson and P. Hofer. *Chemistry and Industry* 377, (1966).

[176] D. C. Rohrer and D. S. Fullerton. *Acta Crystallogr., Sect. B.* **B29**, 1565, (1980).

[177] I. L. Karle and J. Karle. *Acta Crystallogr., Sect. B.* **B25**, 434, (1969).

[178] A. Messerschmidt, E. Höhne, and R. Megges. *Cryst. Struct. Commun.* **10**, 157, (1981).

[179] A. Messerschmidt, E. Höhne, and B. Streckenbach. *Cryst. Struct. Commun.* **10**, 141, (1981).

[180] K. Go and G. Kartha. *Acta Crystallogr., Sect. B* **B36**, 3034, (1980).

[181] G. Reck, A. Messerschmidt, and R. Megges. *Cryst. Struct. Commun.* **10**, 637, (1981).

[182] E. Hohne and D. Pfeiffer. *Studia Biophysica* **97**, 81, (1983).

[183] Sir Colin Dollery, editor. *Therapeutic drugs*, volume 1. Churchill Livingstone, Edinburgh, (1991).

[184] S. J. Halkes, J. Hartog, L. Morsink, and A. M. de Wachter. *J. Med. Chem.* **15**, 1288, (1972).

[185] R. Wiechert and F. Neumann. *Arzneim.-Forsch.* **15**, 244, (1965).

[186] L. J. Chinn and B. N. Desai. *J. Med. Chem.* **18**, 268, (1975).

[187] J. F. Templeton and R. S. Kim. *Steroids* **27**, 581, (1976).

[188] M. Wolff, W. Ho, and M. Honjoh. *J. Med. Chem.* **9**, 682, (1966).

[189] F. T. Bond, W. Weyler, B. Brunner, and J. E. Stemke. *J. Med. Chem.* **19**, 255, (1976).

[190] L. R. Wiseman and D. McTavish. *Drugs* **45**, 66, (1993).

[191] G. E. Ackerman, M. E. Smith, C. R. Mendelson, C. R. MacDonald, and E. R. Simpson. *J. Clin. Endocr. Metab.* **53**, 412, (1981).

[192] J. F. Templeton. Personal communication.

[193] B. Sherry and R. H. Abeles. *Biochemistry* **24**, 2594, (1985).

[194] J. Frank, S. H. Krimpern, P. E. J. Verweil, J. A. Jongejan, A. C. Muler, and J. A. Duine. *Eur. J. Biochem.* **184**, 187, (1989).

[195] J. F. Templeton and C. W. Wie. *Can. J. Chem.* **53**, 1693, (1975).

[196] J. C. Orr, M. J. Newlands, E. J. Gabe, and J. P. Charland. *Steroids* **52**, 37, (1988).

[197] V. Petrow, G. M. Padilla, A. T. McPhail, N. Bruchovsky, and S. L. Schneider. *J. Steroid Biochem.* **32**, 399, (1989).

[198] J. F. Templeton, J. C. Orr, H. Majgier-Baranowska, and K. Marat. *J. C. S. Perkin Trans I* in press, (1995).

[199] N. J. Kuhn and M. S. Briley. *J. Biochem.* **117**, 193, (1970).

[200] J. Matsuda, K. Noda, K. Shiota, and M. Takahashi. *J. Reprod. Fertil.* **88**, 467, (1990).

[201] E. Caspi, T. Arunachalam, and P. A. Nelson. *J. Amer. Chem. Soc.* **105**, 6987, (1983).

[202] E. Caspi, T. Arunachalam, and P. A. Nelson. *J. Amer. Chem. Soc.* **108**, 1847, (1983).

[203] P. A. Cole and C. H. Robinson. *J. Med. Chem* **33**, 2934, (1990).

[204] J. N. Wright and M. Akhtar. *Steroids* **55**, 142, (1990).

[205] S. S. Oh and C. H. Robinson. *J. Steroid Biochem. Molec. Biol.* **44**, 389, (1993).

[206] J. D. Townsley and H. J. Brodie. *Biochemistry* **7**, 33, 1968.

[207] P. A. Cole and C. H. Robinson. *Biochem. J.* **268**, 553, (1990).

[208] D. D. Beusen and D. F. Covey. *J. Steroid. Biochem.* **20**, 931, (1984).

[209] M. Akhtar, M. R. Calder, D. L. Corina, and J. N. Wright. *Biochem. J.* **201**, 569, (1982).

[210] J. F. Templeton, V. G. Paslat, and C. W. Wie. *Can. J. Chem.* **56**, 2058, (1978).

[211] J. F. Templeton and R. K. Gupta. *Unpublished information*, (1994).

[212] J. F. Templeton, Y. Ling, W. Lin, and K. Marat. *Tetrahedron Letters* **35**, 5755, (1994).

[213] J. F. Templeton, Y. Ling, W. Lin, R. J. Pitura, K. Marat, and J. N. Bridson. *J. Chem. Soc. Perkin Trans. I* 1149, (1994).

[214] L. H. Knox, E. Velarde, and A. D. Cross. *J. Amer. Chem. Soc.* **85**, 2533, (1963).

[215] D. D. McIntyre, M. W. Germann, and H. Vogel. *Can. J. Chem.* **68**, 1263, (1990).

[216] T. Drakenberg, P. Brodelius, D. D. McIntyre, and H. J. Vogel. *Can. J. Chem.* **68**, 272, (1990).

[217] M. Kinns and J. K. M. Sanders. *J. Magn. Reson.* **56**, 518, (1984).

[218] J. S. Martin and A. R. Quirt. *J. Magn. Reson.* **5**, 318, (1971).

[219] K. Marat and R. Sebastian. *Bruker Report* 42, 1993.

[220] Wavefunction, Inc., 18401 Von Karman, Suite 370, Irvine, CA, USA. *Spartan Program*, (1994).

[221] L. Birladeanu, T. Hanafusa, and S. Winstein. *J. Amer. Chem. Soc.* **88**, 2315, (1966).

[222] P. E. Hammann, G. G. Habermehl, and H. Kluge. *Magn. Reson. Chem.* **26**, 85, (1988).

[223] P. E. Hammann, H. Kluge, and G. G. Habermehl. *Magn. Reson. Chem.* **29**, 133, (1991).

[224] E. L. Eliel, W. F. Bailey, L. D. Kopp, R. L. Willer, D. M. Grant, R. Bertrand, K. A. Chistensen, D. K. Dalling, M. W. Duch, E. Wenkert, F. M. Schell, and D. W. Cochran. *J. Amer. Chem. Soc.* **97**, 322, (1975).

[225] D. M. Grant and V. B. Cheney. *J. Amer. Chem. Soc.* **89**, 5315, (1967).

[226] N. S. Bhacca, M. E. Wolff, and W. Ho. *Tetrahedron Letters* **52**, 5427, (1968).

[227] U. R. Desai and G. K. Trivedi. *Magn. Reson. Chem.* **29**, 148, (1991).

[228] K. Tori and K. Kitahonoki. *J. Amer. Chem. Soc.* **87**, 386, (1965).

[229] H. H. McConnell. *J. Chem. Phys.* **27**, 226, (1957).